Scaffold Design for Bone Regeneration

Liliana Polo-Corrales[1,2], **Magda Latorre-Esteves**[2], and **Jaime E. Ramirez-Vick**[1,2,*]

[1]Engineering Science and Materials Department, University of Puerto Rico-Mayagüez, Mayagüez, P. R. 00681, USA

[2]Department of Chemical Engineering, University of Puerto Rico-Mayagüez, Mayagüez, P. R. 00681, USA

Abstract

The use of bone grafts is the standard to treat skeletal fractures, or to replace and regenerate lost bone, as demonstrated by the large number of bone graft procedures performed worldwide. The most common of these is the autograft, however, its use can lead to complications such as pain, infection, scarring, blood loss, and donor-site morbidity. The alternative is allografts, but they lack the osteoactive capacity of autografts and carry the risk of carrying infectious agents or immune rejection. Other approaches, such as the bone graft substitutes, have focused on improving the efficacy of bone grafts or other scaffolds by incorporating bone progenitor cells and growth factors to stimulate cells. An ideal bone graft or scaffold should be made of biomaterials that imitate the structure and properties of natural bone ECM, include osteoprogenitor cells and provide all the necessary environmental cues found in natural bone. However, creating living tissue constructs that are structurally, functionally and mechanically comparable to the natural bone has been a challenge so far. This focus of this review is on the evolution of these scaffolds as bone graft substitutes in the process of recreating the bone tissue microenvironment, including biochemical and biophysical cues.

Keywords

Bone Tissue Engineering; Bone Graft; Scaffold; Biomaterials; Biophysical Stimulation; Biochemical Stimulation; Bone; Mesenchymal Stem Cells; Osteoblasts

1. INTRODUCTION

Bone grafts are used for augmenting or stimulating the formation of new bone in cases such as the healing of skeletal fractures or between two bones across a diseased joint, to replace and regenerate lost bone as a result of trauma, infection, or disease, or improve the bone healing response and regeneration of bone tissue around surgically implanted devices, such as artificial joints replacements or plates and screws used to hold bone alignment. The high incidence of these conditions is evidenced by the 2.2 million bone grafts used in orthopedic procedures annually worldwide.[1] The three main types of bone grafts are the autografs,

*Author to whom correspondence should be addressed.

allografts and bone graft substitutes.[2] The tissue regeneration capacity of these bone grafts is measured in terms of their osteogenic, osteoconductive and osteoinductive potential.[3] The osteogenic potential of a bone graft is given by cells involved in bone formation, such as mesenchymal stem cells (MSCs), osteoblasts, and osteocytes. The term osteoconductive refers to the scaffold or matrix which stimulates bone cells to grow on its surface. Osteoinductive capacity of a bone graft is perhaps the most important property in bone healing as it refers to the stimulation of MSCs to differentiate into preosteoblasts to begin the bone-forming process. The most common of these bone grafts is the autograft, which is the transplanting of bone tissue from one site to another in the same patient. It is usually transplanted from the iliac crest, but it can also be from the distal femur or the proximal tibia. This type is considered the standard in bone grafts since it contains both osteogenic cells and an osteoconductive mineralized extracellular matrix where these can grow and proliferate. However, its use is limited by complications such as pain, infection, scarring, blood loss, and donor-site morbidity.[4-6] Another alternative is the allograft, which is bone tissue from cadavers or living donors. Their benefits over autographs include the elimination of donor site morbidity and issues related to their limited supply. However, they lack the osteogenic capacity of autografts and carry the risk of infectious agents or immune rejection.[7,8] Although both types of bone grafts have been widely used, their limitations have prompted the search for other alternatives, which are referred to bone graft substitutes.[9] This type of bone graft is based on the concept of bone tissue engineering, which focused on improving their osteogenic, osteoconductive and osteoinductive potential by incorporating bone progenitor cells and growth factors to stimulate cells into a scaffold made of various natural or synthetic materials or their combination, which mimic the bone microenvironment. This review focuses on the current state of development of these biomimetic scaffolds, and the alternatives and design criteria for their application in bone regeneration applications.

2. BONE PROPERTIES

To design bone biomimetic scaffolds involves building a proper representation of bone, which requires understanding bone biology and physiology. Bone can be seen as an open cell composite material composed of osteogenic cells extracellular matrix (ECM) proteins, growth factors, mineral calcium in the form of calcium hydroxyapatite, and a complex vascular system. The cells that make up the bone represent about 10% of the total volume and include osteoprogenitor cells of mesenchymal origin, i.e., osteoblasts and osteocytes and bone-resorptive cells of hematopoietic origin, i.e., osteoclasts. Pre-osteoblasts are bone progenitor cells located in the periosteum, endosteum, and Haversian canals that derive from MSCs and which are stimulated through growth factors (e.g., bone morphogenetic proteins (BMPs), transforming growth factor-β (TGF-β), fibroblast growth factor (FGF), insulin-derived growth factor (IGF), platelet-derived growth factor (PDGF), and interleukins) into migrating to a specific site, to proliferate and differentiate into osteoblasts. Osteoblast differentiation occurs in three stages: (1) cell proliferation, (2) matrix maturation, and (3) matrix mineralization. During the proliferation stage ECM proteins are expressed and secreted by osteoblasts forming the non-mineralized bone matrix or osteoid. This is followed by the crosslinking of the proteins of the osteoid during matrix maturation, forming a

structure that is stronger and more stable. Crosslinked collagen type I fibrils, the main component of the osteoid, become templates onto which the inorganic minerals are deposited forming the mineralized bone matrix. At the end of this stage, osteoblasts can either: become embedded in the bone as osteocytes, transform into inactive osteoblasts and become bone-lining cells, or undergo programmed cell death (i.e., apoptosis).[10] The osteocytes embedded in bone matrix are the most abundant cell type of bone forming networks connected to each other via long cytoplasmic extensions that occupy tiny canals called canaliculi. Through this network, that is thought to include osteoclasts, they function as strain and stress sensors, signals that are very important for maintaining bone structure.[11] Osteoclasts are large, multinucleated cells that attach to bone matrix through a brush border and solubilize its mineral content via acidification. This process is tightly regulated via the paracrine co-regulation between osteoclasts and osteoblasts in a process called bone remodeling. The main recognized functions of bone remodeling include preservation of bone mechanical strength by replacing older, microdamaged bone, with newer, healthier bone and calcium and phosphate homeostasis. The cortical bone turnover rate is smaller than in trabecular bone, but adequate to maintain biomechanical strength of the tissue. The rate of trabecular bone turnover is higher, more than required for maintenance of the mechanical strength of cortical bone, indicating that is more important for mineral metabolism. This process can also respond to changes in the functional demands of the mechanical loading.[12]

The ECM proteins self-assemble and are composed mainly of collagens, and non-collagenous proteins, which include glycoproteins, proteoglycans and growth factors. The collagens form 90% of the total weight of ECM proteins, which mainly contain collagen type I (97%), with smaller amounts of type III, V, XI and XIII. The non-collagenous proteins form the additional 10% of the bone mass.[13, 14] The glycoproteins include alkaline phosphatase (ALP), osteopontin (OPN), bone sialoprotein (BSP), and osteocalcin (OCN), which modulate the mineralization process and osteonectin that modulates collagen fibril diameter. In addition, there are proteins containing the RGD integrin–binding domain, which include thrombospondins, fibronectin, vitronectin, and fibrillin 1 and 2.[15] The proteoglycans constitute about 10% of the non-collagenous proteins and provide resistance to compressive forces. This property stems primarily from the glycosaminoglycan portion of proteoglycans, which are long-chain polysaccharides whose chemical properties are determined by the types of sugars in the chain. Another property of proteoglycans is their capacity to bind growth factors for future use. For instance growth factors can be stored in the bone ECM by binding to the proteoglycans decorin, biglycan or perlecan, or membrane-bound proteoglycans such as syndecan or betaglycan, which may act as co-receptors for these growth factors.[16]

Bone is a reservoir for calcium in the body, containing 99% of the body's calcium. Bone mineral is mostly (85%) in the form of hydroxyapatite (HA, $Ca_{10}(PO_4)_6(OH)_2$), with calcium carbonate (10%), calcium fluoride (2–3%) and magnesium fluoride (2–3%). Natural hydroxyapatite contains carbonate ions as replacement groups in phosphate and hydroxyl sites of the hydroxyapatite structure. These crystals are about 20 nm in their largest dimension. Bone strength and stiffness is higher along its longitudinal axis.[17] This is due to collagen and mineral crystals being usually oriented in this direction, with the mineral providing stiffness, and the collagen fibrils providing fracture toughness to the bone.[18]

At the histological level, there are two main structural types in bone, the cortical bone which forms a dense outer shell and the cancellous or trabecular bone which forms the porous inner core. Both of these are classified based on their porosity, structure and metabolic activity, which modulate their function and physiology (Fig. 1). Cortical bone is highly dense and consists of a hierarchical structure, each with in a different size scale,[12] see Table I. These range from the solid material (> 3 mm), to the cylindrically organized osteons (10–500 μm), lamellae (3–20 μm), and the collagen-mineral composite (60–600 nm).[19] The osteons give cortical bone its strength and include the central Haversian canal which is composed of blood vessels interconnected with vessels on the surface of the bone through perforating canals (Fig. 1). The lamellae are layers of bone generally 3–7 mm in thickness, which are arranged concentrically around the central Haversian canal in osteonal bone. The primary function of cortical bone is to provide torsion and bending resistance and compressive strength. In contrast, cancellous bone is highly porous, consisting of an interconnected network of trabeculae which is usually filled with marrow. Its hierarchical structure ranges from the solid material (> 3 mm), to the trabeculae (75–200 μm), lamellae (1–20 μm), and the collagen-mineral composite (60–600 nm).[18] The porous trabeculae provide a high surface area which allows for nutrient diffusion and exposure to circulating growth factors. This access allows cancellous bone tissue to be metabolically active and can be remodeled more frequently than that of cortical bone.[20] In contrast to the regular, cylindrically shaped lamellae in cortical bone, in cancellous bone lamellae consist of irregular, semicircular shapes, which allows for deformation and absorption of loads.[21]

Bone is considered an anisotropic material because its mechanical properties vary with anatomical location and the loading direction. For instance, there is great variability in Young's modulus of elasticity, tensile and compressive strengths between the longitudinal and transverse loadings.[20] In contrast, cancellous bone does not show a consistent mechanical strength and varies both longitudinally and from one bone to another. As a result, cancellous bone exhibits much broader mechanical properties compared to those of cortical bone. The trabeculae of cancellous bone follow the lines of stress and can be realigned by changes in the direction of stress.

3. THE EVOLUTION OF BONE GRAFT SUBSTITUTES

The evolution of bone implant devices has resulted with an increase in knowledge about the microenvironment where the replacement will occur, which results in changes in requirements and properties of the biomaterials used. This evolution can be measured by defining three different generations as defined by Hench.[22] As pointed by Navarro et al.[23] these generations are not chronological but technological, since there is currently active research and development for each. First generation bone graft substitutes require the biomaterial to match the physical properties of the tissue to be replaced, while maintaining inertness with the tissue microenvironment. These include metals such as stainless steel, titanium, and alloys; ceramics such as alumina and zirconia; and polymers such as silicone rubber, polypropylene, and polymethylmethacrylate. A common occurrence for all these biomaterials is the formation of fibrous tissue at the biomaterial-tissue interface that would eventually encapsulate the graft subsequently leading to aseptic loosening. This occurs as a non-specific immune response to a material that cannot be phagocytosed, in which an

inflammatory response persists until the foreign body becomes encapsulated by fibrotic connective tissue, shielding it from the immune system and isolating it from the surrounding tissues.[24]

To avoid this non-specific immune response, second generation bone graft substitutes were developed with bioactive interfaces which would elicit a specific biological response (i.e., osteoconduction) to avoid the formation of this fibrous layer and improve osseointegration. The overall strategy is to modify first generation biomaterials with coatings that are bioactive or biodegradable. This bioactivity is provided by a surface chemistry that would either allow mineralization through the heterogeneous nucleation and crystallization of HA, or cover the biomaterial surface with bioactive ceramics such as HA, β-tricalcium phosphate (β-TCP), or bioactive glass. A second type of second generation bone graft substitutes is made biodegradable with the aim that the rate of degradation matches the healing rate of the injured bone tissue. These biomaterials are based on the use of synthetic or natural polymers that can provide a controlled chemical breakdown under physiological conditions into inert products that can be resorbed by the body. Examples of the synthetic polymers include polylactide, poly(ε-caprolactone), and polyglicolide; and chitosan and hyaluronic acid for natural ones.[23] The mechanical and osteoconductive properties of these polymers can be improved by forming composites with bioactive ceramics. Another alternative to improve the polymers is to chemically modify them through the conjugation of osteoinductive biomolecules.

Third generation bone graft substitutes try to get closer to the autograft standard by using biomaterials capable of inducing specific cellular responses at the molecular level, by integrating the bioactivity and biodegradability of second generation devices. This type of bone graft is based on the concept of bone tissue engineering, which focused on creating a device that enhances bone repair and regeneration by incorporating bone progenitor cells and growth factors to stimulate cells into a scaffold made of various natural or synthetic biomaterials or their combination and with sufficient vascularization to allow access to nutrients to support this process.[25] This process of bone regeneration is osteoconductive in which MSCs are recruited and stimulated to differentiate into pre-osteoblast and depends on the microenvironment. This is similar to what happens during new bone formation or immediately after skeletal injury or biomaterial implantation, being particularly active during the first week post-trauma. In contrast, bone repair involves a basic inflammatory response, where fibrous tissue is formed, and does not depend on the osteoinductive potential of the microenvironment.[26]

The osteoprogenitor cells, growth factors and vascularization are all natural components of the bone tissue microenvironment, making the scaffold the only element of this formulation which requires fabrication. This entails defining the necessary design parameters for achieving the cell function leading to bone regrowth, which include cell attachment, proliferation, and differentiation. These design parameters should lead to specific scaffold properties, which include biocompatibility, porosity, micro and nano-scale structure, degradation rate, mechanical strength, and growth factor delivery, all of which dictate the biomaterial to be used or developed.[27] Defining specific design parameters requires knowledge of MSC activity in osteogenesis, including the progression of cellular events and

the sensitivity of cells to biochemical and mechanical stimuli. Biocompatibility is related to a scaffold biomaterial which does not elicit undesirable local or systemic responses in the eventual host and is thus a property of the material itself.[28] Scaffold geometry affects cell adhesion, proliferation and distribution by affecting the access to cell recruitment, vascularization, nutrients and oxygen. This is related to the pore size and interconnectivity, which directly affect the scaffold porosity. Pore structure and overall porosity seem to be able to modulate osteogenesis since osteogenic cells have been shown to respond to particular pore dimensions. For instance, bone growth in canines where the pore diameters range 15–50 mm is fibrovascular, 50–150 mm is osteoid, and 150–500 mm is mineralized.[29] It can be seen why a highly porous scaffold facilitates cell seeding and migration, while smaller pores allow tissue ingrowth. High porosity in excess of 90% is chosen in many scaffold designs since it allows for adequate diffusion of nutrients during tissue culture and provides sufficient surface area for cell–biomaterial interactions. Since the mechanical strength provided by the scaffold decreases with porosity, this value should always be balanced with the mechanical needs of the particular tissue that is going to be replaced. Another important aspect of pore structure is pore interconnectivity, since interconnected pores enhance the diffusion rates to and from the center of the scaffold and facilitates vascularization, thus improving oxygen and nutrient supply and waste removal. Microscale pores allow cell migration, vascular distribution, and diffusion of nutrients and oxygen providing osteoconductivity. In contrast, nanostructured biomaterials significantly enhance cell functions leading to improved osteoinductivity and osseointegrativity, since osteogenic cells interact with nano-scale minerals and proteins.[30] It has been shown that these nano-topographies affect adsorbed protein conformation giving access to motifs that can allow binding by osteogenic cells through integrins, a widely expressed family of transmembrane adhesion receptors, consisting of α and β heterodimers, which bind to specific amino acid sequences, such as the RGD cell binding domain.[31] The rate of degradation of the scaffold must be tuned so that it provides the necessary structural support until the newly grown bone has sufficient mechanical strength to replace this supporting function.[32] If this condition is not met, the scaffold could fracture after being submitted to a mechanical load before the bone healing process is complete. Growth factors such as platelet-derived growth factors (PDGF), bone morphogenetic proteins (BMP), insulin-like growth factors (IGF), and transforming growth factor-β (TGF-β) increase the osteoinductive and osteoconductive potential of osteoprogenitor and osteoblast functions to enhance bone growth by encouraging MSCs to migrate into the scaffold, proliferate, differentiate, and begin ECM production.[33] These can be delivered by methods such as bolus injection, surface adsorbed protein release, osmotic pumps, and controlled release from biodegradable scaffolds. Challenges found by these methods include loss of their bioactivity because of a short half-life, limited control over dose administration, and non-targeted delivery. Among the delivery methods, controlled release from biodegradable scaffolds has proven the most effective.

4. MATERIALS

4.1. Natural Polymers

Bone tissue engineering has focused on the creation of 3D scaffolds that can mimic the ECM, support the formation of new bone, while degrading as new bone is produced. Natural

polymers have attractive properties for the construction of 3D scaffolds, such as biocompatibility and biodegradability. Importantly, control of porosity, charge, and mechanical strength can be controlled by changing polymer concentrations, polymerization conditions, or by introducing various functional groups.[34] Bioactivity can also be controlled by the addition of chemicals, proteins, peptides, and cells.[35] The most commonly studied natural polymers for the purpose of bone engineering are collagen/gelatin, chitosan, silk, alginate, hyaluronic acid, and peptides.[36, 37] Here we discuss recent studies where these natural polymers are studied as 3D scaffolds for bone regeneration, and are modified in different manners in order to improve their osteogenic capabilities.

4.1.1. Collagen—As a primary component of bone, collagen (and gelatin) is an ideal candidate for the design of 3D scaffolds.[38] It is inherently biocompatible and biodegradable, and stimulates proliferation and differentiation of cells as extracellular matrix.[39] However, it has poor mechanical properties.[40] In the following studies, collagen was used as a base for 3D scaffolds and modified with the addition of polymers and other biomolecules in order to improve osteoinductivity.

In one study,[41] the authors combine the mechanical properties of a 3D macrochanneled poly-ε-caprolactone (PCL) scaffold, fabricated via the robotic dispensing technique, with the bioactive properties of collagen. A MSC loaded collagen hydrogel collagen was inserted onto the macrochanneled scaffold. The authors studied the effect of growing these cell-seeded scaffolds in a perfusion bioreactor, to test how osteogenesis was affected by the continuous supply of fresh media and shear stress. The collagen/PCL scaffolds had a statistically significant increase in cell proliferation when grown in the perfusion chamber when compared to cells grown in static conditions. The activity of alkaline phosphatase (ALP), an early osteogenic marker, was also significantly upregulated at 14 days in cells grown in the perfusion chamber. The expression of the osteogenic genes OPN, OCN, and BSP was also significantly upregulated when cells were grown in the perfusion chamber. Results clearly indicate that cell proliferation and differentiation are enhanced by the effects of the perfusion chamber. The authors tested if the shear stress provided to the cells in scaffold by the perfusion chamber could cause upregulation of genes associated with mechanotransduction, a process by which physical forces are converted into biochemical signals that are essential for the formation of bone.[42] This hypothesis was supported by the very substantial increase of the *c*-fos and COX-2 genes in cells grown in the perfusion chamber, factors that have been shown to respond rapidly to mechanical stress.[43]

Collagen hydrogels have also been used to test the ability of MSCs from different sources to undergo osteogenic differentiation.[44] In this study, a scaffold composed of 90% type 1 collagen, which gives bone its tensile strength,[45] and 10% type 3 collagen. In recent years, bone marrow MSCs (BM-MSC) have shown great potential for tissue engineering purposes. They are relatively easy to isolate, retain their multipotency even after several passages, and can be induced to differentiate into bone.[46] However, there is a very low amount that can be harvested from bone marrow, they have limited proliferation, and high senescence.[47] It has recently been reported that MSCs can be isolated from the Wharton's Jelly found in the umbilical cord (UC-MSC), and they are more abundant, more easily expanded and more resistant to cryogenic storage.[48] The adhesion, migration into scaffold, growth, spreading,

osteogenic differentiation, ECM degradation and synthesis of BM-MSCs versus UC-MSCs was compared. The tested collagen scaffold showed excellent cytocompatibility with both cell types and could maintain high proliferation and viability. When stimulated with osteogenic induction medium, both cell types showed comparable osteogenic gene expression, migration and scaffold colonization, and ability to contract the collagen scaffold. It is very interesting to note that UC-MSCs were much more capable of producing an ECM. They showed at least 10-fold higher expression of the ECM marker genes collagen I, collagen III, collagen IV, and laminin than BM-MSCs. Since the production of ECM is an integral component of bone regeneration, UC-MSCs could have a significant impact on bone tissue engineering, and its osteogenic potential should be investigated in additional scaffold compositions.

Several studies have been conducted where other materials are incorporated into collagen in order to enhance mechanical properties and enhanced bone-matrix interface strength. In one such study,[49] a $CaO-P_2O_5-SiO_2$ bioactive glass (BA) was added to a collagen solution to prepare composite scaffolds, in the presence or absence of phosphatidylserine (PS). At higher PS ratios, the porosity (%) of the scaffold increased and compressive strength (MPa) decreased. The scaffold chosen for *in vivo* and *in vitro* studies had a COL-PS/BA ratio (w/w) of 35:65. This scaffold had a porosity of 75.40% and a compressive strength of 1.5469 MPa. As a control, a scaffold composed of COL-BG was used. Rat MSCs were used for *in vitro* studies. Attachment and proliferation of MSCs was higher in the COL-BG-PS than in the COL-PA scaffolds at all time-points tested. When cultured in osteogenic media, ALP activity was significantly higher in COL-BG-PS constructs after day 7, and mineralization was significantly increased in cells grown in the COL-BG-PS scaffolds at day 21. Expression of ALP, OC, and OPN were obviously higher in MSCs in contact with the COL-BG-PS composite. For *in vivo* studies, a rat femur defect model was used. Three groups were analyzed: COL-BG-PS/MSC, COL-BG/MSC, and cell free COL-BG-PS. MSCs were cultured in osteoinductive media prior to seeding into the scaffold. At 6 weeks post-surgery, the femurs of the rats in the COL-BG-PS/MSC group showed the greatest amount of healing, followed by the COL-BG/MSC group. The least amount of healing was observed in the cell free COL-BG-PS group. The data obtained from this work suggests that the addition of PS into other types of scaffolds could enhance their osteogenic potential. In another study, the hydraulic permeability (*k*) of a collagen-based scaffold is manipulated in order to improve mechanical properties, cell–scaffold interactions, oxygen flow and nutrient diffusion.[50] Permeability is the ability of porous structures to transfer fluids through their interstices under applied pressure, and this can be controlled through pore size, number, orientation, distribution and interconnectivity.[51] Collagen scaffolds were prepared and exposed to plastic compression using different static stresses in order to control permeability. Results showed that increasing compression reduces *k*. It was also found that a decrease in *k* correlates with an increase of the modulus and permeability of collagen gels. The authors then went on to test the effect of *k* on MSC proliferation, differentiation and mineralization. When compared to non-compressed gels, compressed gels showed higher proliferation, ALP staining, and mineralization, but no significant difference was found between the different compressed gels. These findings suggest that decreasing *k* provides a good matrix for cell proliferation and osteodifferentiation, but the influence of *k* on

osteoinduction and osteoconduction has not been fully defined. Another study examines the effect of varying gelatin (G) and chitoolisaccharide (COS) ratio on scaffold pore size, and the effect of pore size on osteogenic differentiation.[52] Scaffolds at G/COS mixing ratios of 100:0, 70:30 and 50:50 were fabricated by freeze-drying and glutaraldehyde cross-linking. Gelatin (100:0) scaffolds had the largest pore size and most homogenous distributions and higher compressive moduli than scaffolds prepared at 70:30 and 50:50 ratios. MSCs were seeded into the scaffolds and allowed to proliferate and differentiate in osteogenic media. ALP activity and calcium content was found to be highest for the G:COS 70:30 formulation. This scaffold was then chosen for *in vivo* subcutaneous implantation studies. This scaffold was pre-cultured with MSCs in osteogenic media and then implanted using a cell free scaffold as a control. Calcium was deposited on the surface of scaffolds pre-cultured with MSC at 8 weeks post-implantation. No calcium deposition was observed in control scaffolds. This study shows that the tested formulation supports ectopic calcium deposition, however, the effect of pore size was not evaluated at this stage. The same group also tested the effect of adding magnesium calcium phosphate (MCP) onto gelatin scaffolds in order to find optimal pore size and mechanical properties for osteoinduction.[53] MCP was added to the gelatin solution at 25, 50, 75, and 90 wt%. Porosity was not significantly affected with the addition of MCP, however, the compression moduli (MPa) and amount of magnesium released into cell culture media increased with higher percentages of MCP in the formulation. MSCs were seeded onto the gelatin sponges and tested for proliferation, osteocalcin content, and ALP activity. An increase in MCP content correlated with an increased proliferation, ALP activity, and osteocalcin content. It remains to be determined whether these effects are due to the change in mechanical properties conferred by addition of MCP, or if the amount of magnesium released in the media could have an important impact on these effects.[54]

Collagen scaffolds have also been used as a method for delivery of factors that induce osteogenic differentiation. In one study, bone morphogenetic protein-4 (BMP4) was spatially immobilized in a collagen-poly(lactic-co-glycolic acid) (PLGA) hybrid scaffold.[55] BMP4 has been shown to induce osteogenic differentiation of osteoblasts promote bone formation.[56] MSCs were loaded into collagen-PLGA scaffolds, with or without BMP-4, and cultured in osteoinductive media prior to implantation into the dorsa of athymic nude mice. Four weeks after implantation, scaffolds were removed and analyzed. Only the scaffold with immobilized BMP-4 showed positive staining of deposited calcium. The expression levels of several osteogenic markers were analyzed by RT-PCR. Type 1 collagen, OPN, and OCN were showed a significant increase in expression as compared to the control. However, there was no difference in ALP expression; however, this may be that ALP expression increased prior to analysis of the removed implants. Another group studied the effect of adding basic fibroblast growth factor bFGF into collagen hydrogels,[57] which has been shown to enhance bone formation in organ culture models.[58] Various amounts of bFGF were incorporated into the hydrogel matrix. Release profiles of bFGF from hydrogels were monitored, and it was found that they could liberate up to 76.3% of the original amount in the hydrogel. Proliferation of MSCs in hydrogels containing a broad range of bFGF concentrations (0, 5, 50, and 500 ng per 500 mL hydrogel sample) was examined. Proliferation peaked at the 5 ng concentration but declined at higher concentrations. This concentration was used for the

remainder of the experiments. At 7 days, there was no difference in ALP expression between the bFGF-containing hydrogels and the control, but at day 14 there was a statistically significant increase. Expression of osteogenesis related genes (type 1 collagen, OPN, BSP, and OCN) was measured at 3 different time points, and the presence of bFGF increased the expression of these markers in at least one of the time points tested. It would be interesting to evaluate if controlling the release of bFGF from low to high could allow for an early low release to increase proliferation and a later high release to induce differentiation. In another study, a collagen-based silicified matrix was loaded with stromal cell-derived factor-1 (SDF-1),[59] which is a chemokine-receptor ligand that is involved in mobilization and homing of stem cells to injured tissues.[60] The silicified collagen scaffold (SCS), was first compared to collagen scaffold (CS) in terms of mechanical properties. The tangent modulus values (KPa) from 0–5% strain were 0.80 ± 0.21 for CS and 599.8 ± 166.0 for SCS. The modulus of resilience values (KPa) were 0.18 ± 0.06 for CS and 165.3 ± 4.0 for SCS. *In vitro* analyses showed there was no difference in cell viability when MSCs or endothelial progenitor cells EPCs were in contact with CS or SCS. The formation of extracellular bone nodules in differentiated MSCs was significantly higher in SCS than in CS, and the formation of capillary-like tubes by EPCs was much higher in SCS than in CS. These results indicate that the presence of silica in collagen hydrogels increases its osteogenic and angiogenic potential. The release kinetics of the SDF-1 from SCS hydrogels was analyzed, and it was found that at high concentrations, up to 80% release could be obtained at 30 days. *In vitro* cell homing experiments were conducted with MSCs and EPCs using a transwell migration assay, using SDF-1 concentrations that corresponded to the ones used in the release assay. Both MSCs and EPCs showed higher migration with higher SDF-1 concentrations. For *in vivo* experiments, the ability to promote osteogenesis was compared between SCS loaded with MSCs (cell-seeding approach) and cell-free SDF-1 containing SCS (cell-homing approach). Scaffolds were implanted into subcutaneous pockets of Balb/c mice. Implants were studied after removal, and it was found that ectopic bone formation was similar in both scaffolds. However, ectopic bone formation in scaffolds loaded with SCF-1 showed a statistically significant increase in capillary formation. The results indicate that cell-homing strategies such as this one *must* be further explored, as it reduces the complications of cell seeding and increases angiogenesis, a requirement for the formation of healthy bone.

4.1.2. Chitosan—Chitosan is an excellent natural polymer to consider as a material for the construction of 3D scaffolds for bone tissue engineering. It is biodegradable, biocompatible, has antibacterial, wound healing, and bioadhesive properties.[61] Here we describe several studies where the osteogenic properties of chitosan 3D scaffolds are modified through the addition of other polymers, cells, and bone-inducing factors.

Chitosan and poly(butylene succinate) (CH-PBS) scaffolds were constructed and seeded with human MSCs in order to test their ability to induce osteogenesis.[62] The material was found to have 59% porosity, 144.9 mm pore size, and 60.9% interconnectivity. MSC viability increased for 21 days in the scaffold, and ALP activity also increased for 21 days after MSCs were exposed to osteogenic induction. The ability of the MSC-seeded scaffolds to repair a cranial critical-sized bone defect in mouse was also examined. The cell-scaffold

constructs were cultured in osteogenic-induced medium for two weeks prior to implantation. Cell-free scaffolds were used as a control. The crania were observed 8 weeks after implantation. Bone formation was analyzed using μCT. The results evidently showed an elevated rate of bone formation in the cell-seeded scaffold, evidencing the importance of the existence of stem cells near the area where bone formation is needed. In another study, human bone marrow-derived stem cells (hBMSC) were encapsulated in hydrogels at chitosan/collagen ratios of 100/0, 65/35, 25/75, and 0/100 wt%.[63] Beta-glycerophosphate (β-GP) was added to hydrogels, as it has been shown to be an osteogenic supplement when added to cultures of hBMSC, and has also been used as a catalyst to sol–gel transitions in chitosan hydrogels.[64] The effect of collagen addition to chitosan on matrix mechanical properties was assessed. Stress-strain profiles (0–8% strain) showed that all collagen materials were approximately 3 times stiffer than pure chitosan, which has a modulus of 6.3 kPa. When evaluating cell proliferation, DNA content dropped by about half over 12 days in pure chitosan materials while it increased twofold in materials containing collagen. For these reasons, only collagen-containing materials were examined as to their effect on osteogenic gene expression. hBM-SCs were encapsulated in chitosan-collagen and collagen hydrogels and exposed to osteogenic medium. Hydrogels with a chitosan/collagen ratio of 65/35 had the highest levels of osterix expression, bone sialoprotein expression, and ALP activity. These osteogenic markers started to decrease at lower chitosan concentrations. These results suggest that the presence of collagen was highly beneficial for the osteogenic capabilities of the 3D scaffold, although it remains to be determined if this was caused by the change in mechanical properties, or the intrinsic biological properties of collagen. In a subsequent study, the authors studied the effect of glyoxal crosslinking on chitosan/collagen hydrogels.[65] Glyoxal was used in order to provide stability to the hydrogels. The effect of crosslinking on gel compaction and stiffness was examined in 50:50 chitosan/collagen hydrogels. Crosslinking caused decreased gel compaction. Rheological measurements indicated a six-fold increase as shown from the storage modulus when gels were crosslinked, but no change in the loss modulus, indicating increased matrix stiffness. DNA content, ALP activity, calcium deposition, and osteogenic gene expression was evaluated for hBMSCs embedded in hydrogels with and without crosslinkers and cultured in osteogenic media. Crosslinking inhibited cell proliferation, and decreased ALP activity at day 9 after induction and had no effect on calcium deposition. Osterix expression was higher in non-crosslinked gels on day 9, but higher on crosslinked gels at day 21. Crosslinking inhibited bone sialoprotein expression at all days tested, but had no effect on the expression of type-1 collagen. These results suggest that the mechanical changes conferred to the hydrogel upon crosslinking are not beneficial to the induction of bone formation. Another group prepared porous 3D-scaffolds based on chitosan (CHI), chitosan/silk fibroin (CHI/SF) and chitosan/silk fibroin/hydroxyapatite (CHI/SF/HA).[66] SF/HA scaffolds has been previously reported to be unsuitable for bone tissue engineering, due to insufficient formability and inflexibility.[67] The characteristics imparted by the nature of the chitosan polymer could improve these characteristics. Porosity of the scaffolds was measured by liquid displacement. The CHI scaffolds have a porosity of $94.2 \pm 0.9\%$, which was statistically higher than the one presented by CHI/SF/HA scaffolds, which had a porosity of $89.7 \pm 2.6\%$. The CHI/SF scaffold had a porosity of $91.6 \pm 1.2\%$, which was not significantly different from other materials. SaOs-2 cells were used to measure viability and

differentiation. At day 21, there was a statistically significant increase in cell proliferation and in ALP activity in the CHI/SF/HA scaffolds as compared to CHI and CHI/SF. It is unclear whether it is the presence of HA or the changes in porosity that help promote osteogenesis.

Chitosan has also been used as an injectable biomaterial. Bi et al.[68] produced an injectable composite of tricalcium phosphate (TCP), chitosan, and platelet rich plasma (PRP).[69] A TCP-chitosan composite (TC) was used as control. PRP contains a number of growth factors (i.e., PGDF, TGF-β, IGF, bFGF, and VEGF), which have often been shown to have an important role in bone tissue engineering applications. The composites were fabricated into cylinders for mechanical testing. It was found that the compressive strength (MPa) of both composites increased over time (~9–16 over 7 days), but there was no difference between them. MSCs were seeded onto TCP and TC scaffolds and cell proliferation was measured over 7 days, showing that the amount of cells on PTC was significantly higher than on TC at every time point tested. MSCs grown in plates in osteogenic media (OM) were used as a positive control for osteo-differentiation analysis of the materials being tested. ALP activity was tested at 7 and 14 days. At 7 days, ALP activity was higher in PTC than TC, and PTC and OM had comparable levels. At day 14, ALP activity was significantly higher in PTC than TC and even OM. RT-PCR analysis was used to study the expression of osteogenesis-related genes. Runx-2, type-1 collagen, and osteonectin expression in TCP was comparable to that in OM. Hardly any expression was observed on TC. TCP and TC materials were tested *in vivo* for their capacity to repair osseous defects in goat tibiae; untreated animals were used as a control. Through radiological examination, it was very evident at 16 weeks that bone had been repaired much more effectively in TCP than in TC. Almost no new bone was formed in the blank group. This work shows a promising system where MSCs do not need to be conditioned in osteogenic medium in order to produce robust bone growth. Another study investigated the use of 3D porous chitosan–alginate (CA) scaffolds for critical size calvarial defect repair in Sprague–Dawley rats.[70] The material had a porosity of 97%, with an average pore size of 100 μM. MSCs grown on the CA scaffolds *in vitro* were able to promote cell attachment. For *in vivo* tests, the CA scaffold was modified either with MSCs, bone marrow aspirate (BM), or BMP-2. An empty defect was used as a control. Through micro-CT analysis, percent defect reduction at 4 and 16 weeks were only significantly higher for CA-BMP-2 scaffolds as compared to controls. At 16 weeks, mineralization was studied by Von Kossa staining, showing a significant increase in mineralization as compared to controls was found for the CA-BM and CA-BMP-2 scaffolds. At 16 weeks, osteocalcin staining showed significantly higher intensity for CA-BMP-2 as compared to control, and OPN staining showed significantly higher expression for CA-BM and CA-BMP-2 as compared to controls. This study, along with many others, suggests that the addition of proteins and other factors tends to improve osteoactivity of most scaffolds.

Another group studied porous chitosan alone and in combination with insulin-like growth factor-1 (IGF-1) and bone morphogenetic protein-2 (BMP-2) for their effectiveness in bone healing.[71] The scaffold had a porosity of 85 ± 2%, with pore sizes between 20–900 μM. Pore size and distribution changed when the scaffold was loaded with growth factors, to 27–350 μm and 35–480 μm for chitosan + IGF-1 and chitosan + BMP-2 samples, respectively.

Materials were tested *in vivo* for the treatment of critical size bone defects. In the control group, the bone defect was treated with bare chitosan scaffold, another group was treated with the chitosan- IGF-1 scaffold, and another group was treated with the chitosan BMP-2 scaffold. Radiographs were taken postoperatively for 15–90 days. The scaffolds with IGF-1 and BMP-2 significantly improved bone formation, but the effect was higher with IGF-1. It remains to be elucidated if these improved outcomes are due to changes in the porosity of the materials or the presence of growth factors.

Chitosan-based scaffolds have also been used to immobilize peptides that can contribute to bone formation. In this study, the addition of the RGD peptide into chitosan/hydroxyapatite scaffolds (C/H) was assessed as a means of promoting osteogenesis by improving cell adhesion onto the scaffold.[72] The porosity of the C/H scaffold was calculated to be 88.4%. Pores had an average width of 400 μM. Porosity was not tested after addition of RGD peptide. C/H scaffolds were loaded with two concentrations of RGD peptide, 50 mg/L and 100 mg/L. All materials were cytocompatible with MSCs. The effect of MSC adhesion onto C/S-RGD versus C/S scaffolds was tested. At higher concentrations of RGD there was a tendency for higher cell adhesion, but results were not statistically significant. The effect of RGD on MSC differentiation was tested by ALP activity. MSCs were cultured in the different scaffolds with osteogenic medium for 14 days. ALP activity was 103.1% higher in C/H-RGD scaffolds versus C/H scaffolds (0.00197 ± 0.00031 U/L/ng vs. 0.00097 ± 0.00025 U/L/ng, respectively). These findings suggest that providing a cell attachment site is highly beneficial to the differentiation process, and is a strategy that should be explored in composites of other materials.

4.1.3. Silk—Silk fibroin is a natural polymer that has also been extensively used for tissue engineering applications.[73] This material has impressive mechanical properties, and has environmental stability, biocompatibility, controlled proteolytic biodegradability, and morphologic flexibility. In one study, CaP/silk powders were incorporated into silk scaffolds to improve porous structure and distribution of CaP powders in the composite scaffolds.[74] The scaffolds tested contained pure silk, or silk with 5% or 10% CaP. The pure silk and silk composite scaffolds were prepared using a freeze-drying method. The addition of CaP did not affect the compressive strength of the material (all tested were ~70 KPa) or the compressive modulus (~250 MPa for all materials tested). All scaffolds tested supported BMSC proliferation to comparable levels. However, ALP activity was significantly higher in CaP/silk scaffolds at days 7 and 14. The expression of the osteogenic markers ALP, type 1 collagen, and osteocalcin was also significantly increased in CaP/scaffolds at day 7 and 14 as compared to pure silk scaffolds. *In vivo* bone formation was assessed in a calvarial defect model by micro-CT. Groups studied were silk scaffold, CaP/scaffold, silk scaffold + MSC, and CaP/scaffold + MSC. Defect areas were collected after 4 weeks. When bone formation was measured, it was clear that the addition of CaP into the scaffold significantly increased bone volume in the area. These results suggest that the presence of CaP in the scaffold was sufficient to enhance osteogenesis, as it did not have any effect on the scaffold's mechanical properties. In another study, different amounts of HA were embedded in silk sponges at volume fractions of 0%, 1.6%, 3.1% and 4.6% to enhance the osteoconductive activity and mechanical properties of the scaffolds.[75] hMSCs were cultured on the scaffolds for up to 10

weeks, when they were subsequently analyzed. At increasing HA concentrations, there was an increase in the scaffold equilibrium compressive Young's modulus. The moduli of scaffolds containing 0%, 1.6%, 3.1%, and 4.6% HA were 121 ± 49, 140 ± 70, 201 ± 90, and 251 ± 117 kPa, respectively, at day 0. By 5 weeks, the moduli of scaffolds containing 0%, 1.6%, 3.1%, and 4.6% HA reached 340 ± 99, 594 ± 234, 865 ± 347, and 1005 ± 381 kPa, respectively. There was no difference in cell proliferation between cells seeded in the various scaffolds. Micro-CT imaging was used to measure bone fracture, fracture volume, connectivity density, trabecular number, and trabecular spacing. Decellularized bovine trabecular bone was used for comparison. It was found that these values of these parameters approached the values for bovine trabecular bone in scaffolds with 3.1% and 4.6% HA. Calcium content was studied in all scaffolds at up to 10 weeks, there was an increase over time but there were no differences between groups. These studies demonstrate a system where even if there is no improvement in cell proliferation or calcium deposition with the addition of HA, the presence of certain amounts of HA can lead to the formation of tissue grafts with excellent enhancement of trabecular structure, increased connectivity and superior mechanical properties. Another group studied silk sponge matrices reinforced with silk microparticles to generate protein–protein composite scaffolds with desirable mechanical properties for *in vitro* osteogenic tissue formation.[76] Three different scaffold compositions were tested: Non-reinforced scaffolds (1:0), scaffolds reinforced with a 1:1 mass ratio of silk in solution to silk microparticles (1:1), and scaffolds reinforced with a 1:3 mass ratio of silk in solution to silk microparticles (1:2). Adding silk microparticles increased the compressive modulus from 0.28 ± 0.13 MPa to 1.03 ± 0.45 and 1.93 ± 0.88 MPa for the 1:1 and 1:2 scaffolds, respectively. The reinforced scaffolds showed an increase in yield stress from 22.6 ± 6.3 kPa to 50.4 ± 28.6 and 154.9 ± 77.5 kPa for the 1:1 and 1:2 scaffolds, respectively. The equilibrium modulus also showed a significant increase: 67.19 ± 36.13 kPa for the untreated scaffold, 320.95 ± 145.09 kPa for the 1:1 scaffold and 981.43 ± 311.92 kPa for the 1:2 scaffold. hMSC cells were seeded into the different scaffolds and cultured in osteogenic medium, and analyzed at 3 and 6 weeks. Analysis of osteogenic markers by RT-PCR revealed that type 1 collagen, ALP, and OPN had a significant increase in expression as compared to control at 6 weeks on the 1:2 scaffold. Bone sialoprotein expression was significantly increased at 6 weeks on both the 1:1 and 1:2 scaffolds. Biochemical analysis of the scaffolds at 3 and 6 weeks revealed that there were no significant differences in ALP activity or soluble collagen levels. However, there was a significant increase in calcium deposition in the 1:1 and 1:2 scaffolds at 6 weeks as compared to the 1:0 scaffold. Micro-CT analysis was done to measure bone volume in the scaffolds after 6 weeks in culture. Bone volume fraction for 1:0, 1:1, and 1:2 was 0.0077, 0.0709, and 0.0667, respectively. These results show that improving the mechanical properties of the scaffolds, even though they did not reach the mechanical properties of trabecular bone, improved almost all osteogenesis parameters tested. In another work, the relationship between scaffold degradability and osteogenesis was examined.[77] 3D porous silk fibroin scaffolds were prepared with two different degradation rates. The water-based scaffold was synthesized as the rapidly degrading scaffold (control), and a slower-degrading scaffold was obtained by the addition of hexafluoroisopropanol (HFIP) to induce insolubility in aqueous media (HFIP scaffold). Degradation studies were done, the control scaffold lost more than 90% of its mass at day 7, and the HFIP scaffold's mass remained nearly the same

at 7 days. Various biochemical assays were performed on both scaffolds after seeding with MSCs and culturing for 16 or 56 days. At 56 days, DNA content in the control scaffolds was around 6-fold lower than for HFIP scaffolds. There was no significant difference in ALP activity between the two scaffolds. However, calcium content/DNA ant total collagen/DNA showed a dramatic increase in the rapidly degrading scaffold when compared to the slowly degrading scaffold. RT-PCR was used to measure the expression of osteogenesis-related genes. There was no significant difference in expression of ALP, BSP, Col1a1, or OP between control and HFIP scaffolds. However at day 56, HIF-1 expression was significantly higher in the control than the HFIP scaffold. Studies in transgenic mice have shown that HIF-1 is a critical component of bone regeneration.[78] Markers of metabolic activity, such as glucose consumption rate and lactate synthesis rate were significantly higher in the slowly degrading scaffold. An understanding of the interplay between cellular metabolism and scaffold degradability should aid in the more rational design of scaffolds for bone regeneration needs both *in vitro* and *in vivo* (Fig. 2).

Another study systematically compared 4 different silk scaffolds as to their architecture and biomechanics to develop a greater understanding of the scaffold characteristics that could best induce bone formation.[79] Factors taken into account were solvent (aqueous vs. HFIP), pore size (250–500 μm vs. 500–1000 μm), and structure (lamellar vs. spherical pores). The resulting scaffolds were Aq-250 with the smaller pore size; Aq-500 with the larger pore size; Aq-Lam with the lamellar-shaped pores, and HFIP with pores ranging from 400–600 μM. These scaffolds were tested as to their bone tissue outcomes and compared to decellularized trabecular bone. In this study, adipose stem cells (ASCs) were used to seed the scaffolds, and cultured in osteogenic medium for up to 14 days. Morphometric parameters of the aqueous based solvents were obtained by micro-CT. Aq-250 scaffolds had a porosity of 86.62%, an interconnectivity of 90.97%, an average pore size of 139.74 μM, and a trabeculae thickness of 59.98 μM. Aq-500 scaffolds had a porosity of 75.95%, an interconnectivity of 97.83%, an average pore size of 254.32 μM, and a trabeculae thickness of 56.51 μM. Aq-Lam scaffolds had a porosity of 64.25%, an interconnectivity of 63.25%, an average pore size of 126.24 μM, and a trabeculae thickness of 63.13 μM. Morphometric parameters were not reported for HFIP scaffolds. Cell seeding efficiency was around 80% for all scaffolds tested, and the Aq-Lam scaffold had the least amount of cells per scaffold. The equilibrium modulus was superior in Aq-Lam and HFIP scaffolds. Calcium change, bone volume and ALP activity were not significantly different in any of the scaffolds tested. Although all materials tested showed similar osteogenic properties, it shows that adipose-derived stem cells are a feasible source of bone progenitor cells. Another study was conducted to evaluate the ability of fibroin scaffolds combined with human stem cells, such as dental pulp stem cells (hDPSCs) and amniotic fluid stem cells (hAFSCs) to repair critical-size cranial bone defects.[80] These scaffolds had an 85% porosity and pore diameters ranging from 10–250 μM, and a compressive modulus of 25.69 ± 1.61 kPa. hDPSCs and hAFSCs were seeded onto the scaffolds and grown in osteogenic media for 10 days before implantation into the cranial critical size defect. Groups tested consisted of scaffolds without cells, scaffold + hDPSCs, scaffold + hAFSCs, and empty defect. Thirty days after surgery, radiograph images showed that scaffolds without cells were able to slightly repair the area, but this effect was more pronounced when either kind of stem cell was present.

Hematoxylin/eosin staining showed that there was vascularization present in all scaffolds tested, however, hASFCs seemed to have a greater potential for bone regeneration because it was the only scaffold tested that showed bone in scaffold areas distant to the dura matter. This study gives additional evidence that silk fibroin scaffolds can be engineered to enhance bone formation, and that stem cells from various sources can be used to optimize bone formation in these scaffolds.

One research group reported the effects of different concentrations of silk fibroin protein on 3D scaffold pore microstructure, and its effects on bone formation when cultured with hBMSCs transfected with BMP-7.[81] Untransfected cells were included in the study as a control. At 1% wt silk protein, scaffolds had a porosity of 94% and a pore size ranging from 250–300 μM. At 2% wt protein, porosity was 87% and pore size from 200–250 μM. At 3.5% wt silk protein, scaffolds had a porosity of 80% and a pore size ranging from 150–200 μM. At 2% wt protein, porosity was 71% and pore size from 80–150 μM. MSCs proliferated on all scaffolds, but at day 14 there was a significant decrease in the 5% scaffold. ALP activity was shown to increase in all groups, but there was significantly higher expression in the 3.5% scaffold. After 2 weeks in osteogenic medium, expression of osteogenic markers in transfected and untransfected MSCs in the various scaffolds was analyzed by RT-PCR. ALP, Col1, and OCN had similar levels of expression in all scaffolds tested when they were transfected with BMP-7, except in the 5% scaffold, where there was a significant decrease in marker expression. MSCs that were not transfected showed similar levels of expression to cells cultured in undifferentiated medium. This study indicates that decreased scaffold porosity is detrimental for the promotion of bone formation, and that the presence of BMP-7 greatly enhances the cells capabilities to express osteogenic phenotypes.

4.1.4. Alginate—Alginate is also an attractive polymer for 3D scaffolds for tissue regeneration. It is soluble in water, and forms a gel at room temperature in the presence of divalent cations, allowing for the formation of 3D gels. In one study, A macroporous alginate scaffold was fabricated and mineral-coated using a biomimetic approach.[82] The nucleation of HA was achieved by incubating the scaffold in modified simulated body fluids for up to four weeks. Mineralization of the scaffold was determined by a change in mass, which increased steadily from weeks 1–4. Energy dispersive X-ray spectroscopy revealed a Ca/P ratio of 1.61, when the Ca/P ratio of pure hydroxyapatite (HAP) is 1.67. Viability experiments demonstrated that the HAP coatings support attachment and proliferation of hMSCs. Cell number was significantly higher in the coated scaffolds at all time-points tested. This work shows that a simple scaffold modification, such as immersion in simulated biological fluids, can change the topography and environment of a scaffold in order to improve the osteogenic outcome of the scaffold. In another study, human umbilical cord mesenchymal stem cells (hUCMSCs) were encapsulated in three types of alginate-based microbeads.[83] The three types of microbeads tested were: alginate microbeads (AM), oxidized alginate microbeads (OAM), and oxidized alginatefibrin microbeads (OAFM). Alginate was oxidized to increase its biodegradability. Fibrin was added to decrease biodegradability. Encapsulated hUCMSCs were grown for up to 21 days. Cells in OAFMs always showed the highest viability at all-time points tested, and cells grown in AM always had the lowest viability at all-time points tested. Although all materials were tested for

viability measurements, only the cells in OAFMs were tested for the expression of osteogenic markers and ALP activity. ALP gene expression peaked at day 7, Runx-2 expression peaked at day 14, and OC and collagen I peaked at day 21, as compared to cells that were not grown in the differentiation media. ALP activity steadily increased over time when cells were grown in the OAFMs. Although this study supports that OAFM is a suitable candidate for bone regeneration, it does not address whether the presence of fibrin, thus degradability of the scaffold, truly has a role in enhancing osteogenesis. In another study, a 3D matrix of calcium phosphate cement (CPC) combined with alginate was tested for potential usefulness for drug delivery and tissue engineering of bone.[84] Fiber diameter decreased as the ratio of CPC powder to alginate liquid increased from 1.5 to 2.0, and the needle gauge increased from 23 to 27 G. This allowed for the formation of low (13.6%), medium (34%) and high (53.7%) porosity scaffolds. MSCs actively populated and permeated into the porous network with time of culture and showed a significantly more favorable proliferation on scaffolds with relatively high porosity levels. ALP activity was also significantly higher in the high porosity scaffolds. An *in vivo* pilot study of the CPC–alginate scaffolds with high porosity was implanted into rat calvarium. Examination after 6 weeks revealed the formation of new bone tissue within the scaffold, closing the defect almost completely. This study illustrates that subtle changes in physical properties, such as porosity, can be adjusted to obtain more satisfactory results.

Alginate scaffolds have also been used in combination with proteins and peptides to enhance osteogenesis. One such study aimed to determine if the delivery of human bone marrow stromal cells (HBMSC) seeded onto VEGF/BMP-2 releasing composite alginate scaffolds could enhance the bone regenerative capability in a critical sized femur defect.[85] Release kinetics were fine-tuned so VEGF would be released rapidly and BMP-2 would have a later release. This was achieved by using alginate fibers as a carrier for VEGF, and PDLLA was used as a carrier for BMP-2. Cumulative release experiments confirmed that VEGF release occurred earlier than BMP-2 release, and it was confirmed that the proteins remained active after release. Prior to implantation, scaffolds were seeded with or without HBMSCs. Three groups were examined: control alginate/PDLLA scaffold group, alginate-$VEGF_{165}$/$P_{DL}LA$-BMP-2 scaffold group, and alginate- VEGF/PDLLA-BMP-2 scaffolds seeded with HBMSC. 28 days after implantation, the bone defect was examined in each of the groups by micro-CT. There was a statistically significant increase in bone volume in alginate-VEGF/PDLLA-BMP-2 and alginate VEGF/PDLLA-BMP-2 + HBMSC scaffolds. There was no difference in bone surface to bone volume and trabeculae thickness between groups tested. Bone volume to total volume and trabecular number was only significantly increased in alginate VEGF/PDLLA-BMP-2 + HBMSC scaffolds. There was a significant decrease in trabecular spacing only in alginate VEGF/PDLLA-BMP-2 + HBMSC scaffolds. These data show that adding cells to alginate VEGF/PDLLA-BMP-2 scaffold resulted in better bone regeneration, but it is not clear if the coordinated release of proteins from the scaffold had any effect on this outcome. Another group also used alginate as a scaffold to induce spatiotemporal release kinetics of growth factors.[86] This was accomplished by encapsulating the bone defect in a nanofiber mesh tube and an RGD-functionalized BMP-containing alginate hydrogel was injected inside the tube (Fig. 3). To test this material, three groups were used in this study. Collagen sponge + 5 μg rhBMP-2 (COL), Alginate plug + 5 μg rhBMP-2

(ALG), and Alginate + Nanofiber mesh tube + 5 μg rhBMP-2 (ALG + MESH). Scaffolds were placed in rat femoral segmental defects and evaluated by micro-CT. Two Volumes of Interest (VOI) were established: Central VOI, which was defined as the cylindrical volume that captured the central defect region, and Total VOI, which included entire volume of mineralization, in and around the defect. At 12 weeks, central bone volume (central and total VOI) was significantly higher in ALG and ALG + MESH groups. Bone Volume Accumulation (central and total VOI) was only significantly higher in the ALG + MESH group. Mean density was significantly lower in the ALG + MESH group, and there was no difference in connectivity density between the groups. The biomechanical properties of the regenerated femurs were measured at 12 weeks. Maximum torque, torsional stiffness, and work to failure were significantly increased only in the ALG + MESH set. There was no difference in failure angle between groups. The collective data from this study suggests constraining bone formation within the defect region, in this case by means of a mesh tube, improves bone formation in rat femoral segmental defects. Another group developed a nanoscale calcium sulfate (nCS)/alginate (nCS/A) injectable paste.[87] The nCS/A ratios tested were 85:15 (nCS/15%A), 90:10 (nCS/10%A), or 95:5 (nCS/5%A). The injectability force (N) and flexural strength (MPa) significantly increased in an alginate concentration-dependent matter. The nCS/10%A paste was chosen for the remaining studies becaused it supported increased cell viability. The paste was loaded with bone morphogenetic protein 2 (*BMP*2) gene-modified rat mesenchymal stem cells (MSCs) and effect on bone and blood vessel growth was studied. The injectable paste was studied in rat critical-sized calvarial defects. Groups tested included: no treatment (blank), nCS/10%A, nCS/10%A + untransfected MSCs (nCS/10%A + M), and nCS/10%A + MSCs transfected with BMP-2 (nCS/10%A + M/B2). 7 weeks after implantation, X-ray was used to measure bone formation. The groups treated with nCS/10%A + M/B2 paste showed a significant increase in bone density and bone area measurement when compared to other groups. Very importantly, the nCS/10%A + M/B2 material significantly enhanced the production of blood vessels. The induction of angiogenesis is a significant accomplishment, as it is a requisite for the formation and maintenance of healthy bone.

One study used alginate-based scaffolds to study the effects of co-culturing osteoblast-related SaOS-2 cells and osteoclast-like RAW 264.7 cells.[88] These cells were embedded into beads composed of a Na-alginate-based hydrogel matrix, with (HG:S) or without (HG) the addition of silica, which was used as an inorganic matrix. The advantage of the co-incubation conditions applied here is that under straightforward conditions soluble mediators released from one cell line can diffuse to a compartmentalized second cell line where they can cause a differential response. The mechanical stability of HG and HG:S was tested. The Martens hardness was of 0.548 ± 0.039 GPa for HG and 0.742 ± 0.027 GPa for HG:S. The reduced elastic modulus was of 20.336 ± 0.812 GPa for HG and 22.826 ± 0.579 GPa for HG:S. The expression of OPG was used as a functional indicator of SaOS-2 cells and TRAP as a functional indicator of RAW 264.7 cells. RANKL was used as a reference gene for SaOs-2 cells and TRAF-4 for RAW 264.7 cells. Cellular viability and gene expression analysis was measured in four groups: SaOs-2: HG, SaOs-2 + RAW: HG, SaOs-2: HG:S, and SaOs-2 + RAW: HG:S. Cellular viability was measured for 48 hours and no changes were observed between groups. Expression of OPG/RANKL was significantly higher in the

two groups that contained silica in the hydrogel, but highest in the SaOs-2 + RAW: HG:S group, demonstrating SaOS-2 functionality. The expression of TRAP/TRAF-4 was significantly lower only in the SaOs-2 + RAW: HG:S group, suggesting that the presence of silica and SaOS-2 cells somehow have a combined suppressive effect on the activity of RAW cells. Although these groups were not tested individually to assess bone formation, these results clearly suggest that there was cross-talk between the osteoblast-and osteoclast-like cell lines.

4.1.5. Hyaluronic Acid—Hyaluronic acid (HAc) has also demonstrated potential as bone scaffold material. It is naturally occurring, hydrophilic, nonimmunogenic, and has also been found in the cytoplasm of osteoprogenitor cells.[89] This natural polymer has been used in combination with other materials, factors, and drugs to enhance its osteogenic potential. In one study, a photo-cured HAc hydrogel containing an osteogenesis-inducing drug, Simvastatin (SIM), was designed.[90] SIM has been found to induce osteodifferentiation of human adipose-derived stromal cells. Hydrogel viscoelastic properties were tuned through 2-aminoethyl methacrylate substitution (HAc-AEMA). Three different HAc-AEMA scaffolds were studied: HAc with 20% (wt/wt) AEMA (HAc-AEMA-20), 30% AEMA (HAc-AEMA-30), and 40% AEMA (HAc-AEMA-40). Rheological measurements showed that the elastic storage of the hydrogel increased with increasing AEMA concentration (from 40–80 Pa). Pore size increased with increasing AEMA concentration, but sizes were not reported. MC3T3 fibroblasts were seeded into the hydrogels to test for cytocompatibility, it was found that the material was cytocompatible and that there were no differences in viability between groups. After SIM was loaded into the hydrogel, release kinetic experiments showed that it could sustain release for up to 14 days. HAc-AEMA-40 hydrogel was chosen for the remaining experiments. Loading of 1 mg SIM into HAc-AEMA-40 significantly increased fibroblast proliferation and mineralization at all time-points tested. The presence of SIM also upregulated the expression of OCN and OPN at all time-points tested. The effectiveness of this system was then tested *in vivo* with and without SIM. Hydrogels were implanted in parietal bone defects in rabbits. Cone beam computed tomography was used to assess healing of the bone defect for up to 9 weeks. Healing was only slightly superior at 9 weeks in the SIM containing hydrogel. These results show that substitution with AEMA can improve viscoelastic properties and the addition of SIM into the hydrogel shows improved osteogenesis *in vitro*, although the results were not as notable *in vivo*. In another study, the ability of a HAc-based, cell-adhesive hydrogel that could direct initial attachment and subsequent differentiation of human MSCs into pre-osteoblasts without osteogenic supplements was assessed.[91] This was accomplished by using a novel HAc hydrogel system, referred to as the doubly crosslinked networks (DXNs), comprised of densely crosslinked HAc hydrogel particles (HGPs) physically embedded in or covalently connected to a loosely crosslinked secondary network that is also HAc-based. A HAc-based hydrogel particle system was produced with (gHGP) or without (bHGP) immobilized gelatin. Gelatin was added to impart cell adhesive properties to the hydrogel. Both gHGPs and bHGPs had an average particle size of 5–6 μM. There was no statistically significant difference in the compression moduli of either HGP (24.6 ± 1.6 kPa and 21.3 ± 0.6 kPa for bHGP and gHGP, respectively). hMSCs were seeded on both hydrogels and cultured for up to 28 days. Cell viability did not change between materials tested. Cells cultured on bHGP

control remained rounded and stationary; however, cells grown on gHGP formed branched intracellular networks and had migrated inside the gel. Histochemical analysis revealed that cells grown on gHGP had osteogenic markers, and cells grown in bHGP had adipogenic markers. These results suggest that osteogenic differentiation without osteogenic supplements was achieved by the ability of gHGP to foster the attachment of MSCs.

HAc scaffolds have also been used to enhance osteogenesis via the delivery of growth factors. In one study, HAc hydrogel scaffold systems with tunable degradation properties were developed for the controlled delivery of osteoinductive and angiogenic growth factors (BMP-2 and VEGF).[92] Hydrogels were designed to degrade at fast, intermediate, and slow rates by varying crosslinking parameters. There was relatively little difference between scaffolds for BMP-2 and VEGF release kinetics. The three hydrogel groups were either loaded or not loaded with BMP-2 and surgically implanted into a rat calvarial defect model, and regeneration was measured for up to six weeks by micro-CT. The presence of BMP-2 had an overwhelming effect on mineralization increase, but there was no difference between low, intermediate, and fast-degrading scaffolds. Co-delivery with VEGF was tested on the fast degrading scaffolds. There was not a significant increase in mineralization when only VEGF was present in the scaffold, but when BMP-2 and VEGF were co-delivered, mineralization was significantly higher than BMP-2 by itself. These data indicate that osteoinductive and angiogenic factors can have a synergistic effect on bone mineralization. In another study, an injectable HAc hydrogel was obtained through aldehyde modification of HAc by the incorporation of an amino-glycerol side chain via amidation reaction and selective oxidation of the pendent group.[93] Controlled release of active bone morphogenetic protein-2 (BMP-2) from the hydrogel was achieved. Human dermal fibroblasts were seeded onto the gels in the presence or absence of rhBMP-2. Viability was measured for up to three days and there were no changes between groups. *In vivo* evaluation of this gel as a BMP-2 carrier was performed by injecting gels over the rat calvarium. Bone formation was measured after 8 weeks by peripheral Quantitative Computerized Tomography and histology. There was a correlation between amount of BMP-2 loaded (0, 5 and 150 μg) within the gel and newly formed bone volume. The 150 μg BMP-2 loaded hydrogel produced significantly higher amounts of bone. In addition, histological examination showed newly formed bone with a high expression of OCN, OPN and with angiogenic bone marrow when higher BMP-2 concentration was employed. This system shows great potential, as it induces high mineralization and induces angiogenesis. Another study also shows the potential of combining a hyaluronic acid based system with the presence of BMP-2.[94] Hyaluronan-based hydrogels formulated to include heparin (Heprasil™) were compared to similar gels without heparin (Glycosil™) for their ability to deliver bioactive BMP-2 *in vitro* and *in vivo*. Heparin has been used for many years to stabilize susceptible growth factors such as BMP-2.[95] An examination of BMP-2 release kinetics from both hydrogels showed that more BMP-2 is retained and less is released in the heparin containing gels. For *in vivo* experiments, the ability of both BMP-2 loaded hydrogels to form bone in a rat ectopic model was assessed. The bone-forming capacity of Glycosil/BMP-2 or Heprasil/ BMP-2 hydrogels were quantitatively assessed by micro-CT bone volume measurements. There was negligible bone formation in the control, Glycosil, or Heprasil hydrogels. However, there was bone formation in both Glycosil/BMP-2 and Heprasil/BMP-2

hydrogels, with approximately a 1.5 fold increase in Glycosil/BMP-2 as compared to Heprasil/BMP-2. Non-Heprasil loaded hydrogels resulted in a more efficacious outcome *in vivo*, emphasizing the therapeutic importance of an increased release of BMP-2.

Another study evaluated whether covalent grafting of an integrin-specific ligand into an HAc hydrogel could improve cell attachment and further enhance the osteogenic potential of rhBMP-2.[96] Hydrazide-thiol HAc (HAc-hy-SH) and aldehyde-derivatized HAc (HAc-al) were prepared from hyaluronic acid. HAc-al and HAc-hy-SH were mixed together at equal ratios to form the hydrogel. A fibronectin (FN) fragment containing an integrin-binding domain of full-length FN was engineered and incorporated into the hydrogel (HAc-FN). The mechanical properties of the hydrogels were analyzed by rheological testing. The elastic moduli for HAc before and after swelling were 2520 ± 30 Pa and 405 ± 78 Pa, respectively. These values for HAc-FN were 2600 ± 30 Pa and 325 ± 31 Pa before and after swelling, respectively. There was no cytotoxicity of either hydrogel towards MSCs after 48 hours of incubation. The percent of adhered cells was statistically higher in HAc-FN than in HAc. For *in vivo* experiments, a rat ectopic bone model was selected. HAc and HAc-FN hydrogels were prepared with or without rhBMP-2, and hydrogels were implanted subcutaneously. After seven weeks, quantitative analysis of the bone volume normalized to the total tissue volume (BV/TV) by micro-CT revealed there was significantly higher for BV/TV in the HA-FN loaded with rhBMP-2 than in the HA hydrogels loaded with rhBMP-2. There was no bone formation in either of the hydrogels in the absence of BMP-2. Histological measurements show the delivery of rhBMP-2 through HA-FN resulted in morphologically more homogenous bone tissue with better organization of collagen fibers. This work suggests that HA hydrogel with an integrin ligand enhances the osteogenic potential of rh-BMP-2.

4.1.6. Peptide Hydrogels—Self-assembling peptide hydrogels are a novel class of materials that are currently being investigated for tissue engineering applications. They can easily be modified to contain bioactive motifs. Their basic units are biocompatible and biodegradable. They are composed of self-complementary amphiphilic peptides, and when gelled they provide a 3D structure that has many similarities to the ECM.[97] In one study, self-assembling peptide nanostructured gels were constructed using peptide amphiphile (PA) materials with or without phosphoserine residues near their surfaces and with or without an RGDS peptide.[98] The phospho-residues contribute to mineralization and the RGDS peptide contributes to cell adhesion. The authors propose that the architecture of these PA materials is highly biomimetic of the fibrous elements commonly found in ECM such as collagen fibrils. The system was tested in a rat femoral critical-size defect. Four types of implants were tested *in vivo*: Phosphorylated Serine (PS), Phosphorylated Serine combined with RGDS (PS-R), Filler with RGDS (F-R), and Serine (S). These were compared to demineralized bone matrix and empty defect as controls. Micro computed tomography was used to quantify new bone formation. Only PS-R gels and PS gels exhibited similar bone volume values as those treated with demineralized bone matrix, which is the current clinical standard. The results of this study suggest that a 3D matrix that supports mineralization and cell-adhesion is favorable for bone formation, but the outcome is not superior to implantation with demineralized bone tissue. In another study, the commercially available

peptidic hydrogel, Puramatrix™, was evaluated as a candidate to assess its potential for osteogenic differentiation of dedifferentiated fat cells (DFATs).[99] Puramatrix™ is composed of 8–16 L-amino acid residues, and forms a 3D scaffold that is biocompatible and biodegradable.[97] In this study, it is denoted as RADA16. DFATs are an attractive alternative to hMSC's as they are derived from subcutaneous fat that can be obtained through minimally invasive procedures. The cell suspension was mixed at a 1:1 ratio with the hydrogel. Cell/hydrogel mixture was placed in either a control medium (CM) or an osteogenic medium (OM). DNA content was significantly higher in the DFATs/RADA16 hydrogels cultured in the OM than in those cultured in the CM on days 7 and 21. DFAT/ hydrogel cultured in OM showed significantly higher osteocalcin content on days 7 and 14 and significantly higher calcium contents on days 7, 14, and 21 than those cultured in CM. However, on quantitative examination, no ALP activity was found in either of the studied conditions. These results indicate that commercially available Puramatrix™ can support the osteogenic differentiation route, and that DFATs are a viable alternative to MSCs that should further be explored in regard to bone regeneration. In another study, varying concentrations of Puramatrix™ were added to the hydrogel to control matrix stiffness.[100] Peptide concentrations varied from 0.15 to 0.5% w/v. As measured by rheometry, material stiffness increased from 120 Pa at 0.15% peptide concentration to 1480 Pa at. 50% concentration. MC3T3-E1 cells were embedded in the different hydrogels. At low peptide concentrations (0.15% peptide), or more compliant gels, cellular network was maintained and became denser. Cell elongation and construct contraction were clearly hindered at higher stiffness values (0.30%, material stiffness 510 Pa), where cells could hardly overcome the matrix resistance. Contraction degree at 4 days cellular seeding was highest at the lower peptide concentration. In addition, inhibiting contraction with a cell contractility inhibitor (Rho kinase inhibitor) abrogated cell elongation, migration, and 3D culture contraction. Osteogenesis was induced by placing encapsulated cells in contact with osteogenic media. The shear modulus for constructs increased from 84 G/Pa 4 days after seeding to 9,445 G/Pa after 30 days. Osteogenic marker expression was examined by RT-PCR at different time points. Cells grown in the 0.15% 3D hydrogel showed an increase in collagen type I, bone sialoprotein, and osteocalcin as compared to cells grown in 2D culture. Interestingly, it was found that even without addition of osteogenic media, cells spontaneously upregulate the expression of the tested bone-related proteins, indicating that the 3D environment enhances their osteogenic potential. However, the addition of dexamethasone was required to acquire a final mature phenotype characterized by features such as matrix mineralization and ALP activity.

Peptide hydrogels composed of Pro–Asp–(Phe–Asp)$_5$–Pro (P$_{FD}$-5), were synthesized as bone regeneration scaffolds in another study.[101] The peptide chosen is based on previous reports that show that peptides that constitute alternating hydrophilic and hydrophobic amino acids tend to form β-sheet structures that spontaneously assemble into hydrogels that mimic ECM.[102] Hydrogels were either loaded or not loaded with TCP. The effect of unloaded hydrogels, TCP loaded hydrogels, or a clinically approved β-TCP ceramic was evaluated for cell proliferation and for bone regeneration in bone defects in rat femora. hFOB cells were seeded on P$_{FD}$-5 hydrogels, β-TCP particulates and β-TCP-loaded P$_{FD}$-5 hydrogels. Cell proliferation was similar in all materials tested, but ALP activity was

significantly increased in hydrogel and TCP-containing hydrogel, with the TCP-containing hydrogel having the most significant increase in ALP activity of all groups tested. The *in vivo* ability of the materials tested to induce bone regeneration was tested in a non-critical sized defect in a rat femur. Regenerated bone was analyzed by micro-CT. Bone volume/total volume (BV/TV) in the volume of interest and trabecular number per millimeter was highest in TCP-loaded hydrogel, followed by the TCP particulates. These results suggest that the TCP mineral and peptide hydrogel act synergistically to enhance bone regeneration.

Another group developed a novel class of amino acid-based poly(ester urea)s (PEU) materials, which are biodegradable *in vivo*.[103] Materials (poly(1-LEU-6) and poly(1-PHE-6)) were covalently crosslinked with 0.5% or 1% osteogenic growth peptide (OGP) and were synthesized as plugs. For poly(1-PHE-6) hydrogels, Young's modulus increased from 3.41 GPa at 0.5% OGP to 4.18 kPa at 1.0% OGP. *In vitro* proliferation assays perfomed in MC3T3-E1 osteoblasts and primary murine fibroblasts gave different results. Osteoblast proliferation increased and fibroblast proliferation decreased in both poly(1-LEU-6) and poly(1-PHE-6) 1% OPG hydrogels, indicating there is a cell-type specific effect. For *in vivo* experiments, incisions were made in the dorsum of rats, approximately 1 cm from the spine where thin plugs of polymers were inserted and skin incisions were closed. Experimental groups were: poly(1-LEU-6), with 0.0, 0.5 or 1% OPG, and poly (1-PHE-6) with 0.0, 0.5 or 1% OPG. Controls were poly lactic acid plugs. After 4 or 12 weeks post-surgical insertion, four animals from each group were euthanized and tissues containing the polymers were collected histologically evaluated. Through histological examination, the materials were found to be generally biocompatible, and crosslinking with OPG improved biodegradability. It would have been interesting to see if these materials could have promoted better bone growth *in vivo* if they had been pre-seeded with osteoprogenitor cells.

4.2. Synthetic Polymers

4.2.1. Polyesters—Aliphatic polyesters such as polyglycolic acid, polylactic acid, and polycaprolactone are the most commonly used polyesters for tissue engineering applications. Their degradation products are present in the human body and can be removed by natural metabolic pathways. 3D scaffolds from these materials can be fabricated through various techniques, and tuning the molar ratios of these polymers can influence mechanical properties and degradation rates.[104,105]

In one study, PCL scaffolds incorporating HA particles were fabricated by combined solvent casting and particulate leaching techniques.[106] The presence of HA slightly increased the density of the scaffold but had no significant effect on the porosity values of the scaffolds. With increasing HA concentrations, there was a significant correlation with an increase in the compressive modulus. Viability assays showed that the number of primary human bone cells that had been cultured on the PCL/HA scaffolds was greater than that of the cells that had been cultured on the neat PCL scaffolds at both 24 and 48 h after cell culturing. Cell proliferation studies showed that the number of primary human bone cells that had been cultured on the PCL/HA scaffolds was greater than that of the cells that had been cultured on the neat PCL scaffolds at both 24 and 48 h after cell culturing. Expression levels of type I collagen and osteocalcin were evaluated by RT-PCR and were significantly greater in cells

cultured on the PCL/HA scaffolds than those in cells cultured on the neat PCL scaffolds on day 10. The formation of mineralized nodules of the cells cultured on the PCL/HA scaffolds was significantly greater than that of the cells cultured on the neat PCL scaffolds. For *in vivo* experiments, a circular calvarial defect in mouse was used as a model. Six weeks post-implantation, histomorphometric analysis indicated a statistically significant increase in the amount of new bone formation in the PCL/HA scaffolding implants as compared to neat PCL counterparts.

In another study, ultrasound was used to prepare compatibilized blends of PCL and poly(diisopropyl fumarate) (PDIPF).[107] The addition of PDIPF to PCL did not significantly affect the resistance of the scaffold as evaluated by the elastic modulus, however, there was a nearly 50% decrease in ultimate tensile stress (7.5 MPa), and 84% decrease in elongation-at-break of compatibilized blend (60%). Biocompatibility of the PCL/PDIPF blend was compared to that of homo-polymeric PCL and PDIPF films with UMR106 and MC3T3E1 osteoblastic cells. Cell adhesion and proliferation was significantly higher on polymer blends than on homopolymers. There was no significant difference in ALP activity between the materials tested. Interestingly, collagen production was higher in MC3T3E1 cells in the copolymer blend but higher in UMR106 cells in the neat PCL scaffold. These results suggest that the changes in mechanical properties imparted by the addition of PDIPF to PCL could have an effect on bone formation, but that this effect is cell type-dependent. In an extension of this work, the PCL–PDIPF composite (Blend) was synthesized with the addition of hydroxyapatite (Blend-HA) to improve osteoconductivity.[108] PCL by itself with or without HAP was tested for comparison. The addition of HA increased the elastic modulus of the Blend from 143 to 182 MPa. The ultimate tensile stress of polymer was not affected by addition of HA. The addition of HA decreased strain at failure from 60 to 20%. UMR106 rat osteosarcoma and MC3T3E1 mouse calvaria cells were used to test material potential for osteoblastic growth and differentiation. Addition of 1% HA in PCL and Blend significantly increased cell proliferation after 24 hours. ALP activity and collagen production was measured in UMR106 cells after 48 hours and MC3T3E1 cells after 2 weeks. ALP activity was only increased in the BLEND-HA composite in UMR106 cells. However, in MC3T3E1 cells that were induced to differentiate in an osteogenic medium for 2 weeks, the presence of HA significantly inhibited ALP expression. In both UMR106 and MC3T3E1 cells, HA increased collagen production only in the Blend material. The expression of the osteogenesis-related transcription factor, Runx-2, was examined by RT-PCR. Addition of HA to PCL and Blend increased Runx-2 expression in both cell lines. These results suggest that the change in mechanical properties and presence of a mineral component can work together to enhance osteogenesis. PCL has also been added to calcium phosphate cement (CPC) in order to improve CPC osteoconductivity *In Vitro* and *In Vivo* Osteoconductivity of Bone Marrow Stromal Cells in Biomimetic Polycaprolactone/Calcium Phosphate Cement Composites.[109] At PCL:CPC mass ratios of 70:30, the composite material was able to promote attachment, proliferation and osteoblastic differentiation of rat BMSCs *in vitro. In vivo*, the ability of the composite to regenerate bone was tested in a critical-sized mandibular rat model. BMSCs were able to attach to the composite, proliferate, and undergo osteogenesis.

The porous scaffolds composed of Poly(L-lactide-co-ε-caprolactone (poly(LLA-co-CL)) and poly(L-lactide-co-1,5-dioxepan-2-one), (poly(LLA-co-DXO)) were evaluated and compared for potential use in bone tissue engineering constructs.[110] Bone marrow stromal cells (BMSCs) were seeded onto the scaffolds and cultured *in vitro* for up to 21 days in osteogenic medium. Wettability of the scaffolds was measured by static-contact-angle measurements. Poly(LLA-co-CL) and poly(LLA-co-DXO) yielded significantly different contact angles of 85° and 75°, respectively. Porosity of both scaffolds used in this experiment was ~90%. Rat BMSCs were used for *in vitro* tests. There was no significant difference in cell proliferation on the two separate scaffold types. Both materials were able to support osteogenic differentiation of BMSCs as evidenced through analysis of a panel of osteogenic markers as measured by RT-PCR, however there were no differences in the level of response between the experimental copolymer scaffolds that were being compared.

Another group investigated a biocompatible dipeptide polyphosphazene-polyester blend (BLEND), which was electrospun to produce fibers in the diameter range of 50–500 nm to emulate dimensions of collagen fibrils present in the natural bone extracellular matrix.[111] Parameters were optimized to control for (a) uniformity, (b) porosity, and (c) mechanical strength. The PPHOS-PLAGA blend was compared to PLAGA for its osteogenic enhancing capabilities. BLEND nanofiber matrices presented a very high porosity of 87.2% as compared to 63.3% for PLAGA matrices. The elastic modulus values were found to be 132 ± 13 MPa and 151 ± 14 MPa for PLAGA and BLEND nanofiber matrices, respectively, and tensile strengths were found to be 1.8 ± 0.7 MPa PLAGA matrices and 1.5 ± 0.4 MPa for BLEND matrices. Nanofiber strips were seeded with primary rat osteoblasts and incubated in mineralized media. Both nanofiber matrices showed incremental and comparable cell growth with culture time suggesting good osteocompatibility. ALP activity of osteoblasts cultured on BLEND nanofibers was significantly higher than on PLAGA nanofibers at day 3, indicative of the early phenotypic expression induced by polyphosphazene component. However, ALP expression on the two matrices was comparable at day 7 as osteoblasts reached confluence. Results indicate that the porosity and mechanical properties of the BLEND composite resulted in an earlier induction of ALP activity, which could be desirable for bone engineering applications. This same group fabricated PLAGA scaffolds with a different technique to create potential osteoinductive scaffolds. PLAGA sintered microsphere scaffolds were developed by sintering together PLAGA microspheres followed by nucleation of minerals in a simulated body fluid.[112] VEGF was incorporated to the PLAGA (as control) and mineralized PLAGA scaffolds via direct adsorption. Mineralized PLAGA scaffolds (a) retained more than double the protein and (b) showed slower release kinetics than unmineralized scaffolds. Compressive properties of the mineralized PLAGA scaffolds were tested over the 10-day mineralization period. The compressive modulus remained around 400 MPa and the compressive strength remained around 15 MPa for the 10 days tested. Scaffolds were seeded with endothelial cells to assess the angiogenic potential of VEGF. Cell proliferation was assessed on

  i.   PLAGA scaffolds,

  ii.   mineralized PLAGA scaffolds,

  iii. VEGF-incorporated PLAGA scaffolds, and

> **iv.** VEGF-incorporated mineralized PLAGA scaffolds.

Cell proliferation was significantly higher when VEGF was incorporated in the mineralized PLAGA scaffolds. The authors propose that the significantly higher metabolic activity observed on VEGF-incorporated mineralized PLAGA scaffolds can be attributed to the combined effect of bioactivity associated mineralized scaffolds and the angiogenic potential of VEGF. However, no markers of osteogenesis were examined.

The scaffolds were produced by means of a rapid prototyping technique (three-dimensional plotting) to avoid the use of organic solvents.[113] Scaffolds were composed of either poly(hydroxymethylglycolide-co-ε-caprolactone) (pHMGCL) or PCL. Porosity of the scaffolds was calculated to be 69.7% and 72.8% for the PCL and pHMGCL scaffolds, respectively. Human MSCs were dynamically seeded onto each scaffold on an orbital shaker. After 11 days of culture, cells had proliferated and filled the pores of the pHMGCL scaffold, but did not fill the pores of the PCL scaffold. Authors attribute this to the higher hydrophilicity of pHMGCL due to the presence of hydroxyl groups. The osteogenic differentiation potential of the human MSCs was investigated in both scaffold types by evaluating the expression of ALP. Although ALP expression was not quantified, fluorescence microscopic examinations indicate that there was higher expression of ALP in the cells in pHMGCL scaffolds. These results indicate that the increased pore size and hydrophilicity of the pHMGCL scaffold makes it better suited than PCL for bone engineering applications.

Another group created 3D PCL scaffolds that were coated with an artificial extracellular matrix composed of collagen with or without either chondroitin sulfate (CS) or a high sulfated hyaluronan derivative (HSH).[114] Non-coated scaffolds were used as a control. Cells were also exposed to pulsed electric fields via transformer-like coupling. Human MSCs were seeded into scaffolds. Cell culture was performed in either expansion or osteogenic media. When grown in expansion or osteogenic media, collagen coating increased cell proliferation when measured at 28 days, but neither CS nor HSH showed an additional effect. However, at 28 days, ALP activity was significantly increased from the rest of the materials only when cells were grown in the PCL-Collagen-HSH material. The same tendency was observed when the cells were grown in both the expansion and osteogenic media, however, ALP activity was much higher in cells grown in osteogenic media. Gene expression analysis of bone related proteins was carried out to assess the effect of that matrix composition on osteogenic differentiation. Runx-2 expression was not altered by the scaffold composition. At 14 days in osteogenic medium, ALP expression was significantly higher in scaffolds with collagen and HSH. Interestingly, there was also a statistically significant difference in ALP expression in cells cultured in expansion media and grown on PCL-Collagen-HSH material. At 14 days, OPN expression was increased only in cells grown in the PCL-Collagen-HSH material. At 28 days, cells grown in materials coated with collagen versus uncoated materials, showed a much greater expression of OPN but the addition of CS either CS or HSH did not produce any effects. OCN expression was increased in respect to PCL controls only in scaffolds with collagen and HSH. Electric stimulation did not affect cell proliferation. However, even though ALP activity did not change with electrical stimulation in cells grown in expansion media, it did increase

significantly when cells were grown in osteogenic media. The highest level of ALP activity was obtained in cells grown in PCL-Collagen-HSH material and exposed to electric fields. RUNX2 expression was not affected by electrical stimuli. ALP, OCN, and OPN activity did however show a synergistic effect when grown in osteogenic media and exposed to electrical stimulus. These results demonstrate that physical factors, such as electrical stimuli, can complement and enhance the properties of 3D scaffolds for applications such as bone engineering.

4.2.2. Copolymers—Copolymers in general are attractive for tissue engineering applications because their physicochemical properties are highly controllable. Gel formation dynamics, crosslinking density, and material mechanical and degradation properties can be controlled by regulating molecular weights, block structures, degradable linkages, and crosslinking modes.[115]

In one study, the authors had previously developed a novel BMP-2 related peptide (P24) that was shown to enhance the osteoblastic differentiation of bone marrow stromal cells. The purpose of this study was to incorporate P24 into a modified PLGA-(PEG-ASP)n copolymer to promote bone formation.[116] PLGA and PLGA-(PEG-ASP)n membranes were fabricated by solvent-coating and evaporating technique. The terminal carboxyl groups of the P24 peptide were activated by NHS and then reacted with the amino groups of the PLGA-(PEG-ASP)n copolymer. The porosity of the scaffolds was over 80%. In *in vitro* release studies, ~70% peptide had been released after 14 days. Adhesion and proliferation studies were performed with BMSCs, and it was found that PLGA-(PEG-ASP)n scaffolds, with and without p24, promoted cell adhesion and proliferation as compared to PLGA control. There was no difference between PLGA-(PEG-ASP)n and PLGA-(PEG-ASP)n-p24 scaffolds in either cell adhesion or proliferation. However, in cell differentiation studies, the PLGA-(PEG-ASP)n-p24 scaffold was shown to enhance differentiation at each time point tested for up to 20 days, as determined by ALP activity. *In vivo* studies were also performed. Subcutaneous pockets were prepared in the back of the animal by blunt dissection. Four weeks after operation, spot-like shadows were observed in PLGA-(PEG-ASP)n-P24 group, and the shadow density was lower than that of normal bone. Block-like shadows were found on the CT image with density identical to that of normal bone 12 weeks after operation. In contrast, no high-density shadows were observed in groups of PLGA-(PEG-ASP)n. Results show that this composite successfully delivered the synthetic peptide, and that incorporation of PEG segments and aspartic acid into PLGA greatly improved its bioactivity. PLGA-based scaffolds have also been used for the controlled release of the osteogenic stimulator, simvastatin.[117] The half-life of simvastatin is approximately two hours, which hinders its ability to promote long-term bone formation. In one study, a PLGA/hydroxyapatite nanofibrous scaffold was designed with the ability to continually release simvastatin for 56 days. *In vitro* tests showed that this material was able to support MC3T3-E1 cell proliferation and ALP activity. *In vivo* studies took place in a rat calvarial defect model. Results showed that the scaffold with simvastatin was more effective at inducing bone formation than the bone scaffold alone.

A novel three-component biomimetic hydrogel composed of triblock PEG–PCL–PEG copolymer (PECE), collagen and nano-hydroxyapatite (*n*-HA) was successfully prepared.[118]

The temperature-sensitive property of the PECE/Collagen/n-HA hydrogel composite was investigated by a test tube-inverting method and rheological analysis. At room temperature, the composite could flow freely, yet it lost its flowability at 37 °C. Rheological measurements showed the composite had low elastic modulus (G') and viscous modulus (G'') while the temperature was less than 30 °C, revealing that composite was a flowable fluid with low viscosity. When the temperature exceeded 30 °C, G' and G'' values increased observably and reached the maximum at about 37 °C, confirming that the PECE/Collagen/n-HA hydrogel composite had thermal sensitivity. *In vivo* biocompatibility of the PECE/Collagen/n-HA hydrogel composite was tested by implanting the composite into the dorsal muscle pouches of Wistar rats for 3, 7, and 14 days. Some inflammation occurred during the degradation process, but by day 14 the inflammatory response disappeared completely. The activity of bone regeneration was evaluated by reconstructing two rectangular defects in rabbit craniums. The untreated left defects were used as control and the right defects were packed with PECE/Collagen/n-HA hydrogel composite. At 20 weeks, as determined by histological staining, the right defect has been filled completely with new bone, and the amount of high-density tissue in the control defect was visibly less than the treatment defect. Although the authors show that the composite is better at regeneration than the self-healing process, they do not address how the individual components of their copolymer contribute to this effect. In another study, copolymer blends of PCL–PEG–PCL (CEC) was synthesized through electrospinning and evaluated for its osteogenic potential in the presence and absence of nanohydroxyapatite (nHAP) (Nanohydroxyapatite Incorporated Electrospun polycaprolactone/Polycaprolactone-Polyethyleneglycol-Polycaprolactone Blend Scaffold for Bone Tissue Engineering Applications.[119] The system was tested with rabbit adipose-derived mesenchymal stem cells (ADMSCs). The presence of nHAP in the scaffold affected the degradation rate of the scaffolds after 90 days, this in turn caused a decrease in tensile strength, from 83% to 75%. In addition, cell viability, proliferation, and ALP activity where all enhanced in osteogenic-induced ADM-SCs grown in the nHAP-containing scaffolds.

The electrospinning was used to fabricate fibrous 3D scaffolds made of a poly(ethylene oxide terephthalate)/poly(butylene terephthalate) copolymer to mimic the physical microenvironment of ECM.[120] Applied radio-frequency oxygen plasma treatment for 5, 10, 15 and 30 minutes was used to create nanoscale roughness. AFM measurements determined an exponential increase of surface roughness with plasma treatment time, for roughness R_a values of less than 10 nm for the 5 minute-treated surface to approximately 25 nm for the 30 minute-treated surface. An increase in hydrophilicity after plasma treatment was observed, which was associated with higher oxygen content in plasma treated scaffolds compared to untreated ones. hMSCs were cultured on untreated, 15 and 30 min treated scaffolds. SEM analysis confirmed cell attachment and a pronounced spindle-like morphology on all scaffolds. No significant differences were observed between different scaffolds regarding the amount of DNA, metabolic activity and ALP activity after 7 days of culture, however, after 21 days, ALP staining of cells on plasma treated meshes appeared more pronounced than on untreated meshes. The expression of osteogenic markers BSP, ON, OC, OP, Col-I and ALP in cells cultured on untreated, 15 and 30 min plasma treated scaffolds in basic medium was assessed using RT-PCR after 7 days of culture. An increase in gene expression of ON and BSP was observed with increasing plasma treatment time and a significant

upregulation was observed in the 30 min-treated scaffolds compared to untreated scaffolds. Surface treatment had no effect on the expression of ALP, Col-I or OC. This study indicates that controlling surface roughness of a scaffold gives a level of control over MSC differentiation.

Another research group synthesized poly(lactide-co-ε-caprolactone) (PLCL) scaffolds that were modified with collagen (Coll) and HA to design a nontoxic scaffold with both composition and microstructure suitable for bone tissue engineering.[121] The porosity of the material obtained was 84.54%, with a density of 0.187 g/cm². The compressive force and Young's modulus of the PLCL and the Coll/HA/PLCL scaffolds was compared. With the added collagen and HA, the compressive force of the Coll/HA/PLCL scaffold was significantly higher compared to that of the PLCL model (from around 25 to 15 kPa), and no reduction of Young's modulus was recorded (around 5 kPa for both scaffolds). After subjecting the scaffold to up to 10 cyclic compressions, its calculated recovery ratio remained constant and was higher than 90% of the initial length. The authors claim the Coll/HA improved recovery ratio but did not compare this to the PLCL scaffold by itself. Saos-2 osteosarcoma cells were seeded onto both scaffolds. Cell growth on the Coll/HA/PLCL scaffold was increased as compared to the PLCL scaffold. RT-PCR was used to assess expression of osteogenic genes at days two and four after seeding. ALP expression significantly increased in the Coll/HA/PLCL scaffold at day 2 compared to that in the PLCL scaffold, but at day 4 there were no differences between the materials tested. Osteocalcin expression showed a greater increase in the Coll/HA/PLCL scaffold than in the PLCL scaffold only on day 4. This scaffold showed promising results, and it should be tested with other types of cells that have not been committed towards the osteogenic route, such as MSCs.

In another study, biodegradable and electroactive poly(ester amide)s containing conjugated segments of amino-capped tetraaniline (PEA-g-TA) was prepared.[122] Composites were prepared under different feed weight percentages of TA (3.5, 8.4, and 15.5%). The copolymer solutions were cast onto a super flat polytetrafluoroethylene plate and placed for 5 h under room temperature to form thin films. Conductivity increased with increasing TA percentage (7.11×10^{-7}, 8.01×10^{-6}, and 2.45×10^{-6} S/cm for 3.5, 8.4, and 15.5%, respectively), but all scaffolds had conductivity values adequate to transfer bioelectrical signals *in vivo*. The PEA-g-TA#2 copolymer (8.4% feeding ratio) was highly distensible with breaking elongation rate of $105 \pm 10\%$, and the tensile modulus of copolymer was 20 ± 2.5 MPa. These values were not reported for the other scaffolds. Mouse MC3T3-E1 cells showed more than 90% viability in all copolymers tested. Cells were stimulated by pulsed electrical signal for two hours every day for 14 days. Osteogenic differentiation of MC3T3-E1 cells was assessed by the intracellular free calcium concentration and ALP enzyme activity. After 14 days, there were no dignificant differences between the materials tested, however, the cells that were stimulated by the electric signal had higher intracellular calcium concentration and ALP enzyme activity. This work illustrates that combining appropriate materials with physical stimulation such as electrical impulses can produce superior responses.

4.3. Ceramic Scaffolds

Over the last four decades, ceramics have been used in medical applications to reconstruct and replace damaged body parts and for skeletal repair. These ceramics are recognized as Bioceramics[123-126] and are classified in two groups: bioinert or bioactive, and bioactive ceramics are categorized as resorbable or non-resorbable.[126]

Ceramics are used due to their chemical properties and similar crystallinity to bone mineral components. These materials exhibit excellent biocompatibility and bioactivity. The inorganic fraction of bone is composed of HA and calcium phosphates, which allow the formation of bone tissue on its surface.[127-130] This type of material is excellent as an implant, but presents particular problems with its mechanical properties in terms of fracture and fatigue.[124] Common ceramic materials used for bone repair or regeneration are Bioglass, calcium phosphates and ceramic scaffold derived from corals. Here, we report some studies where these materials are studied both *in vitro* and *in vivo* to assess their osteogenic potential.

4.3.1. Bioglass—Since 45S5 bioactive glasses were discovered by Hench in 1969, they have been used for interface bonding of implant and tissue repair and regeneration of bone.[131] The necessity of finding a material that forms a living bond with tissues led Hench to develop Bioglass repair tissues during the Vietnam War.[126,131] Bioglass offers advantages such as control of rate of degradation, excellent osteoconductivity, bioactivity, and capacity to deliver cells,[132] but they present limitations in certain mechanical properties such as low strength, toughness, and reliability.[130, 132]

Wu et al.[133] prepared 45S5 Bioglass® by foaming with rice husks and sintering at high temperature, obtaining favorable results in compressive testing and degradability in simulated body fluid (SBF). This study reported compressive strength values in the ranges of trabecular bone. Porous bioactive glass-ceramic (45S5) was tested with human umbilical vein endothelial cells (HUVECs) and human osteoblast-like cell (HOBs).[134] The results of this study demonstrated that the proliferation of HOB and HUVEC co-cultures seeded on scaffolds was higher than commercial HA scaffolds.

Wu and coworkers[135] studied HOB attachment, proliferation and differentiation on bioactive diopside scaffold ($CaMgSi_2O_6$). Cell proliferation increased with incubation time. In addition, porous $CaSiO_3$ and akermanite ($Ca_2MgSi_2O_7$) ceramic scaffolds were compared to β-TCP ceramic scaffolds, demonstrating *in vivo* bone formation and potential applications in bone tissue regeneration.[136, 137] Other studies related to the formation of porous bioglass were developed by Moawad et al.[138] They fabricated nano-macroporous soda lime phosphosilicate glass scaffolds using sucrose as a macropore former, and established process parameters such as weight ratio of glass/sucrose, particle size of glass/sucrose powders, and time/temperature of sucrose dissolution.

Studies have demonstrated improvement of osteoblastic function on nanophase ceramics.[139] Nazhat and coworkers[140] demonstrated an increase in scaffold stiffness and osteoblastic function regulation by accelerating mineralization of dense collagen-nano bioactive glass hybrid gel (DC-nBG). Results indicated high surface area and reactivity of nBG-induced

calcium phosphate formation, which was detected within processed DC-nGB hybrid gel scaffolds.

Amorphous bioactive glass may be crystallized under higher temperatures. Chang and coworkers[141] fabricated a novel SiO_2–CaO–MgO–P_2O_5 bioactive glass (BG20), reporting an advanced technique based on heat-treating to create BG20 powders with different crystallization structures. *In vitro* studies showed cell proliferation using mouse fibroblast (NIH3T3) and BMSCs. Moreover, RT-PCR on two representative marker genes demonstrated early osteogenesis and endochondral ossification fate of BMSCs. Bhakta et al.[142] studied the osteoconductive activity of modified potassium fluorrichterite glass-ceramics by immersion in simulated body fluid but the phase transition of glass during heat treatment was not reported.

A comparative study of the optimization of composition, structure and mechanical strength between Bioglass and Bioglass-CEL2 was reported by Baino et al.[143] In this study, the scaffolds were mechanically tested and studied *in vitro*. Bioglass-CEL2 exhibited mechanical strength twice that of Bioglass, and a 7 day soak in SBF demonstrated the excellent bioactivity of all produced scaffolds. Rahaman and coworkers[144] used Bioactive glass (13–93) scaffolds fabricated by robotic deposition for structural bone repair. Compression tests were performed *in vitro* in SBF and implanted in a rat subcutaneous model. The results showed a more rapid degradation as a result of faster conversion to HA. SEM image of this material is shown in Figure 4. Recent studies have shown that silicate 13–93 and 6P53B glass scaffolds fabricated by robo-casting have compressive strengths comparable to those of human cortical bone.[145,146] Studies using bioactive glass scaffolds are summarized in the Table II.

4.3.2. Calcium Phosphate—Calcium phosphates appears in the scientific literature as a materials for bone defect repair in the form of TCP, ceramic HA granules, and self-hardening calcium phosphate cements (CPC).[147] Tricalcium phosphate was first used in 1920 by Albee and Morrinson.[148] The study reported cases of fracture with bone loss where more rapid bone growth and union was observed when TCP was injected into the gap between the bone ends than did the controls without its use. Also, it was demonstrated that osteogenesis was stimulated by this material in conjunction with the fracture microenvironment. In 1951, Ray and Ward[149] reported the use of granular synthetic HA to repair defects in long bone and iliac wings of dogs and bur holes in the crania of cats, demonstrating that this material could be replaced by new bone, but they were not as effective as autologous bone grafts in repairing the defects.[147] In 1986, Brown and Chow[150] developed a CPC composed of a mixture of tetracalcium phosphate (TECP) [$Ca_4(PO_4)_2O$] and dicalcium phosphate anhydrous (DCPA) ($CaHPO_4$). Such materials formed a paste of HA ($Ca_{10}(PO_4)_6(OH)_2$) as a final product when mixed with aqueous liquid.[151] Calcium phosphate-based scaffolds exhibit osteoconductivity, bioactivity and resorbability *in vivo* due to their complex chemical composition (Ca/P ratio) and physical properties such as crystallographic structure and porosity.[152]

In studies combining calcium phosphate cement (CPC) paste with hydrogel microbeads to encapsulate human umbilical cord MSCs (*h*UCMSCs)[153] with chitosan fibers[154] *h*UCMSCs

viability and differentiation capacity was observed. Lopez-Lacomba and coworkers[155] evaluated the biological properties of Solid Free Form Designed Ceramic (SFF) scaffolds combined with an osteoinductive growth factor (i.e., BMP-2) using the mouse myoblastic cell line C2C12 *in vitro* and pig maxillary defect *in vivo*. *In vitro* results showed that these scaffolds are adequate for cell attachment, proliferation and colonization. The *in vivo* studies showed bone formation in control scaffolds, and thtat muscle tissue and fibrous tissue were stimulated by the BMP-2. Figure 5 shows images of the implantation of the SFF scaffolds in rabbit bone.

The use of ceramic scaffolds with integrated magnetic nanoparticles have been shown to stimulate bone growth. Panseri et al.[156] developed a novel porous ceramic composite made of HA with incorporated magnetite at three different compositions. Human osteoblast-like cells and an *in vivo* bone defect were used for this study. Results indicated an overall increase in cell proliferation and a good level of histocompatibility. No alterations on cellular ALP activity by the applied magnetic field were observed.

An important aspect in the design of calcium phosphate scaffolds is the geometry of their porous structure, which encourages bone formation and facilitates mass transfer into pore networks. Teraoka et al.[157] evaluated the osteogenic influences of mosaic-like ceramics fabrication products (MLPC) composed of HA units on the differentiation of rat bone-marrow-derived MSCs *in vitro* and *in vivo*. In this study, two types of assembly of the MLPC led to different pore size and diameter in the scaffold. High ALP activity was observed in the BMSCs/MLPC scaffold, and new bone formation was indicated by osteocalcin secretions of BMSCs on MLPC-HA scaffold.

Spark plasma sintering method (SPS)[158] and selective laser synthering (SLS)[159] are some of the techniques used to fabricate β-TCP scaffolds. The biological properties of scaffolds prepared by SLS have been evaluated in *in vitro* experiments, where a crystalline mineral layer of carbonate apatite phase was obtained with a gradual increase of immersion times in SBF.

Studies have demonstrated that HA/β-TCP ratio is a key parameter in controlling scaffold performance for bone repair applications.[160] A combination of different HA/β-TCP compositions for ceramic scaffold by robo-casting was studied by Houmard et al.[161] The results indicate that at similar volume porosity, the mechanical strength of the sintered scaffolds increased with decreasing rod diameter. Increasing surface area of the scaffolds allows cells to obtain higher surface reactivity, which in turn influences their proliferation and osteogenic differentiation. Oreffo and coworkers[162] studied the effect of porosity of a HA/β-TCP ceramic scaffold with two types of pore sizes on skeletal stem cell growth. *In vitro* and *in vivo* analysis confirmed cell viability, proliferation and differentiation capacity in both systems. Recently, a Comparative Study of Bone Formation Following Grafting with Different Ratios of Particle Dentin and Tricalcium Phosphate Combinations was elaborated by Seung-Chan Jin.[163] This study evaluated the bone regeneration using the rabbit cranium defect model showing new bone formation.

It is known that ceramic scaffolds are only osteoconductive, which limit their clinical use. However, the combination of calcium aluminate with osteoinductive materials such as melatonin and platelet-rich plasma was used by Clafshenkel et al.[164] to form a bone filler substitute with regenerating properties similar to that of natural bone. *In vitro* results showed adhesion, viability, and proliferation of normal human osteoblasts cells but not that of NIH3T3 fibroblasts. *In vivo* studies in critical size calvarial defects in rats indicated that the scaffold was biocompatible, biodegradable, osteoconductive and osteoinductive. In addition, other biomolecules such as bioactive peptides have been attached to this type of scaffold using bifunctional organic molecules as linkers.[165]

Bioactive glass has a high negative-surface charge density by silanols, which promote the adsorption of serum proteins; therefore, a bioglass-calcium phosphate composite could be a candidate ceramic scaffold biomaterial. Wu and coworkers[166] designed a novel injectable calcium phosphate cement-bioactive glass (CPC-BG) composite for bone regeneration. *In vitro* studies reported cell differentiation evaluated by ALP activity of rat osteoblast cultured on CPC-BG; while *in vivo* studies showed biocompatibility, biodegradability and osteogenesis. A summary of studies using calcium phosphate scaffolds is shown in Table III.

4.3.3. Coral—Corals are attractive materials for scaffolds because they present microstructures with highly controlled pore sizes and an interconnected porous architecture similar to trabecular bone.[123,167,168] In the mid-1970s, natural coral exoskeleton was introduced as a bone-graft substitute and used clinically to treat a variety of orthopedic and craniofacial bone defects.[168-170] After 1991, Ripamonti reported the first study of the morphogenesis of bone in porous bioceramics (coral-derived HA) in the rectus abdominis muscle of adult non-human primates *Papio ursinus*, demonstrating the use of coralline replicas of hydroxyapatite with an average pore size of 600 μm as bone grafts for the controlled formation of bone in humans.[171]

Coral scaffolds using adipose derived MSCs (AMSCs) have been used to repair cranial bone defects in a canine model,[172] showing adipogenic differentiation and good biocompatibility to support the proliferation of AMSCs *in vitro*; Subsequent implantation *in vivo* showed new bone formation. Certain types of proteins such as ALP, OPN, and OCN are employed to identify the activity of osteoblast-specific proteins. Suzina and coworkers[173] reported an increase in expression of specific genetic markers from osteoblasts such as Runx-2, OPN, ALP and OCN in the *Porites sp* coral.nx-*Goniopora* coral which was implanted in orthotropic calvarial defects of the adult non-human primate *P. ursinus*.[174] *In vivo* results showed an increase in ALP activity from 2 to 12 months and induction of bone in the concavities; however, limited conversion of HA/calcium carbonate (HA/CC) was observed. In contrast, it was reported in previous studies that there was partial HA/CC conversion, but that the system did not promote bone formation by induction.[175]

A great challenge for scaffold design is the enhancement of vascularization. A preliminary study in nude mice reported the vascularization of tubular coral scaffold with cell sheets.[176] In this study, cells promoted new bone formation through an endocrine process. In addition, Xiao and coworkers[177] observed an organized vascular pedicle of saphenous arteriovenous network in fibular defects of beagle dogs using an MSC-coral-HA scaffold (Fig. 6).

Zheng et al.[178] evaluated the feasibility of mandibular condyle constructs engineered from human BMSCs. *In vitro* studies reported that human BMSCs induced differentiation into osteoblasts and chondroblasts, and seeded scaffolds implanted into nude mice showed neovascularization in the temporomandibular joint (TMJ) detected by bFGF expression. Natural coral scaffolds (*Porites Lutea*) also promoted the differentiation of human MSCs into osteoblasts when they were grown in osteogenic medium and enriched with FGF9 and vitamin D2.[179]

Recently, the osteogenic potential of MSCs seeded onto granules of *Acropora* coral scaffold in sheep was evaluated; adhesion and proliferation of MSCs was observed *in vitro*, and increased bone formation was observed *in vivo*.[180] Recently, Cui and coworkers[181] demonstrated that allogeneic osteo-differentiated ASCs combined with coral scaffolds could regenerate bone in a canine cranial CSD model. A summary of studies using natural coral scaffolds are shown in Table IV.

4.4. Metallic Scaffolds

In 1909, the first patent of a metallic framework for an artificial tooth root for fixation by bone ingrowth was accredit to Greenfield.[182-184] He recognized the limitations of natural tooth implantation and started experimenting with the implantation of artificial hollow-cylinders made of iridoplatinum wire soldered with 24 kt gold.[183] Later in 1971, Galante and coworkers[185] were pioneers in developing open-pore fiber metals for clinical use as porous coatings in hip and knee arthroplasty.

Since metals are materials with high mechanical strength and fracture toughness, they are frequently used as metallic biomaterials in the dental and orthopedic fields to replace and offer support for damaged and healing bone.[186,187] The most common metals used as standard surgical implants are stainless steel 316 L (ASTM F138), Co-based alloys (mainly ASTM F75, and ASTM F799) and titanium alloys; where Ti-6Al-4V (ASTM F67 and F136).[186-188] However, these metallic biomaterials present disadvantages such as the possible release of toxic metallic ions and/or particles through corrosion or wear processes that cause inflammation and allergic reactions, affecting biocompatibility and tissue loss. Also, they produce poor stimulation of new bone growth due to the elastic moduli, which does not correspond with natural bone tissue.[186,187] Despite this, it has been reported that Ti-based metals can be used as bone substitute due to its elasticity, mechanical properties, shape memory effect, porous structure and biocompatibility.[189,190] Also, 3D microporous NiTi and Ti scaffolds have been produced by powder metallurgy obtaining a hydrophilic surface to facilitate the deposition of HA and stimulate cell attachment and proliferation.[190] Osteoconductive properties and biological performance of Ti and TiO_2 scaffolds have been investigated[191, 192] in rabbit tibia peri-implant osseous defects and rabbit peri-implant defects, showing osteoconductivity and osseointegration.[69, 70] The fixation of porous Ti implants in rabbits is shown in Figure 7.

It is known that applied electromagnetic fields can stimulate osteogenic cell function.[193] Fassina et al.[194] modified the surface of titanium fiber-mesh with calcified extracellular matrix to electromagnetically stimulate Saos-2 human osteosarcoma cells. Electromagnetic stimulation (magnetic field intensity, 2 mT; frequency, 75 Hz) produced higher cell

proliferation and differentiation revealed by RT-PCR analysis of transcripts specific for decorin, OPN, and type-I collagen. Coating metallic bone-ingrowth scaffolds with silica glass layers enables release of proteins and drugs into body fluid.[195] Researchers incorporated soybean trypsin inhibitor (STI) into porous Ti scaffold by means of sol gel silica demonstrating that biochemical activity of the STI protein was not affected by encapsulation procedure.

In order to promote fibroblast and osteoblast cell adhesion on the scaffold surface, researchers have fabricated ceramic TiO_2 scaffolds[196, 197] from cleaned Kronos TiO_2 raw powder with excellent mechanical strength. Also, Ti6Ta4Sn scaffolds have been studied by Li et al.[198] In this study, the cell adhesion density was directly proportional to pore sizes in the range of 25–75%, but was inversely proportional in the range of 75–900 μm. Surface modification by different treatments enhanced osteoblast-like cell adhesion.

Recently, W4-Mg alloys[199] and Fe-Mn alloys[200] have been used to fabricate metallic scaffolds. Witte and coworkers developed a cytocompatible and biocompatible, degradable, open-pore, mechanically adaptable metal scaffold fabricated of magnesium alloy W4 melt-extracted short fibers. Mechanical studies showed highest values for compression strength and Young's modulus when testing perpendicular to the fiber deposition direction. *In vitro* studies reported viability and proliferation under certain conditions, bone formation, and biocompatibility *in vivo*. In earlier studies[201] using Mg scaffolds, a negative salt-pattern molding process was found to not be suitable for implant production. Also, MC3T3-E1 pre-osteoblast cells seeded on iron-manganese scaffold reported *in vitro* cytocompatibility, cell viability, and good tensile mechanical properties. Studies using metallic scaffolds are summarized in Table V.

4.5. Composites

Composite scaffolds have been developed to obtain a material with different functionalities such as surface reactivity, bioactivity, mechanical strength, and capable of drug or growth factor delivery. They take advantage of the properties of different materials in order to obtain a synergistic effect in their resulting properties.[202, 203] In 1963, Smith and coworkers[204, 205] developed a ceramic-plastic composite known as Cerosium®, which was used for mandibular prostheses. It is as strong as bone and has the same modulus of elasticity and is composed of a mixture of alumina, silica, calcium carbonate, and magnesium carbonate built with 18 to 25 p open-cell pores impregnated with a diepoxide 0 type epoxy resin.[205]

Commonly, composite scaffolds are fabricated using a different type of matrix with a dispersed phase such as polymer/ceramics, ceramic/metals and polymer/metals.[203]

4.5.1. Polymer/Ceramics—In the last five years, polymer/ceramic based scaffolds have been studied by many researchers. Combinations of calcium phosphate/polyesters for scaffold production has been investigated by Kaplan and coworkers,[206] who developed a scaffold from silk fibroin-polyaspartic acid coated with calcium phosphate. *In vitro* studies showed cell-viability, proliferation and osteogenic differentiation; however, non-uniform distribution of cells due to mineral deposition was observed. Li et al.[207] used two

biocompatible and biodegradable polymers, PLGA and PCL, with a layer of calcium phosphate and a gelatin coating. MC3T3 cells adhered to regions with higher calcium phosphate content along the scaffold, which indicate that the mineralization gradient affects the adhesion/proliferation of cells and physical properties of the scaffold. With relation to the mechanical properties, the local strain varied along the long axis of the scaffold and the Young's modulus increased with increasing levels of calcium phosphate.

Habibovic and coworkers[208] developed a scaffold for bone using a polyester block copolymer (PEO-PBT) with a calcium phosphate layer. Cell attachment, osteogenic differentiation, and bioactivity of the scaffold were evaluated both *in vitro* and *in vivo*. hMSCs were isolated and shown to proliferate for several days. Osteogenic differentiation and new bone formation was observed in the scaffold; however, mechanical properties were poor, which suggest that the scaffold should be reinforced, such as a combination of 3D printing with electrospinning.[209]

A biodegradable membrane system-based nano-apatite (*n*Ap) and PCL for guided tissue or bone regeneration was reported by Jansen and coworkers.[210] In this study the mechanical properties, cell proliferation and differentiation analysis using Rat bone marrow (RBM) cell culture was evaluated. The material showed a proportional increase of stress and strain, but as strain increased, the curve deviated from the line proportionally. Also, the tensile modulus, yield strain, and energy per volume of the membrane increased with the addition of *n*Ap. *In vitro* studies showed that the membranes enhanced bioactivity supporting osteoblast-like cell proliferation and that the presence of *n*Ap provided early cell differentiation.

TCP has been used to generate biocompatible and biomechanical scaffolds[211] *in vivo* studies using this type of scaffold reported significant biocompatibility, sufficient mechanical strength; osteogenic differentiation, and bone growth (Fig. 8). It has also been demonstrated that the incorporation of collagen into this type of system improves hydrophobicity and differentiation capacity.[212, 213] Wang et al.[214] reported a novel scaffold composed of PLGA/β-TCP skeleton wrapped with type I collagen. The aim of this study was to analyze the physical properties and the biocompatibility of the core-sheath structure composite scaffold *in vitro*, in comparison to the PLGA/β-TCP skeleton. No differences were observed in the porosity ratio, compressive strength, or the Young's modulus of the scaffolds. MTT analyses indicated that BMSCs showed better adhesion and proliferation activity on the surface of the core-sheath structure composite scaffold than on the PLGA/β-TCP skeleton. In a previous study,[215] this scaffold was fabricated via low temperature deposition manufacturing (LDM), but its hydrophobicity did not promote adequate cell adhesion, proliferation, and osteoblastic differentiation.

Xu and Thein-Han[216] developed for the first time a novel scaffold from collagen-CPC, using *h*UCMSCs for *in vitro* analysis. Good mechanical properties, *h*UCMSC attachment, viability and osteogenic differentiation were observed. Previously, studies were made using collagen-calcium phosphate (collagen-CP) scaffolds but they were not moldable or injectable.[217, 218] HA has also been employed to fabricate ceramic/polymer scaffolds.[117, 119, 219-221] Kim et al.[222] and Reza Foroughi and coworkers[97] developed this type of scaffold demonstrating

that the combination of PGA-PLGA-HA improves their osteogenic capacity.[223] Hollinger and coworkers used a combination of PCLF-PVA-HA with rhBMP-2 and the pre-osteoblast cell line MC3T3-E1 obtaining good cell viability and proliferation, bioactivity, bone regeneration and an increase in compressive modulus with an increase in HA; however, micro-CT showed a non-uniform distribution of the porogen indicating that the degradation process, porosity and pore interconnectivity needed to be improved. Reza Foroughi and coworkers also fabricated and evaluated a porous composite from nHA, porous HA and poly-3-hydroxybutyrate (P_3HB). In this work, ceramic scaffolds with different porosities and P_3HB coating were synthesized to improve mechanical properties. The results showed significantly cell viability and bone formation. In a previous study, Yang and coworkers,[224] used a nHA-coated chitosan scaffold to test the *in vitro* viability and differentiation of periodontal ligament stem cells (PDLSCs). Matsumoto and coworkers[225] reported studies using ZrO_2/HA composite scaffolds, where *in vitro* results showed that cell adhesion and proliferation in the ZrO_2/HA scaffold substantially improved when compared to the scaffold made with ZrO_2 alone. Studies *in vivo* showed that BMSCs-loaded ZrO_2/HA scaffold provided a suitable 3D environment for BMSC survival and enhanced bone regeneration around the implanted material. Mechanical properties of this material reported that the porosity and the compressive strength of a ZrO_2/HA scaffold increased when the ZrO_2 content increased from 50 to 100 wt%. The problem presented in this study was fragility, which limits its clinical application especially for large bone defects.

Another type of ceramic used for elaboration of ceramic/polymer scaffolds is bioactive glass. Osyczka and coworker[226] developed a 3D scaffold from PLGA combined with bioactive glass from Silica (S2) and Calcium (A2). The results obtained in this study showed good mechanical properties for both bioglass types, but better bioactivity and osteoblast differentiation on A2 bioactive glass, as determined by higher levels of OPN expression. Studies have indicated that the incorporation of bioglass into PCL scaffolds improves their hydrophilicity and bioactivity.[227] Ngothai and coworker[228] fabricated a scaffold from magnesium phosphate (MP)/PCL composite where mechanical analysis showed low values of compressive modulus compared to trabecular bone; thus, this scaffold was found not to be appropriate for high-load-bearing applications. It was also reported that the degradation rate of the composite scaffolds could be modulated by varying the amount of MP particles introduced into the polymer matrix.

Others studies have demonstrated the use of α and β-Chitin hydrogel/nanobiactive glass ceramic/nanosilver composite scaffold for periodontal regeneration and antibacterial activity.[229] This composite scaffold showed characteristics such as antibacterial activity, bioactivity and controlled degradation. Also observed were cell attachment and cell proliferation.

Studies using polymer/ceramic scaffolds are summarized in Table VI.

4.5.2. Metal/Ceramic—Over the past five years, many studies have reported the development of metal/ceramic scaffolds, which have been shown to possess favorable characteristics, regarding mechanical properties and bioactivity (cell attachment, proliferation, and differentiation). Yang and coworkers[230] developed a biodegradable and

bioactive scaffold composed of magnesium with a coating of β-TCP. Mechanical testing reported deformation was similar for different porosities and that a decrease in strength corresponded to an increase in porosity. *In vitro* results showed good cell adhesion and bioactivity. In similar studies, when tantalum and titanium were used as metals, osteoconductivity and osteinductivity was improved *in vivo*.[231]

Hypoxia promotes the expression of a number of genes associated with bone tissue regeneration and skeletal tissue development, and therefore plays an essential role during angiogenesis, osteogenesis and the differentiation process.[232-234] Wu et al.[234] reported the fabrication of a hypoxia-mimicking MBG (mesoporous bioactive glass) scaffolds by incorporating Co^{2+} ions into the MBG scaffold. Results showed that MBG scaffolds had no significant cytotoxicity and that the incorporation of ionic Co^{2+} ions enhanced VEGF secretion, HIF-1a expression, and bone-related gene expression in BMSCs. Also, the Co-MBG scaffolds supported BMSC attachment and proliferation.

It has been reported that ZrO_2 itself does not have good cellular and tissue affinity[235] although, *in vitro* and *in vivo* studies have demonstrated that ZrO_2 is not toxic.[236] Lee and coworkers[237] fabricated a scaffold composed of (biphasic calcium phosphate) ZrO_2 and PCL layers. The scaffold presented a compressive strength of 12.7 MPa and a porosity of 78 vol%, and showed excellent MG63 cell attachment, and OCN and collagen expression. It was also shown that PCL incorporated into BCP gave scaffolds high biodegradability, cell attachment and proliferation.

Some *in vivo* studies have demonstrated copper release decreases the risk of ischemia and promotes vascularization around a cross-linked hyaluronic acid hydrogel,[238] promoting angiogenic potential.[202] Boccaccini and coworkers[202] synthesized and characterized a new boron-containing bioactive glass-based scaffold coated with alginate cross-linked with copper ions. Compressive strength of the alginate-coated scaffolds was found to be higher than that of the uncoated scaffold. The coated scaffolds exhibited bioactivity comparable to the uncoated one. The development of strontium-substituted calcium polyphosphate (SCPP) scaffolds was reported by Gu et al.[239] where a murine monocyte/macrophage cell line and osteoclasts were co-cultured on calcium polyphosphate (CPP) and SCPP scaffolds. Proliferation of macrophages seeded on SCPP and CPP scaffolds was observed. It was also demonstrated that the substitution of Sr for calcium in CPP could reduce osteoclast activity in cultures.

Studies have reported the use of alkali metal and strontium ion co-substituted in ceramic scaffolds.[240] Li and coworkers[241] reported a novel ion doping method applied in CPP-based bioceramic scaffolds to be substituted by potassium and strontium ions (K/Sr). The K/Sr-CPP scaffolds, which showed a higher compressive strength, cell biocompatibility, biodegradability, osteoinductivity and osteoconductivity and better degradation properties than the pure CPP scaffolds; however, the mechanical strength of K/Sr–CPP was not very good after degradation.

Studies have suggested that direct mixing Cu^{2+} ions with bioactive materials improve angiogenesis.[242] Xiao and coworkers[243] prepared copper (Cu)-containing mesoporous

bioactive glass (Cu-MBG) scaffolds with interconnected large pores. Attachment, proliferation, and ALP activity of hBMSCs on Cu-MBG scaffolds was observed, and ionic products of Cu-MBG extracts enhanced the osteogenic differentiation of hBMSCs.

Recent studies using porous ceramic coated TiO_2 as scaffolds have been reported by Dimitriesvska et al.[244] In this study, adhesion, growth and osteoblastic differentiation of hMSCs in the TiO_2-HA nanocomposite were evaluated; however, applications in bone implants are limited by their bioinertness. Also, Haugen et al.[191] reported *in vitro* results that showed cell viability of the mouse osteoblastic cell line MC3T3-E1, no cytotoxic effects from the TiO_2-HA scaffolds were found. It was also reported that healing occurred when this scaffold was implanted into rabbit defects. Gomez-Florit et al.[197] investigated the distribution, growth and differentiation of MC3T3-E1 osteblast over time using a 3D porous TiO_2 scaffold. The results showed good proliferation, cell adhesion (fibronectin and integrins), and osteoblast differentiation. In another studies,[245] MnO_2 substituted 45S5 bioactive-glasses were obtained by controlled crystallization of bioactive glasses and were analyzed *in vitro* bioactivity in SBF for different periods. Results obtained reported that crystallization process decreases the vitrobioactivity. Studies using metal/ceramic scaffolds are summarized in Table VII.

4.5.3. Metal/Polymers—Chemical and physical properties play a crucial role in the osteointegration of implant surface, allowing protein adsorption between implanted biomaterials and the biological environment. Thus, numerous strategies to create a bond between the implant and the living host tissue have been developed. Recently, the use of metallic implants with polymer coating has been reported by many for these purposes. Ti, TiO_2 and Ti-alloy combined with polyester coatings have been intensively studied to fabricate scaffolds. Lagoa et al.[246] developed a partially biodegradable implant from titanium, polylactide, HA, and calcium carbonate. The implant presented mechanical stability, biocompatibility, and partial biodegradability. Helary and coworkers have used poly(sodium styrene sulfonate) polyNaSS on oxidized or grafted Ti samples[247] and poly-NaSS/(Methylacrylic acid) MA grafted onto Ti6Al4V alloy surfaces.[248] They reported that cell adhesion and differentiation on Ti (grafted) was higher than on oxidized titanium and titanium due to the presence of active sites that interact with extracellular proteins. Besides, polyNaSS/MA grafted onto Ti6Al4V alloy in femoral rabbit model showed lamellar trabecular bone with wide haversian canals lined by osteoblasts; however, the high levels of Na, P, Ca, Zn, etc., indicated that the piranha treatment used to oxidize the alloy surface was very intense.

Oughlis et al.[249] developed a scaffold from polyNaSS polymer and titanium. The results showed cell viability, proliferation and osteoblastic differentiation of hMSCs on this scaffold. The authors of this study argued that this type of scaffold improved biocompatibility, but that it requires many chemical reactions that could affect biomolecules or biocompatibility of the material. Another work employs a chromatographic approach combined to 2-DE gels and mass spectrometry for the analysis and identification of proteins adsorbed on polyNaSS/Ti surfaces.[249] Studies using metal/polymer scaffolds are summarized in Table VIII.

5. MECHANICAL PROPERTIES

For bone regeneration, the mechanical properties of a biomaterial are critical to the success of the implant and depend on the tissues into which they are implanted.[250] The mechanical requirements of the scaffold are being studied to repair load-bearing bone defects,[251] where such requirements are not fully defined; however, a strategy considering mechanical properties values of bone and scaffold are required. Another indispensable aspect to consider is the porosity and pore size and architecture in the scaffolds.[252] An increase in these properties helps bone ingrowth but reduce the mechanical strength compromising their structural integrity. Strength, elasticity, tension and compression are tested factors in the scaffold design. The rheological parameters related to these factors are:[253]

   a. *Elastic modulus*: (relation between measured tensile stress and tensile strain),

   b. *Flexural modulus* (relation of bending stress to resulting strain in flexural deformation),

   c. *Tensile strength* (maximum stress that a material can withstand before failing or breaking) and

   d. *Maximum strain* (related to the ductility of the material)

Some derived properties of these factors are:[254]

   (e) *Tangent modulus* (slope of the compressive stress–strain curve at any specified strain) the tangent modulus is equivalent to the Young's modulus below the proportional limit, indicating the stiffness of the scaffold,

   (f) *Modulus of resilience* (area under the stress–strain curve), represent the energy consumed in deformation of the scaffold under particular strain and represents the toughness of material under elastic deformation,

   (g) *Weibull modulus* (dimensionless parameter known as "shape parameter," which is related to the strength variability of the material[255] and

   (h) *work-of-fracture* (fracture energy), which is directly proportional to the relation between the stress and Young's modulus).[256]

Some of these mechanical properties can be controlled by the fabrication method used. Deng et al.[257] obtained good uniformity, appropriate mechanical strength, and suitable porosity in dipeptide-substituted polyphosphazene-polyester blend by optimization of electrospinning conditions. Heat treatment of BG20 (bioactive glass) scaffolds modified the percentage of crystallization changing their mechanical strength, biodegradability and bioactivity.[141] Compressive strength of the TiO_2 scaffolds improved using multiple recoating processes.[196] Mechanically adaptive structures can be manufactured by the crucible melt extraction (CME) process and sintering of MgY4 fibers.[199] GTR/GBR membranes fabricated by electrospinning and the addition of hydroxyapatite improved the mechanical properties in HA/PCL scaffolds.[210] In the Tables II-X some mechanical properties for scaffolds of different materials (polymers, ceramics, metals and composites) are reported.

6. CELLS

Although the most heavily investigated area in bone tissue engineering is the creation of appropriate scaffolds from a wide-range of materials, it is becoming increasingly evident that these materials fall short when it comes to mimicking the natural bone healing process, i.e., promoting osteoblast formation and stimulating the vascularization process. Most studies rely on the utilization of one specific cell type (usually stem cells or osteoblast-like cells). In recent years, a number of studies have employed co-culture systems with the purpose of improving bone engineering properties of 3D scaffolds and also importantly, to understand more about the fundamental processes that occur *in vivo* in the bone healing process.

In studies that specifically aim to promote vascularization in new bone formation, the co-culture of stem cells or osteoblasts with endothelial cells is a common approach. In one study, the synthetic polyester-urethane DegraPol® (DP) foam was used as a scaffold to co-culture human osteoblasts (OB) and human endothelial cells (EC).[258] These seeded scaffolds were used to study early bone formation in the chorioallantoic membrane model (CAM assay) *ex vivo*. Scaffolds were incubated into the CAM assays for seven days, when the scaffold was removed and prepared for histological analyses. Conditions studied were (i) scaffolds seeded with OB, (ii) scaffolds seeded with EC, and (iii) scaffolds seeded with OB/EC co-cultures. Cell proliferation was obviously increased in the co-culture system as compared to the other systems, as was 3D growth into the scaffold material, formation of ECM, and density of avian erythrocytes. MRI was used to quantify the blood perfusion of these systems. The co-culture system showed significantly higher perfusion than in the OB-only system, but not the EC-only system. These results indicate that in this instance the co-culture system had better angiogenic properties, although the formation of bone was not addressed in this study. In another study, Matrigel was used as a scaffold to study the effects of co-culturing bone marrow endothelial progenitor cells (BM-EPCs) and mesenchymal stem cells (MSCs) on vascularization.[259] BM-EPCs and MSCs were cultured in a 1:1 ratio. The cells were analyzed for up to 14 days by fluorescent microscopy. BM-EPCs and MSCs growing in their normal culture media were used as a control. From day 3, it was evident that in the co-culture system there was more cellular migration and organization than in the control systems, and cell–cell contacts had been established between the two cell types, suggesting the establishment of specialized unions. A Matrigel tube-forming assay was used to assess tubulogenesis in the co-culture system. BM-EPCs and MSCs supplemented with VEGF were used as positive controls. The co-culture system demonstrated the highest tubulogenic activity, a more than two-fold increase, as compared to the VEGF-stimulated positive controls. RT-PCR was used to evaluate the presence of a panel of 18 angiogenesis-related genes, the co-culture system presented upregulation and downregulation of genes consistent with the activation of an angiogenic phenotype. These results clearly suggest that a simple co-culture system can be obtained without the addition of exogenous growth factors.

In another study, silk fibroin scaffolds were seeded with a co-culture of human microcapillary endothelial cells (HDMEC) and primary human osteoblast cells (HOS) in order to determine how these scaffolds behaved *in vivo* when subcutaneously implanted into

immunodeficient mice.[260] The co-culture scaffold system was compared to scaffolds with monocultures of HDMEC and HOS. The behavior of co-culture and monocultured scaffolds were analyzed *in vitro* by fluorescence microscopy. It was determined that scaffolds containing the co-culture and the HDMEC monoculture were able to form vascularized networks starting at day 7. As soon as the scaffolds showed microcapillary formation, they were implanted into the animals. After 14 days, scaffolds were analyzed. In co-culture scaffolds microcapillary structures were observed on the surface of the silk fibroin as well as within the scaffold. However, in the HDMEC monoculture scaffold, microcapillaries were only found surrounding the scaffolds. Histomorphometric analysis was performed to quantify the degree of vascularization. In the monoculture system, degree of vascularization was 8.81 vessels/mm^3; while in the coculture system it was found to be 107.34 vessels/mm^3, a very significant increase. This study establishes a system where microvas-culature can be pre-formed in a scaffold without angiogenic factors and will successfully vascularize *in vivo*. However, it remains unclear how the presence of osteoblast cells contributes to this phenomenon.

In another study, human umbilical vein endothelial cells (HUVECs) and human osteoblast-like cells (HOB) were co-cultured into poly(L-lactide)-co-(1,5-dioxepan-2-one) [poly(LLA-co-DXO)] scaffolds at ratios of 5:1 (5:1 group) and 2:1 (2:1 group).[261] Scaffolds were histologically examined for up to 25 days in culture, and results showed that cells were able to proliferate and form capillary-like structures in both groups. Cell viability analysis showed there were no statistically significant differences between the 2:1 group and the 5:1 group. RT-PCR results showed that ALP, BMP-2, and IGF-1 were significantly upregulated in the 5:1 group. TGF-β3 expression was significantly higher in the 2:1 group. No differences were found in the expression of ColI, VEGFa, ITGA1, TGF-beta1, PCNA, or Runx-2 between groups. The differences in gene expression found between groups underscores the importance of examining the effect that different cell ratios have on the outcome of angiogenesis and bone formation. Taken together, the described studies demonstrate that the addition of endothelial cells to stem cells and osteoblast-like cells is a promising approach to promote the essential process of angiogenesis in the formation of new bone. However, more systematic approaches that study the combined effects of scaffold properties, endothelial cell type origin, and co-culture ratios are still needed.

Co-culture systems that aim to enhance the deposition of new bone through osteoclast formation are usually based on stem cells and osteoclast-precursor systems. In one study, murine primary osteoblasts and osteoclast precursors were seeded on a resorbable porous ceramic scaffold based on silicon-stabilized tricalcium phosphate and grown in normal culture (N) or osteogenic medium (O).[262] After 40 days, the percentage of osteoclast precursors was 34% and 23% for cells grown in N and O, respectively. The percentage of osteoblasts in cells grown in N and O was 66% and 77%, respectively. Interestingly, Runx-2 and Osterix expression was higher in cells grown in normal culture, however the expression of osteoclast differentiation markers such as cathepsin K and TRAP was higher in cells grown in osteogenic medium. The data obtained from this study indicates that this co-culture environment can promote osteoblast and osteoclast differentiation; however, it would have been useful to compare the expression of bone-related markers in the same system but with

the individual monoculture components. In a later study by the same group, the same co-culture system was analyzed in terms of bone deposition and biodegradation. In this study, osteoblast/osteoclast co-culture systems were compared to osteoblast monoculture systems.[263] After 8 weeks of culture in osteogenic media, scaffolds were harvested an analyzed by X-ray computed microtomography. Bone deposition was detected in both scaffolds, although in the co-culture systems the bone tissue was much more organized. The co-culture systems also showed higher amounts of fibrous osteoid tissue as well as lower scaffold volume, which is consistent with the higher degradation expected in the presence of osteoclasts. The results from this study further illustrate the importance of understanding how the individual components of co-cultures behave, in order to better understand the interactions within the system as a whole.

A co-culture system of the osteoblast-like SaOs-2 cells and the osteoclast-like RAW 264.7 cells was studied for its effect on the osteogenic differentiation of SaOs-2 cells.[88] SaOs-2 cells were either grown by themselves or with RAW 264.7 cells in alginate or alginate/silica hydrogels in the presence of dexamethasone. There was no change in cell viability between the monocultured or co-cultured cells. As measured by RT-PCR, levels of SaOs-2 osteoprotegerin, which is expressed in osteoblasts, increased under co-culture conditions. However, the expression of *TRAP*, which is a marker for osteoclast differentiation, was inhibited in RAW 264.7 cells when they were cultured in the presence of SaOs-2 cells. These results suggest that in this co-culture system, osteogenesis could be improved through osteoblast activation and osteoclast inhibition, and that there is some molecular crosstalk between SaOs-2 and RAW 264.7 cells. However, no experiments were performed that specifically measured bone formation or mineral deposition.

The effect of co-culturing monocytes/macrophages, which are closely related to osteoclasts,[264] with hBMSCs, on their early osteogenic differentiation.[265] The co-cultures were assembled through porous trans wells that allowed interaction between cells through the secretion of paracrine factors, and cultured in osteogenic media. The authors hypothesize that the secretion of BMP-2 from monocytes/macrophages would enhance osteogenic differentiation. To support this hypothesis, some of the co-cultures were supplemented with anti-BMP-2 antibody. It was found that there was a statistically significant increase in hBMSC proliferation in the presence of monocytes/macrophages, but this effect was abrogated in the presence of the BMP-2 antibody. At seven days, ALP activity was significantly increased in the co-culture experiment, again, this effect was eliminated in when the co-culture system was supplemented with BMP-2 antibody. As measured by RT-PCR, the expression of OCN and OPN underwent a very significant decrease when there was BMP-2 antibody in the co-culture system. These results indicate that the secretion of BMP-2 by monocytes/macrophages influences the osteogenic differentiation of hBMSCs. This study is significant because it attempts to understand the molecular mechanisms by which a co-culture system can improve osteogenic differentiation. Taken together, these results suggest that the *in vivo* interplay between osteoblasts and osteoclasts can be at least partially recapitulated in co-culture systems. These studies should drive the field to investigate co-culture systems in depth.

7. BIOCHEMICAL AND BIOPHYSICAL STIMULATION

A major goal in the design of bone graft substitutes to promote healing is a formulation that can recreate the bone tissue microenvironment, since it is responsible for regulating the osteoprogenitor cell function to maintain homeostasis.[266] Essential to this micronenvironment are stimulating factors that promote the osteoinductive capacity of the bone graft substitute and which include biochemical, mechanical and electromagnetic stimuli. A discussion of each of these stimuli is presented next in the context of bone tissue regeneration.

7.1. Biochemical Stimulation

Osteogenesis is directed by the coordinated expression of many molecules, including growth factors, and transcription factors, which induce cellular and molecular stimuli to guide cellular commitment and differentiation. A strategy in bone tissue engineering to enhance osteogenic cell function has been to incorporate these growth and transcription factors into scaffolds for their release during the healing process. Growth factors are protein molecules that start a signaling cascade through binding to specific cell surface receptors. This leads to signal transduction into the nucleus where transcription factors are activated, affecting gene expression, which influence critical functions, such as cell division, matrix synthesis and tissue differentiation. Prominent among these growth factors in bone formation and repair are TGF-β, BMPs, FGFs, IGFs, PDGF, Wnt, and sonic hedgehog (Shh) signaling. Although there are many transcription factors involved in osteogenesis the most important include TAZ, Runx-2 and osterix, which control commitment and differentiation, while inhibiting adipogenesis. Gene expression patterns of transcription and growth factors suggest that these are co-regulated. For instance, transcription factors are thought to activate the expression of growth factors in response to the signaling of growth factors produced from the adjacent tissue, thus regulating tissue growth.[267]

At the early stages of bone formation or healing, TGF-β recruits and stimulates osteoprogenitor cells to proliferate, providing a pool of pre-osteoblasts.[268] Then later during osteoblast differentiation, TGF-β inhibits differentiation and mineralization, perhaps by inhibiting the expression of the Runx-2 and OCN genes, whose expression is controlled by Runx-2 and mediated by MAPKs and Smad2/3 pathways.[269] Most BMPs belong to the TGF-β superfamily, of which, BMP-2, -4, -6 and -7 are known to have key roles in osteoblast commitment and differentiation. These regulate the transcription factors TAZ, Runx-2 and osterix. Recent studies have shown crosstalk between BMP signaling and Wnt, Notch, FGF and Shh signaling on osteoblast differentiation and bone formation.[270] A problem with the implementation of biodegradable scaffolds for the controlled release of BMPs has been that they require concentrations about six orders of magnitude higher than the physiological to have an equivalent effect.[271] Although FGF signaling and its role in bone healing is currently an active area of research, FGF-2, FGF-9, and FGF-18 have been shown to be regulators of bone cell functions, which seem to act as autocrine/paracrine factors for bone cells.[272] Still, there is limited understanding of the complex roles of FGF signaling in fracture healing and its action mechanisms, limiting any therapeutic measures can be applied clinically to improve bone regeneration.[273] There are two IGF family

members, IGF-1 and IGF-2, the first with greater osteogenic potential and the second being the most abundant in bone tissue. Although the role of IGF-2 is not clear, IGF-1 is known to stimulate osteoblast mobility and activity *in vitro*, and increase bone formation *in vivo*. In addition, IGF-1 has demonstrated a synergistic effect when in the presence of TGF-β in bone healing, specifically in callus mineralization and improving the torsional stiffness of bone after injury.[274] Although PDGF is synthesized by osteoprogenitor cells, it has not shown to have strong osteoinductive properties. It is thought that the role of PDGF in bone healing is related to cell recruitment and angiogenesis.[33] There is increasing evidence for the role of Wnt/β-catenin signaling in controlling osteoblast differentiation and skeletal development by activating Runx-2 gene expression in MSCs, similarly to BMP and TGF-β.[275] In addition, evidence also suggests cross-talk between FGF-2 and the Wnt/β-catenin pathway, through the stimulation of osteoblast differentiation and bone formation.[276] Shh has been shown to induce osteoblast commitment and promote differentiation in MSCs.[277] It has shown a synergistic effect with BMP-2 in osteoblast differentiation and it is thought to be its upstream regulator.[278]

What emerges from the considerable advances made in understanding the regulation of osteoprogenitor cells by growth factors is that there is extensive cross-talk between the signaling pathways activated by them. When looking at these from the temporal perspective of osteoprogenitor cell development an overall pattern can be seen of a carefully regulated sequence of coordinated growth factor expression (Fig. 9). The use of biodegradable scaffolds for the controlled release of these growth factors in third generation bone graft substitutes has proven an effective delivery method. Most studies using biodegradable scaffolds for growth factor delivery include mostly one and perhaps two of these as part of their formulation, when results point to the need of multiple factors at different stages of the osteoprogenitor cell differentiation. In addition, effective delivery of these biochemical stimuli has proven a challenge because of loss of bioactivity, limited control over dose administration, non-targeted delivery, and lack of availability of required growth factors. Strategies to improve control over the microenvironment include the development bioreactor technology capable of allowing constant or dynamic gradients of growth factors bound to the matrix substratum. More research is needed in this area to overcome these challenges which are faced not only by the tissue engineering community but by drug delivery researchers as well.

7.2. Mechanical Stimulation

In addition to biochemical stimulus by growth factors, exogenous mechanical stimulus affects the bone tissue microenvironment and it is also an essential component for maintaining bone health and homeostasis.[279] This mechanical stimulus is converted into biochemical signals that are then integrated into cellular responses through mechanotransduction. Bone tissue can be seen as a cellular network where the osteocytes serve as sensory cells responsible for this mechanotransduction, while osteoblasts and osteoclasts are the effector cells. The current mechanotransduction paradigm states that loads applied to a whole bone causes pulsatile fluid flow through osteocyte canaliculi. The osteocytes can sense the shear stress generated by this flow over its surface and then produce signaling molecules that regulate bone remodeling by osteoclasts and osteoblasts.[280]

Although the precise signaling events involved in the mechanotransduction process are not clear, it is known that mechanical strain and pulsatile fluid flow induce the synthesis of signaling molecules by osteocytes.[33] The effects of mechanical loading on the mechanical strain and pulsatile fluid flow induced on bone cells is thought to be the effect of tensile strain due to hydrostatic pressure and compression/relaxation of the ECM, and shear stress due to fluid flow.[281] Bone loading *in vivo* generates all of these forces concurrently, so transient pressure waves cannot be separated from the effects of fluid shear stress or cell strain. It is of interest in bone tissue engineering to use these compressive or tensile loading mechanisms to mechanically stimulate 3D scaffold constructs seeded with osteoprogenitor cells to produce bone matrix before implantation. This requires the use of bioreactors to impart the different mechanical forces, which mimic the mechanical stimuli that occur *in vivo*.[282] Various groups have studied the effect of cyclic hydrostatic pressure on osteoprogenitor cells showing that this type of stimuli enhances their functions related to new bone formation.[283-285] Fluid shear stress stimulation has been shown to induce osteogenic differentiation and mineralization. It is estimated that in response to loading, the *in vivo* shear stress experienced by bone cells is 8–30 dyn/cm^2.[281] Perfusion bioreactors are the choice configuration for inducing fluid shear stress in 3D scaffolds by pumping media through a cartridge containing the scaffold.[282] In all these studies it is evident that the cell response varies with the intensity and duration of the mechanical stimuli.[281] More recently, mechanical stimulation of MSCs by tagging magnetic nanoparticles to mechanosensitive membrane receptors by electromagnetic field activation induced osteoprogenitor cell differentiation toward an osteogenic lineage.[286]

It is clear that underlying mechanotransduction mechanisms are complex and that development of the clinical applications of mechanical stimulation are yet to come, partially because of our limited understanding of the signaling events involved, but mainly because of a varied and dynamically changing mechanical environment allows for these to be co-regulated. Further investigations on the effect of stimuli intensity and duration are needed to allow the development of therapies that can be applied clinically. In addition, the synergistic effect of biochemical stimulation should be explored to have a system that more closely resembles the physiological condition.

7.3. Electromagnetic Stimulation

Early studies trying to elucidate the osteogenic effect of mechanical stimulation on bone examined its bioelectric properties and concluded that electrical pathways were key aspects of this response.[287] This led to the development of three methods of administering electrical current to bone, which have been used in clinical practice and include direct current, capacitive coupling, and inductive coupling. Of these, inductive coupling enhances bone healing by using electrical/electromagnetic stimulation. Inductive coupling is formed by placing current-carrying Helmholtz coils on the skin over the fracture site.[288] As current flows through the coils, an electromagnetic field is generated within the fractures site.[288] The electrical field that is formed varies in size because of the type of tissues at the fracture site and the properties of the applied magnetic field.[289] Electromagnetic fields varying from 0.01 to 2.0 T have been used to create an electrical field at the fracture site of 1 to 100 mV/cm.[290] This type of treatment option is attractive as it is noninvasive, painless, and

surgery free.[288] In addition, low-frequency pulsed electromagnetic fields (PEMF) have been shown to induce bone and vascular growth[288] and increase the expression of the osteogenic factor Runx-2 and a decrease of the expression of the adipogenic factor PPARγ, which co-repress each other.[291]

However, the molecular mechanisms underlying the response of cells to electric fields are still far from being completely understood.[292] Several *in vitro* studies have been performed showing inconsistent and somewhat controversial data. While several groups have demonstrated an increase in proliferation after exposing cells to electric/electromagnetic fields,[288,291,293] other groups did not detect significant differences following exposure of cells to such fields.[294,295] Similarly, effects on osteogenic differentiation are also controversial. Such differences in responses may result from a number of variables. Among these are differences in cell types, the maturation stage of the cells, as well as characteristics of the electric field parameters. Similarly to mechanical stimulation, the underlying mechanisms involved in electromagnetic stimulation are complex. In addition, there is limited understanding of these signaling events and the effect of stimuli intensity and duration are lacking. In addition, the synergistic effect of biochemical stimulation should be explored to have a system that more closely resembles the physiological condition.

8. CONCLUSION AND FUTURE DIRECTIONS

With the goal of providing an alternative to the autograft bone tissue engineers have focused on the development a bone graft substitute which closely mimics the bone tissue microenvironment. This type of bone graft is designed to enhance bone repair and regeneration by incorporating bone progenitor cells and growth factors to stimulate cells into a scaffold made of various natural or synthetic biomaterials or their combination which provide the necessary support and with sufficient vascularization to allow access to nutrients to support this process. We have presented through this review the current state of the art of this technology and the current development requirements which need to be met to develop a bone graft substitute which closely mimics the bone tissue microenvironment. These needs include:

1. a scaffold that matches the biomaterial degradation rate with the bone regeneration rate,

2. a multi-analyte growth factor delivery strategy with proper control over its release kinetics,

3. a strategy for stimulating scaffold vascularization (e.g., co-cultures, growth factor, etc.),

4. development of a bioreactor technology capable of preparing scaffolds for implantation, and

5. development of biophysical stimulation technologies that can be brought to the clinic.

The developments also require knowledge about the bone regeneration process, including:

1. temporal and multi-growth factor requirements (Fig. 9),

> **2.** signaling pathway cross-talk after growth factor stimulation, and
>
> **3.** signaling pathway cross-talk after biophysical stimulation.

At this point most of the studies in the development of these third generation bone graft substitutes have been limited to *in vitro* testing. Although this is a first stage in viability assessment, *in vivo* testing is required, since it brings the complexity of extracellular fluids, inflammation and mechanical stimulation, of the clinical situation. In addition, there is still much to learn about the dynamics of the bone tissue microenvironment to allow for proper simulation. All these challenges will surely be met through the close interdisciplinary collaboration of material scientists, engineers, medical doctors, chemists, and physicists.

Acknowledgments

References and Notes

1. Neighbour T. The Global Orthobiologics Market: Players, Products and Technologies Driving Change. Espicom Business Intelligence. 2008; 2

2. Brydone A, Meek D, Maclaine S. Proc Inst Mech Eng H. 2010; 224:1329. [PubMed: 21287823]

3. Albrektsson T, Johansson C. Eur Spine J. 2001; (Suppl 2):S96. [PubMed: 11716023]

4. Myeroff C, Archdeacon M. J Bone Joint Surg Am. 2011; 93:2227. [PubMed: 22159859]

5. Oppenheim J, Segal D, Spitzer D. Neurosurgery. 2002; 51:854. [PubMed: 12229871]

6. Silber J, Anderson D, Daffner S, Brislin B, Leland J, Hilibrand A, Vaccaro A, Albert T. Spine. 2003; 28:134. [PubMed: 12544929]

7. Mankin H, Hornicek F, Raskin K. Clin Orthop Relat Res. 2005; 432:210. [PubMed: 15738824]

8. Graham S, Leonidou A, Aslam-Pervez N, Hamza A, Panteliadis P, Heliotis M, Mantalaris A, Tsiridis E. Expert Opin Biol Ther. 2010; 10:885. [PubMed: 20415596]

9. Laurencin C, Khan Y, El-Amin S. Expert Rev Med Devices. 2006; 3:49. [PubMed: 16359252]

10. Jayakumar P, Silvio LD. Proc Inst Mech Eng H. 2010; 224:1415. [PubMed: 21287829]

11. Franz-Odendaal T, Hall B, Witten P. Dev Dyn. 2006; 235:176. [PubMed: 16258960]

12. Buck D II, Dumanian G. Plast Reconstr Surg. 2012; 129:1314. [PubMed: 22634648]

13. Gentili C, Cancedda R. Curr Pharm Des. 2009; 15:1334. [PubMed: 19355972]

14. Anselme K. Biomaterials. 2000; 21:667. [PubMed: 10711964]

15. Clarke B. Clin J Am Soc Nephrol. 2008; 3:S131. [PubMed: 18988698]

16. Lamoureux F, Baud'huin M, Duplomb L, Heymann D, Rédini F. Bioessays. 2007; 29:758. [PubMed: 17621645]

17. Sasaki N, Matsushima N, Ikawa T, Yamamura H, Fukuda A. J Biomech. 1989; 22:157. [PubMed: 2540205]

18. Zioupos P, Currey JD, Hamer A. J Biomed Mater Res. 1999; 45:108. [PubMed: 10397964]

19. Martin, R.; Burr, D. Structure Function, and Adaptation of Compact Bone. Raven Press; New York: 1989.

20. Rho J, Kuhn-Spearing L, Zioupos P. Med Eng Phys. 1998; 20:92. [PubMed: 9679227]

21. Keaveny, TM. Cancellous bone. In: Black, J.; Hastings, G., editors. Handbook of Biomaterial Properties. Chapman and Hall; London: 1998. p. 15

22. Hench L, Polak J. Science. 2002; 295:1014. [PubMed: 11834817]

23. Navarro M, Michiardi A, Castaño O, Planell J. J R Soc Interface. 2008; 5:1137. [PubMed: 18667387]

24. Anderson JM. Annu Rev Mater Res. 2001; 31:81.

25. Amini A, Laurencin C, Nukavarapu S. Crit Rev Biomed Eng. 2012; 40:363. [PubMed: 23339648]

26. Jayakumar P, Silvio LD. Proc Inst Mech Eng H. 2010; 224:1415. [PubMed: 21287829]

27. Sundelacruz S, Kaplan D. Semin Cell Dev Biol. 2009; 20:646. [PubMed: 19508851]

28. Williams D. Biomaterials. 2008; 29:2941. [PubMed: 18440630]

29. Hulbert S, Young F, Mathews R, Klawitter J, Talbert C, Stelling F. J Biomed Mater Res. 1970; 4:433. [PubMed: 5469185]

30. Rivera-Chacon D, Alvarado-Velez M, Acevedo-Morantes C, Singh S, Gultepe E, Nagesha D, Sridhar S, Ramirez-Vick J. J Biomed Nanotechnol. 2013; 9:1092. [PubMed: 23858975]

31. García A. Biomaterials. 2005; 26:7525. [PubMed: 16002137]

32. Freed L, Vunjak-Novakovic G, Biron R, Eagles D, Lesnoy D, Barlow S, Langer R. Biotechnology. 1994; 12:689. [PubMed: 7764913]

33. Hughes F, Turner W, Belibasakis G, Martuscelli G. Periodontol. 2006; 41:48.

34. Lee KY, Yuk SH. Prog Polym Sci. 2007; 32:669.

35. Lee S-H, Shin H. Advanced Drug Delivery Reviews. 2007; 59:339. [PubMed: 17499384]

36. Vagaská B, Bacáková L, Filová E, Balík K. Physiol Res. 2010; 59:309. [PubMed: 19681662]

37. Semino CE. J Dent Res. 2008; 87:606. [PubMed: 18573978]

38. Aravamudhan A, Ramos DM, Nip J, Harmon MD, James R, Deng M, Laurencin CT, Yu X, Kumbar SG. J Biomed Nanotechnol. 2013; 9:719. [PubMed: 23621034]

39. Hiraoka Y, Kimura Y, Ueda H, Tabata Y. Tissue Eng. 2003; 9:1101. [PubMed: 14670098]

40. Harley BA, Leung JH, Silva ECCM, Gibson LJ. Acta Biomaterialia. 2007; 3:463. [PubMed: 17349829]

41. Yu H-S, Won J-E, Jin G-Z, Kim H-W. Biores Open Access. 2012; 1:124. [PubMed: 23515189]

42. Huang C, Ogawa R. FASEB J. 2010; 24:3625. [PubMed: 20505115]

43. Kawata A, Mikuni-Takagaki Y. Biochem Biophys Res Commun. 1998; 246:404. [PubMed: 9610372]

44. Schneider RK, Puellen A, Kramann R, Raupach K, Bornemann J, Knuechel R, Pérez-Bouza A, Neuss S. Biomaterials. 2010; 31:467. [PubMed: 19815272]

45. Roeder BA, Kokini K, Sturgis JE, Robinson JP, Voytik-Harbin SL. J Biomech Eng. 2002; 124:214. [PubMed: 12002131]

46. Qi H, Aguiar DJ, Williams SM, Pean AL, Pan W, Verfaillie CM. PNAS. 2003; 100:3305. [PubMed: 12631704]

47. Bruder SP, Jaiswal N, Haynesworth SE. J Cell Biochem. 1997; 64:278. [PubMed: 9027588]

48. Ennis, J.; Sarugaser, R.; Gomez, A.; Baksh, D.; Davies, J. Isolation, Characterization, and Differentiation of Human Umbilical Cord Perivascular Cells (HUCPVCs). In: Jennie, PM., editor. Methods in Cell Biology. Vol. 86. Academic Press; Oxford, UK: 2008. p. 121

49. Xu C, Su P, Chen X, Meng Y, Yu W, Xiang AP, Wang Y. Biomaterials. 2011; 32:1051. [PubMed: 20980051]

50. Serpooshan V, Julien M, Nguyen O, Wang H, Li A, Muja N, Henderson JE, Nazhat SN. Acta Biomaterialia. 2010; 6:3978. [PubMed: 20451675]

51. O'Brien FJ, Harley BA, Waller MA, Yannas IV, Gibson LJ, Prendergast PJ. Technol Healt Care. 2007; 15:3.

52. Ratanavaraporn J, Damrongsakkul S, Kanokpanont S, Yamamoto M, Tabata Y. J Biomater Sci Polym Ed. 2011; 22:1083. [PubMed: 20615314]

53. Hussain A, Bessho K, Takahashi K, Tabata Y. Tissue Eng, Part A. 2012; 18:768. [PubMed: 21995670]

54. Staiger MP, Pietak AM, Huadmai J, Dias G. Biomaterials. 2006; 27:1728. [PubMed: 16246414]

55. Lu H, Kawazoe N, Kitajima T, Myoken Y, Tomita M, Umezawa A, Chen G, Ito Y. Biomaterials. 2012; 33:6140. [PubMed: 22698726]

56. Pang E-K, Im S-U, Kim C-S, Choi S-H, Chai J-K, Kim C-K, Han S-B, Cho K-S. J Periodontol. 2004; 75:1364. [PubMed: 15562914]

57. Oh S-A, Lee H-Y, Lee JH, Kim T-H, Jang J-H, Kim H-W, Wall I. Tissue Eng Part A. 2012; 18:1087. [PubMed: 22145747]

58. Pitaru S, Kotev-Emeth S, Noff D, Kaffuler S, Savion N. J Bone Miner Res. 1993; 8:919. [PubMed: 8213254]

59. Niu L-N, Jiao K, Qi Y-P, Nikonov S, Yiu CKY, Arola DD, Gong S-Q, El-Marakby A, Carrilho MRO, Hamrick MW, Hargreaves KM, Diogenes A, Chen J-H, Pashley DH, Tay FR. FASEB J. 2012; 26:4517. [PubMed: 22859369]

60. Kitaori T, Ito H, Schwarz EM, Tsutsumi R, Yoshitomi H, Oishi S, Nakano M, Fujii N, Nagasawa T, Nakamura T. Arthritis Rheum. 2009; 60:813. [PubMed: 19248097]

61. Costa-Pinto AR, Reis RL, Neves NM. Tissue Eng Part B Rev. 2011; 17:331. [PubMed: 21810029]

62. VMC, Costa-Pinto AR. J Tissue Eng Regen Med. 2011; 6:21. [PubMed: 21312336]

63. Wang L, Stegemann JP. Biomaterials. 2010; 31:3976. [PubMed: 20170955]

64. Hoemann CD, Chenite A, Sun J, Hurtig M, Serreqi A, Lu Z, Rossomacha E, Buschmann MD. J Biomed Mater Res A. 2007; 83:521. [PubMed: 17503494]

65. Wang L, Stegemann JP. Acta Biomaterialia. 2011; 7:2410. [PubMed: 21345389]

66. Lima PAL, Resende CX, de Almeida Soares GD, Anselme K, Almeida LE. Materials Science and Engineering: C. 2013; 33:3389. [PubMed: 23706225]

67. Wang L, Li C. Carbohydrate Polymers. 2007; 68:740.

68. Bi L, Cheng W, Fan H, Pei G. Biomaterials. 2010; 31:3201. [PubMed: 20116844]

69. Kiuru J, Viinikka L, Myllylä G, Pesonen K, Perheentupa J. Life Sciences. 1991; 49:1997. [PubMed: 1749310]

70. Florczyk SJ, Leung M, Li Z, Huang JI, Hopper RA, Zhang M. J Biomed Mater Res A. 2013; 101:2974. [PubMed: 23737120]

71. Nandi SK, Kundu B, Basu D. Materials Science and Engineering: C. 2013; 33:1267. [PubMed: 23827571]

72. Qu Z, Yan J, Li B, Zhuang J, Huang Y. Biomed Mater. 2010; 5:065001. [PubMed: 20924135]

73. Vepari C, Kaplan DL. Prog Polym Sci. 2007; 32:991. [PubMed: 19543442]

74. Zhang Y, Wu C, Friis T, Xiao Y. Biomaterials. 2010; 31:2848. [PubMed: 20071025]

75. Bhumiratana S, Grayson W, Castaneda A, Rockwood D, Gil ES, Kaplan DL, Vunjak-Novakovic G. Biomaterials. 2011; 32:2812. [PubMed: 21262535]

76. Rockwood DN, Gil ES, Park S-H, Kluge JA, Grayson W, Bhumiratana S, Rajkhowa R, Wang X, Kim SJ, Vunjak-Novakovic G, Kaplan DL. Acta Biomaterialia. 2011; 7:144. [PubMed: 20656075]

77. Park S-H, Gil ES, Shi H, Kim HJ, Lee K, Kaplan DL. Biomaterials. 2010; 31:6162. [PubMed: 20546890]

78. Wan C, Gilbert SR, Wang Y, Cao X, Shen X, Ramaswamy G, Jacobsen KA, Alaql ZS, Eberhardt AW, Gerstenfeld LC, Einhorn TA, Deng L, Clemens TL. PNAS. 2008; 105:686. [PubMed: 18184809]

79. Correia C, Bhumiratana S, Yan L-P, Oliveira AL, Gimble JM, Rockwood D, Kaplan DL, Sousa RA, Reis RL, Vunjak-Novakovic G. Acta Biomaterialia. 2012; 8:2483. [PubMed: 22421311]

80. Riccio M, Maraldi T, Pisciotta A, La Sala GB, Ferrari A, Bruzzesi G, Motta A, Migliaresi C, De Pol A. Tissue Eng Part A. 2012; 18:1006. [PubMed: 22166080]

81. Zhang Y, Fan W, Ma Z, Wu C, Fang W, Liu G, Xiao Y. Acta Biomaterialia. 2010; 6:3021. [PubMed: 20188872]

82. Suárez-González D, Barnhart K, Saito E, Vanderby R, Hollister SJ, Murphy WL. J Biomed Mater Res A. 2010; 95A:222. [PubMed: 20574984]

83. Zhou H, Xu HHK. Biomaterials. 2011; 32:7503. [PubMed: 21757229]

84. Lee G-S, Park J-H, Shin US, Kim H-W. Acta Biomaterialia. 2011; 7:3178. [PubMed: 21539944]

85. Kanczler JM, Ginty PJ, White L, Clarke NMP, Howdle SM, Shakesheff KM, Oreffo ROC. Biomaterials. 2010; 31:1242. [PubMed: 19926128]

86. Kolambkar YM, Boerckel JD, Dupont KM, Bajin M, Huebsch N, Mooney DJ, Hutmacher DW, Guldberg RE. Bone. 2011; 49:485. [PubMed: 21621027]

87. He X, Dziak R, Mao K, Genco R, Swithart M, Li C, Yang S. Tissue Eng Part A. 2013; 19:508. [PubMed: 22994418]

88. Schloßmacher U, Schröder HC, Wang X, Feng Q, Diehl-Seifert B, Neumann S, Trautwein A, Müller WEG. RSC Adv. 2013; 3:11185.

89. Pavasant P, Shizari TM, Underhill CB. J Cell Sci. 1994; 107:2669. [PubMed: 7533172]

90. Bae MS, Yang DH, Lee JB, Heo DN, Kwon Y-D, Youn IC, Choi K, Hong JH, Kim GT, Choi YS, Hwang EH, Kwon IK. Biomaterials. 2011; 32:8161. [PubMed: 21821281]

91. Jha AK, Xu X, Duncan RL, Jia X. Biomaterials. 2011; 32:2466. [PubMed: 21216457]

92. Patterson J, Siew R, Herring SW, Lin ASP, Guldberg R, Stayton PS. Biomaterials. 2010; 31:6772. [PubMed: 20573393]

93. Martínez-Sanz E, Ossipov DA, Hilborn J, Larsson S, Jonsson KB, Varghese OP. J Control Release. 2011; 152:232. [PubMed: 21315118]

94. Bhakta G, Rai B, Lim ZXH, Hui JH, Stein GS, van Wijnen AJ, Nurcombe V, Prestwich GD, Cool SM. Biomaterials. 2012; 33:6113. [PubMed: 22687758]

95. Ruppert R, Hoffmann E, Sebald W. Eur J Biochem. 1996; 237:295. [PubMed: 8620887]

96. Kisiel M, Martino MM, Ventura M, Hubbell JA, Hilborn J, Ossipov DA. Biomaterials. 2013; 34:704. [PubMed: 23103154]

97. Holmes TC. Trends in Biotechnology. 2002; 20:16. [PubMed: 11742673]

98. Mata A, Geng Y, Henrikson KJ, Aparicio C, Stock SR, Satcher RL, Stupp SI. Biomaterials. 2010; 31:6004. [PubMed: 20472286]

99. Kishimoto N, Momota Y, Hashimoto Y, Omasa T, Kotani J. J Oral Tissue Eng. 2011; 8:151.

100. Marí-Buyé N, Luque T, Navajas D, Semino CE. Tissue Eng Part A. 2013; 19:870. [PubMed: 23157379]

101. Amosi N, Zarzhitsky S, Gilsohn E, Salnikov O, Monsonego-Ornan E, Shahar R, Rapaport H. Acta Biomaterialia. 2012; 8:2466. [PubMed: 22503952]

102. Rughani RV, Salick DA, Lamm MS, Yucel T, Pochan DJ, Schneider JP. Biomacromolecules. 2009; 10:1295. [PubMed: 19344123]

103. Stakleff KS, Lin F, Smith Callahan LA, Wade MB, Esterle A, Miller J, Graham M, Becker ML. Acta Biomaterialia. 2013; 9:5132. [PubMed: 22975625]

104. Sachlos E, Czernuszka JT. Eur Cell Mater. 2003; 5:29. [PubMed: 14562270]

105. Wang D, He Y, Bi L, Qu Z, Zou J, Pan Z, Fan J, Chen L, Dong X, Liu X, Pei G, Ding J. Int J Nanomedicine. 2013; 8:1855. [PubMed: 23690683]

106. Chuenjitkuntaworn B, Inrung W, Damrongsri D, Mekaapiruk K, Supaphol P, Pavasant P. J Biomed Mater Res A. 2010; 94:241. [PubMed: 20166220]

107. Fernandez JM, Molinuevo MS, Cortizo AM, McCarthy AD, Cortizo MS. J Biomat Sci -Polym E. 2010; 21:1297.

108. Fernandez JM, Molinuevo MS, Cortizo MS, Cortizo AM. J Tissue Eng Regen Med. 2011; 5:126.

109. Wang S, Zhao P, Lin C, Huang Y. J Biomater Tissue Eng. 2013; 3:512.

110. Dånmark S, Finne-Wistrand A, Wendel M, Arvidson K, Albertsson A-C, Mustafa K. Journal of Bioactive and Compatible Polymers. 2010; 25:207.

111. Deng M, Kumbar SG, Nair LS, Weikel AL, Allcock HR, Laurencin CT. Adv Funct Mater. 2011; 21:2641.

112. Jabbarzadeh E, Deng M, Lv Q, Jiang T, Khan YM, Nair LS, Laurencin CT. J Biomed Mater Res B Appl Biomater. 2012; 100B:2187. [PubMed: 22915492]

113. Seyednejad H, Gawlitta D, Dhert WJA, van Nostrum CF, Vermonden T, Hennink WE. Acta Biomaterialia. 2011; 7:1999. [PubMed: 21241834]

114. Hess R, Jaeschke A, Neubert H, Hintze V, Moeller S, Schnabelrauch M, Wiesmann H-P, Hart DA, Scharnweber D. Biomaterials. 2012; 33:8975. [PubMed: 22995709]

115. Drury JL, Mooney DJ. Biomaterials. 2003; 24:4337. [PubMed: 12922147]

116. Lin Z-Y, Duan Z-X, Guo X-D, Li J-F, Lu H-W, Zheng Q-X, Quan D-P, Yang S-H. Journal of Controlled Release. 2010; 144:190. [PubMed: 20184932]

117. Jiang L, Sun H, Yuan A, Zhang K, Li D, Li C, Shi C, Li X, Gao K, Zheng C, Yang B, Sun H. J Biomed Nanotechnol. 2013; 9:1921. [PubMed: 24059091]

118. Fu S, Ni P, Wang B, Chu B, Zheng L, Luo F, Luo J, Qian Z. Biomaterials. 2012; 33:4801. [PubMed: 22463934]

119. Remya KR, Joseph J, Mani S, John A, Varma HK, Ramesh P. J Biomed Nanotechnol. 2013; 9:1483. [PubMed: 23980497]

120. Nandakumar A, Birgani ZT, Santos D, Mentink A, Auffermann N, Werf KVD, Bennink M, Moroni L, Blitterswijk CV, Habibovic P. Biofabrication. 2013; 5:015006. [PubMed: 23229020]

121. Akkouch A, Zhang Z, Rouabhia M. J Biomed Mater Res A. 2011; 96:693. [PubMed: 21284080]

122. Cui H, Liu Y, Deng M, Pang X, Zhang P, Wang X, Chen X, Wei Y. Biomacromolecules. 2012; 13:2881. [PubMed: 22909313]

123. Hench LL. J Am Ceram Soc. 1991; 74:1487.

124. Doremus RH. J Mater Sci. 1992; 27:285–297.

125. Hench LL. J Am Ceram Soc. 1998; 81:1705.

126. Best SM, Porter AE, Thian ES, Huang J. J Europ Ceram Soc. 2008; 28:1319.

127. Yuchun L, Jing L, Swee-Hin T. Biotechnol Adv. 2013; 31:688. [PubMed: 23142624]

128. Lichte P, Pape HC, Pufe T, Kobbe P, Fischer H. Injury Int J Care Injured. 2011; 42:569.

129. Bose S, Roy M, Bandyopadhyay A. Trends Biotechnol. 2012; 30:546. [PubMed: 22939815]

130. Rezwan K, Chen QZ, Blaker JJ, Boccaccini AR. Biomaterials. 2006; 27:3413. [PubMed: 16504284]

131. Hench LL. J Mater Sci: Mater Med. 2006; 17:967. [PubMed: 17122907]

132. Fu Q, Saiz E, Rahaman MN, Tomsia AP. Mater Sci Eng C Mater Biol Appl. 2011; 31:1245. [PubMed: 21912447]

133. Wu S-C, Hsu H-C, Hsiao S-H, Ho W-F. J Mater Sci: Mater Med. 2009; 20:229. [PubMed: 18758915]

134. Deb S, Mandegaran R, Silvio LD. J Mater Sci : Mater Med. 2010; 21:893. [PubMed: 20091103]

135. Wu C, Ramaswamy Y, Zreiqat H. Acta Biomaterialia. 2010; 6:2237. [PubMed: 20018260]

136. Huang Y, Jin X, Zhang X, Sun H, Tu J, Tang T. Biomaterials. 2009; 30:5041. [PubMed: 19545889]

137. Wu C, Chang J. J Biomed Mater Res B Appl Biomater. 2007; 83:153. [PubMed: 17318828]

138. Moawad HM, Jain H. J Mater Sci : Mater Med. 2012; 23:307. [PubMed: 22042462]

139. Webster TJ, Ergun C, Doremus RH, Siegel RW, Bizios R. Biomaterials. 2000; 21:1803. [PubMed: 10905463]

140. Marelli B, Ghezzi CE, Mohnc D, Stark WJ, Barralet JE, Boccaccini AR, Nazhat SN. Biomaterials. 2011; 32:8915. [PubMed: 21889796]

141. Zhou Y, Li H, Lin K, Zhai W, Gu W, Chang J. J Mater Sci : Mater Med. 2012; 23:2101. [PubMed: 22699712]

142. Bhakta S, Pattanayak DK, Takadama H, Kokubo T, Miller CA, Mirsaneh M, Reaney IM, Brook I, Noort Rv, Hatton PV. J Mater Sci Mater Med. 2010; 21:2979. [PubMed: 20725768]

143. Baino F, Ferraris M, Bretcanu O, Verne E, Vitale-Brovarone C. J Biomater Appl. 2013; 27:872. [PubMed: 22207602]

144. Liu X, Rahaman MN, Hilmas GE, Bal BS. Acta Biomaterialia. 2013; 9:7025. [PubMed: 23438862]

145. Doiphode N, Huang T, Leu M, Rahaman M, Day D. J Mater Sci Mater Med. 2011; 22

146. Deliormanli A, MN MR. J Eur Ceram Soc. 2012; 32:3637.

147. Chow L. Dent Mater J. 2009; 28:1. [PubMed: 19280963]

148. Albee F, Morrison H. Ann Surg. 1920; 71:32. [PubMed: 17864220]

149. Ray, R.; Ward, A, Jr. Surgical Forum. Vol. 429. American College of Surgeons WB Saunders Co; Philadelphia: 1951.

150. Chow, B. A New Calcium Phosphate, Water-Setting Cement. American Ceramic Society; Westerville, Ohio: 1987. p. 352

151. Yu L, Li Y, Zhao K, Tang Y, Cheng Z, Chen J, Zang Y, Wu J, Kong L, Liu S, Lei W, Wu Z. PLoS ONE. 2013; 8:e62660. [PubMed: 23671620]

152. Shepherd JH, Best SM. JOM. 2011; 63:83.

153. Zhao L, Weir M, Xu H. Biomaterials. 2010; 31:3848. [PubMed: 20149437]

154. Zhao L, Weir MD, Xu HHK. Biomaterials. 2010; 31:6502. [PubMed: 20570346]

155. Abarrategi A, Moreno-Vicente C, Martinez-Vazquez FJ, Civantos A, Ramos V, Sanz-Casado JV, Martinez-Corria R, Perera FH, Mulero F, Miranda P, Lopez-Lacomba JL. PLoS ONE. 2012; 7:34117.

156. Panseri S, Cunha C, D'Alessandro T, Sandri M, Russo A, Giavaresi G, Marcacci M, Hung CT, Tampieri A. PLoS ONE. 2012; 76:38710.

157. Teraoka K, Kato T, Hattori K, Ohgushi H. J Biomed Mater Res A. 2013; 00A:1.

158. Zhang F, Lin K, Chang J, Lu J, Ning C. J Eur Ceram Soc. 2007; 28:539.

159. Shuai C, Zhuang J, Hu H, Peng S, Liu D, Liu J. Biotechnol Appl Biochem. 2013; 60:266. [PubMed: 23600577]

160. Daculsi G, Passuti N, Martin S, Deudon C, Legeros R, Raher S. J Biomed Mater Res. 1990; 24

161. Houmard M, Fu Q, Genet M, Saiz E, Tomsia AP. J Biomed Mater Res, Part B. 2013; 101:1233.

162. Aarvold A, Smith JO, Tayton ER, Lanham SA, Chaudhuri JB, Turner IG, Oreffo ROC. J Biomed Mater Res Part A. 2013; 00A:1.

163. Jin S-C, Kim S-G, Oh J-S, Lee S-Y, Jang E-S, Piao Z-G, Lim S-C, Jeong M-A, Kim J-S, You J-S, Park S-C, Cho Y-S, Yang S-S, Yu S-K. J Biomed Nanotechnol. 2013; 9:475. [PubMed: 23621004]

164. Clafshenkel WP, Rutkowski JL, Palchesko RN, Romeo JD, McGowan KA, Gawalt ES, Witt-Enderby PA. J Pineal Res. 2012; 53:206. [PubMed: 22462771]

165. Merolli A, Santin M. Molecules. 2009; 14:5367. [PubMed: 20032899]

166. Yu L, Li Y, Zhao K, Tang Y, Cheng Z, Chen J, Zang Y, Wu J, Kong L, Liu S, Lei W, Wu Z. PLoS ONE. 2013; 8:e62570. [PubMed: 23638115]

167. Guillemin G, Meunier A, Dallant P, Christel. J Biomed Mater Res. 1989; 23:765. [PubMed: 2738087]

168. Hannouche D, Petite H, Sedel L. J Bone Joint Surg [Br]. 2001; 83-B:157.

169. Vuola J, Bohling T, Kinnunen J, Hirvensalo E, Asko-Seljavaara S. J Bioimed Mater Res. 200; 51:117.

170. de-la-Caffiniere JY, Viehweger E, Worcel A. Rev Chir Orthop Reparatrice Appar Mot. 1998; 84:501. [PubMed: 9846323]

171. Ripamonti U. J Bone Joint Surg Am. 1991; 73:692. [PubMed: 1675218]

172. Cui L, Liu B, Liu G, Zhang W, Cen L, Sun J, Yin S, Liu W, Cao Y. Biomaterials. 2007; 28:5477. [PubMed: 17888508]

173. Foo LH, Suzina AH, Azlina A, Kannan TP. J Biomed Mater Res Part A. 2007; 87:215.

174. Ripamonti U, Crooks J, Khoali L, Roden L. Biomaterials. 2009; 30:1428. [PubMed: 19081131]

175. Ripamonti U, Ma S-S, Reddi A. Plast Reconstr Surg. 1992; 89:731. [PubMed: 1312241]

176. Gao Z, Chen F, Zhang J, He L, Cheng X, Ma Q, Mao T. Br J Oral Maxillofac Surg. 2009; 47:116. [PubMed: 18992973]

177. Cai L, Wang Q, Gu C, Wu J, Wang J, Kang N, Hu J, Xie F, Yan L, Liu X, Cao Y, Xiao R. Biomaterials. 2011; 32:8497. [PubMed: 21855129]

178. Zheng Y-H, Su K, Jian Y-T, Kuang S-J, Zhang Z-G. J Tissue Eng Regen Med. 2011; 5:540. [PubMed: 21695795]

179. Tran CT, Gargiulo C, Thao HD, Tuan HM, Filgueira L, Strong DM. Cell Tissue Bank. 2011; 12:247. [PubMed: 20703817]

180. Manassero M, Viateau V, Deschepper M, Oudina K, Logeart-Avramoglou D, Petite H, Bensidhoum M. Tissue Eng Part A. 2013; 19:1554. [PubMed: 23427828]

181. Liu G, Zhang Y, Liu B, Sun J, Li W, Cui L. Biomaterials. 2013; 34:2655. [PubMed: 23343633]

182. Greenfield, EJ. Inventor, Mounting of artificial teeth. U S Patent Office. 478360. 1909.

183. Rudy RJ, Levi PA, Bonacci FJ, Weisgold AS, Engler-Hamm D. Compendium. 2008; 29:2.

184. Levine B. Adv Eng Mater. 2008; 10:788.

185. Galante J, Rostoker W, Lueck R, Ray RD. J Bone Joint Surg Ser A. 1971; 53:101.

186. Alvarez K, Nakajima I. Materials. 2009; 2:790.

187. Staiger MP, Pietak AM, Huadmai J, Dias G. Biomaterials. 2006; 27:1728. [PubMed: 16246414]

188. Kokubo T, Kim H-M, Kawashita M, Nakamura T. J Mater Sci -Mater Med. 2004; 15:99. [PubMed: 15330042]

189. Bansiddhi A, Sargeant TD, Stupp SI, Dunand DC. Acta Biomaterialia. 2008; 4:773. [PubMed: 18348912]

190. Wu S, Liu X, Hu T, Chu PK, Ho JPY, Chan YL, Yeung KWK, Chu CL, Hung TF, Huo KF, Chung CY, Lu WW, Cheung KMC, Luk KDK. Nano Lett. 2008; 8:3803. [PubMed: 18950232]

191. Haugen HJ, Monjo M, Rubert M, Verket A, Lyngstadaas SP, Ellingsen JE, Rønold HJ, Wohlfahrt JC. Acta Biomaterialia. 2013; 9:5390. [PubMed: 22985740]

192. Wohlfahrt JC, Monjo M, Rnold HJ, Aass AM, Ellingsen JE, Lyngstadaas SP. Clin Oral Impl Res. 2010; 21:165.

193. Fassina L, Visai L, Benazzo F, Benedetti L, Calligaro A, Angelis MCD, Farina A, Maliardi V, M GG. Tissue Eng. 2006; 12:1985. [PubMed: 16889527]

194. Fassina L, Saino E, Visai L, Silvani G, Angelis MGCD, Mazzini G, Benazzo F, Magenes G. J Biomed Mater Res A. 2008; 87:750. [PubMed: 18200542]

195. Reiner T, Kababya S, Gotman I. J Mater Sci : Mater Med. 2008; 19:583. [PubMed: 17619961]

196. Tiainen H, Lyngstadaas SP, Ellingsen JE, Haugen HVJ. J Mater Sci : Mater Med. 2010; 21:2783. [PubMed: 20711636]

197. Gómez-Florit M, Rubert M, Ramis JM, Haugen HJ, Tiainen H, Lyngstadaas SP, Monjo M. J Biomater Tissue Eng. 2012; 2:336.

198. Li Y, Xiong J, Hodgson PD, Wen CE. J Alloys Compd. 2010; 494:323.

199. Bobe K, Willbold E, Morgenthal I, Andersen O, Studnitzky T, Nellesen J, Tillmann W, Vogt C, Vano K, Witte F. Acta Biomaterialia. 2013; 9:8611. [PubMed: 23542554]

200. Chou D-T, Wells D, Hong D, Lee B, Kuhn H, Kumta PN. Acta Biomaterialia. 2013; 9:8593. [PubMed: 23624222]

201. Witte F, Reifenrath J, Müller P, Crostack H, Nellesen J, B F, Bormann D, Ruder M. Materialwissenschaft und Werkstofftechnik Special Issue: Biomaterials. 2006; 37:504.

202. Erol MM, Mouri o V, Newby P, Chatzistavrou X, Roether JA, Hupa L, Boccaccini AR. Acta Biomaterialia. 2012; 8:792. [PubMed: 22040685]

203. Liu Y, LIm J, Teoh S-H. Biotechnol Adv. 2013; 31:688. [PubMed: 23142624]

204. Smith L. Arch Surg. 1963; 87:653. [PubMed: 14056248]

205. Cook GB, Andrew W, Schewe EJ. Am J Surg. 1965; 110:568. [PubMed: 5825169]

206. Kim HJ, Kim U-J, Kim HS, Li C, Wada M, Leisk GG, Kaplan DL. Bone. 2008; 42:1226. [PubMed: 18387349]

207. X, Li; Xie, I.; Lipner, J.; Yuan, X.; Thomopoulos, S.; Xia, Y. Nano Lett. 2009; 9:2763. [PubMed: 19537737]

208. Nandakumar A, Yang L, Habibovic P, Blitterswijk CV. Langmuir. 2010; 26:7380. [PubMed: 20039599]

209. Moroni L, Schotel R, Hamann D, Wijn JRd, Blitterswijk CAV. Adv Funct Mater. 2008; 18:53.

210. Yang F, Both SK, Yang X, Walboomers XF, Jansen JA. Acta Biomaterialia. 2009; 5:3295. [PubMed: 19470413]

211. Reichert JC, Wullschleger ME, Cipitria A, Lienau J, Cheng TK, Schütz MA, Duda GN, Nöth U, Eulert J, Hutmacher DW. Int Orthop (SICOT). 2011; 35:1229.

212. Gibson LJ. J Biomech. 1985; 18:317. [PubMed: 4008502]

213. Schofer A, Veltum C, T E, et al. J Mater Sci -Mater Med. 2011; 22:1753. [PubMed: 21604139]

214. Wang C, Meng G, Zhang L, Xiong Z, Liu J. J Biomed Biotechnol. 2012; 2012:1. [PubMed: 21836813]

215. Gao C, Hu X, Hong Y, Guan J, Shen J. J Biomater Sci Polym Ed. 2003; 14:937. [PubMed: 14661871]

216. Thein-Han WW, Xu HHK. Tissue Eng Part A. 2011; 17:2943. [PubMed: 21851269]

217. Brodie JC, Goldie E, Connel G, Merry J, Grant MH. J Biomed Mater Res A. 2005; 73:409. [PubMed: 15892144]

218. Parenteau-Bareil R, Gauvin R, Berthod F. Materials. 2010; 3:1863.

219. Lee JB, Park HN, Ko W-K, Bae MS, Heo DN, Yang DH, Kwon IK. J Biomed Nanotechnol. 2013; 9:424. [PubMed: 23620998]

220. Shalumon KT, Sowmya S, Sathish D, Chennazhi KP, Nair SV, Jayakumar R. J Biomed Nanotechnol. 2013; 9:430. [PubMed: 23620999]

221. Sun F, Kang HG, Ryu S-C, Kim JE, Park EY, Hwang DY, Lee J. J Biomed Nanotechnol. 2013; 9:1914. [PubMed: 24059090]

222. Kim J, Sharma A, Runge B, Waters H, Doll B, McBride S, Alvarez P, Dadsetan M, Yaszemski MJ, Hollinger JO. Tissue Eng Regen Med. 2012; 6:404.

223. Zaky SH, Cancedda R. J Dent Res. 2009; 88:1077. [PubMed: 19897785]

224. Ge S, Zhao N, Wang L, Yu M, Liu H, Song A, Huang J, Wang G, Yang P. Int J Nanomedicine. 2012; 7:5405. [PubMed: 23091383]

225. An S-H, Matsumoto T, Miyajima H, Nakahira A, Kim K-H, Imazato S. Dent Mater. 2012; 28:1221. [PubMed: 23018082]

226. Pamula E, Kokoszka J, Cholewa-Kowalska K, Laczka M, Kantor L, Niedzwiedzki L, Reilly GC, Filipowska J, Madej W, Kolodziejczyk M, Tylko G, Osyczka AM. Ann Biomed Eng. 2011; 39:2114. [PubMed: 21487840]

227. Li X, Shi JL, Dong XP, Zhang LX, Zeng HY. J Biomed Mater Res Part A. 2008; 84A:84.

228. Wu F, Liu C, O'Neill B, Weib J, Ngothai Y. Appl Surf Sci. 2012; 258:7589.

229. Srinivasan S, Kumar PTS, Nair SV, Nair SV, Chennazhi KP, Jayakumar R. J Biomed Nanotechnol. 2013; 9:1803. [PubMed: 24059080]

230. Geng F, Tan L, Zhang B, Wu C, He Y, Yang J, Yang K. J Mater Sci Technol. 2009; 25:123.

231. Barrere F, CM VDV, Meijer G, Dalmeijer RA, Groot KD, Layrolle P. J Biomed Mater Res B Appl Biomater. 2003; 67:655. [PubMed: 14528464]

232. Basini G, Grasselli F, Bussolati S, Baioni L, Bianchi F, M MM, Careri M, Mangia A. Steroids. 2011; 76:1433. [PubMed: 21827779]

233. Fan W, Crawford R, Xiao Y. Biomaterials. 2010; 31:3580. [PubMed: 20153522]

234. Wu C, Zhou Y, Fan W, Han P, Chang J, Yuen J, Zhang M, Xiao Y. Biomaterials. 2012; 33:2076. [PubMed: 22177618]

235. Masonis JL, Bourne RB, Ries M, McCalden RW, Salehi A, Kelman DC. J Arthroplasty. 2004; 19:898. [PubMed: 15483807]

236. Manicone PF, Iommetti PR, Raffaelli L. J Dent. 2007; 35:819. [PubMed: 17825465]

237. Mondal D, So-Ra S, Sarkar SK, Min YK, Yang HM, Lee BT. J Biomater Appl. 2012; 28:462. [PubMed: 23064831]

238. Giavaresi P, Torricelli PM, Fornasari R, Giardino R, Leone G. Biomaterials. 2005; 26:3001. [PubMed: 15603795]

239. Gu Z, Hao Wang, Li L, Wang Q, Yu X. Biomed Mater. 2012; 7:1.

240. Wang Q, Song W, Wang Q, Zhang X, Yu X, Wan C. J Funct Mater. 2009; 40:1506.

241. Xie H, Wang Q, Ye Q, Wan C, Li L. J Mater Sci : Mater Med. 2012; 23:1033. [PubMed: 22311075]

242. Ewald A, Kappel C, Vorndran E, Moseke C, Gelinsky M, Gbureck U. J Biomed Mater Res A. 2012; 100:2392. [PubMed: 22528604]

243. Wu C, Zhou Y, Xu M, Han P, Chen L, Chang J, Xiao Y. Biomaterials. 2013; 34:422. [PubMed: 23083929]

244. Dimitrievska S, Bureau MN, Antoniou J, Mwale F, Petit A, Lima RS, Marple BR. J Biomed Mater Res Part A. 2011; 98A:576.

245. Srivastava AK, Pyare R, Singh SP. J Biomater Tissue Eng. 2012; 2:249.

246. Lagoa ALC, Wedemeyer C, Knoch Mv, Löer F, Epple M. J Mater Sci : Mater Med. 2008; 19:417. [PubMed: 17607522]

247. Helary G, Noirclere F, Mayingi J, Migonney V. Acta Biomaterialia. 2009; 5:124. [PubMed: 18809363]

248. Michiardi A, Hélary G, Nguyen P-CT, Gamble LJ, Anagnostou F, Castner DG, Migonney V. Acta Biomaterialia. 2010; 6:667. [PubMed: 19733698]

249. Oughlis S, Lessim S, Changotade S, Bollotte F, Poirier F, Helary G, Lataillade JJ, Migonneya V, Lutomskia D. J Chromatogr B. 2011; 879:3681.

250. Shoichet MS. Macromolecules. 2010; 43:581.

251. Johnson AJW, Herschler BA. Acta Biomaterialia. 2011; 7:16. [PubMed: 20655397]

252. Karageorgiou V, Kaplan D. Biomaterials. 2005; 26:5474. [PubMed: 15860204]

253. Dhandayuthapani B, Yoshida Y, Maekawa T, Kumar DS. Int J Polymer Sci. 2011; 290602:1.

254. Niu L-N, Jiao K, Qi Y-P, Nikonov S, Yiu CKY, Arola DD, Gong S-Q, El-Marakby A, Carrilho MRO, Hamrick MW, Hargreaves KM, Diogenes A, Chen J-H, Pashley DH, Tay FR. FASEB J. 2012; 26:4517. [PubMed: 22859369]

255. Gong J, Si W, Guan Z. J Mater Sci. 2001; 36:2391.

256. Bazant ZP. J Eng Mech. 1996; 122:138.

257. Deng M, Kumbar SG, Nair LS, Weikel AL, Allcock HR, Laurencin CT. Adv Funct Mater. 2011; 21:2641.

258. Buschmann J, Welti M, Hemmi S, Neuenschwander P, Baltes C, Giovanoli P, Rudin M, Calcagni M. Tissue Eng Part A. 2011; 17:291. [PubMed: 20799888]

259. Aguirre A, Planell JA, Engel E. Biochemical and Biophysical Research Communications. 2010; 400:284. [PubMed: 20732306]

260. Unger RE, Ghanaati S, Orth C, Sartoris A, Barbeck M, Halstenberg S, Motta A, Migliaresi C, Kirkpatrick CJ. Biomaterials. 2010; 31:6959. [PubMed: 20619788]

261. Xing Z, Xue Y, Finne-Wistrand A, Yang Z-Q, Mustafa K. J Biomed Mater Res Part A. 2013; 101:1113.

262. Tortelli F, Pujic N, Liu Y, Laroche N, Vico L, Cancedda R. Tissue Eng Part A. 2009; 15:2373. [PubMed: 19292676]

263. Ruggiu A, Tortelli F, Komlev VS, Peyrin F, Cancedda R. J Tissue Eng Regen Med. 201210.1002/term.1559

264. Haynes DR, Crotti TN, Loric M, Bain GI, Atkins GJ, Findlay DM. Rheumatology (Oxford, England). 2001; 40:623.

265. Pirraco RP, Reis RL, Marques AP. J Tissue Eng Regen Med. 2013; 7:392. [PubMed: 22392849]

266. Voog J, Jones D. Cell. 2010; 6:103.

267. Chen, Y.; Maas, R. Signaling loops in the reciprocal epithelialmesenchymal interactions of mammalian tooth development. In: Chuong, C-M.; Landes, RG., editors. Molecular Basis of Epithelial Appendage Morphogenesis. Austin, TX: 1998. p. 282-365.

268. Centrella M, Horowitz M, Wozney J, McCarthy T. Endocr Rev. 1994; 15:27. [PubMed: 8156937]

269. Maeda S, Hayashi M, Komiya S, Imamura T, Miyazono K. EMBO J. 2004; 23:552. [PubMed: 14749725]

270. Chen G, Deng C, Li Y. Int J Biol Sci. 2012; 8:272. [PubMed: 22298955]

271. Service R. Science. 2000; 289:1498. [PubMed: 10991738]

272. Shimoaka T, Ogasawara T, Yonamine A, Chikazu D, Kawano H, Nakamura K, Itoh N, Kawaguchi H. J Biol Chem. 2002; 277:7493. [PubMed: 11741978]

273. Du C, Meijer GJ, Valk Cvd, Haan RE, Bezemer JM, Hesseling SC, Cui FZ, Groot Kd, Layrolle P. Biomaterials. 2002; 23:4649. [PubMed: 12322986]

274. Simpson A, Mills L, Noble B. J Bone Joint Surg Br. 2006; 88:701. [PubMed: 16720758]

275. Gaur T, Lengner C, Hovhannisyan H, Bhat R, Bodine P, Komm B, Javed A, Wijnen Av, Stein J, Stein G, Lian J. J Biol Chem. 2005; 280:33132. [PubMed: 16043491]

276. Fei Y, Xiao L, Doetschman T, Coffin D, Hurley M. J Biol Chem. 2011; 286:40575. [PubMed: 21987573]

277. Yuasa T, Kataoka H, Kinto N, Iwamoto M, Enomoto-Iwamoto M, Iemura S, Ueno N, Shibata Y, Kurosawa H, Yamaguchi A. J Cell Physiol. 2002; 193:225. [PubMed: 12385000]

278. Cai J, Huang Y, Chen X, Xie H, Zhu H, Tang L, Yang Z, Huang Y, Deng L. Cell Biol Int. 2012; 36:349. [PubMed: 22149964]

279. Luu Y, Pessin J, Judex S, Rubin J, Rubin C. Bonekey Osteovision. 2009; 6:132. [PubMed: 22241295]

280. Huang C, Ogawa R. FASEB J. 2010; 24:3625. [PubMed: 20505115]

281. Thompson W, Rubin C, Rubin J. Gene. 2012; 503:179. [PubMed: 22575727]

282. Yeatts A, Choquette D, Fisher J. Biochim Biophys Acta. 2013; 1830:2470. [PubMed: 22705676]

283. Ferraro J, Daneshmand M, Bizios R, Rizzo V. Am J Physiol Cell Physiol. 2004; 286:831.

284. Nagatomi J, Arulanandam B, Metzger D, Meunier A, Bizios R. Ann Biomed Eng. 2003; 31:917. [PubMed: 12918906]

285. Hess R, Douglas T, Myers K, Rentsch B, Rentsch C, Worch H, Shrive N, Hart D, Scharnweber D. J Biomech Eng. 2010; 132:021001. [PubMed: 20370238]

286. Kanczler J, HS HS, Magnay J, Green D, Oreffo R, Dobson J, Haj AE. Tissue Eng Part A. 2010; 16:3241. [PubMed: 20504072]

287. Bassett C, Pawluk R, Pilla A. Ann N Y Acad Sci. 1974; 238:242. [PubMed: 4548330]

288. Evans R, Foltz D, Foltz K. Clin Podiatr Med Surg. 2001; 118:79. [PubMed: 11344981]

289. Aaron R, Ciombor D, Simon B. Clin Orthop Relat Res. 2004; 419:21. [PubMed: 15021127]

290. Aaron R, Steinberg M. Semin Arthroplasty. 1991; 2:214. [PubMed: 10149658]

291. Yang Y, Tao C, Zhao D, Li F, Zhao W, Wu H. Bioelectromagnetics. 2010; 31:277. [PubMed: 20041434]

292. Hronik-Tupaj M, Kaplan D. Tissue Eng Part B Rev. 2012; 18:167. [PubMed: 22046979]

293. Creecy C, O'Neill C, Arulanandam B, Sylvia V, Navara C, Bizios R. Tissue Eng Part A. 2013; 19:467. [PubMed: 23083071]

294. Diniz P, Shomura K, Soejima K, Ito G. Bioelectromagnetics. 2002; 23:398. [PubMed: 12111759]

295. Jansen J, Jagt OVD, Punt B, Verhaar J, Leeuwen JV, Weinans H, Jahr H. BMC Musculoskelet Disord. 2010; 11:188. [PubMed: 20731873]

296. Currey, JD. Cortical bone. In: Black, J.; Hastings, G., editors. Handbook of Biomaterial Properties. Chapman and Hall; London: 1998. p. 3

297. Jee, W. The skeletal tissues. In: Weiss, L., editor. Histology: Cell and Tissue Biology. Elsevier Science Ltd.; New York: 1983. p. 206

298. Athanasiou K, Zhu C, Lanctot D, Agrawal C, Wang X. Tissue Eng. 2000; 6:361. [PubMed: 10992433]

299. Wang X, Li Y, Hodgson P, Wen C. Mater Forum. 2007; 31:156.

300. Ratanavaraporn J, Damrongsakkul S, Kanokpanont S, Yamamoto M, Tabata Y. J Biomater Sci. 2011; 22:1083.

301. Nandi SK, Kundu B, Basu D. Materials Science and Engineering: C. 2013; 33:1267. [PubMed: 23827571]

302. Wang L, Stegemann JP. Biomaterials. 2010; 31:3976. [PubMed: 20170955]

303. Correia C, Bhumiratana S, Yan L-P, Oliveira AL, Gimble JM, Rockwood D, Kaplan DL, Sousa RA, Reis RL, Vunjak-Novakovic G. Acta Biomaterialia. 2012; 8:2483. [PubMed: 22421311]

304. Riccio M, Maraldi T, Pisciotta Alessandra, Sala GBL, Ferrari A, Bruzzesi G, Motta A, Migliaresi C, Pol AD. Tissue Eng Part A. 2012; 18:9.

305. Zhao L, Weir MD, Xu HHK. Biomaterials. 2010; 31:6502. [PubMed: 20570346]

306. Suarez-Gonzalez D, Barnhart K, Saito E, Vanderby R, Hollister SJ, Murphy WL. J Biomed Mater Res Part A. 2010; 95A:222.

307. Jha AK, Xu X, Duncan RL, Jia X. Biomaterials. 2011; 32:2466. [PubMed: 21216457]

308. Kisiel M, Martino MM, Ventura M, Hubbell JA, Hilborn J, Ossipov DA. Biomaterials. 2013; 34:704. [PubMed: 23103154]

309. Mari-Buye N, Luque T, Navajas D, Semino CE. Tissue Eng Part A. 2013; 19:870. [PubMed: 23157379]

310. Tsai W-B, Chen Y-R, Liu H-L, Lai J-Y. Carbohydrate Polymers. 2011; 85:129.

311. Jabbarzadeh E, Deng M, Lv Q, Jiang T, Khan YM, Nair LS, Laurencin CT. J Biomed Mater Res Part B. 2012; 100B:2182.

312. Seyednejad H, Gawlitta D, Dhert WJA, Nostrum CFV, Vermonden T, Hennink WE. Acta Biomaterialia. 2011; 7:1999. [PubMed: 21241834]

313. Grafahrend D, Heffels K-H, Beer MV, Gasteier P, Möller M, Boehm G, Dalton PD, Groll J. Nat Mater. 2010; 10:67. [PubMed: 21151163]

314. Dånmark S, Finne-Wistrand A, Wendel M, Arvidson K, Albertsson A-C, Mustafa K. Journal of Bioactive and Compatible Polymers. 2010; 25:207.

315. Fernandez JM, Molinuevo MS, Cortizo AM, McCarthy AD, Cortizo MS. J Biomater Sci. 2010; 21:1297.

316. Lin Z-Y, Duan Z-X, Guo X-D, Li J-F, Lu H-W, Zheng Q-X, Quan D-P, Yang S-H. Journal of Controlled Release. 2010; 144:190. [PubMed: 20184932]

317. Nandakumar A, Birgani ZT, Santos D, Mentink A, Auffermann N, derWerf KV, Bennink M, Moroni L, Blitterswijk CV, Habibovic P. Biofabrication. 2013; 5:1.

318. Wu C, Ramaswamy Y, Zhu YF, Zheng R, Appleyard R, Howard A, Zreigat H. Biomaterials. 2009; 30:2199. [PubMed: 19203787]

319. Shuai C, Zhuang J, Hu H, Peng S, Liu D, Liu J. Biotechnol Appl Biochem. 2013; 60:266. [PubMed: 23600577]

320. Manassero M, Oudina K, Viateau Vr, Logeart-Avramoglou D, Petite H, Deschepper M, Bensidhoum M. Tissue Eng Part A. 2013; 19:1554. [PubMed: 23427828]

321. Huang S-L, Wen B, Bian W-G, Yan H-W. Med Sci Monit. 2012; 18:435.

322. Martel-Estrada SA, Olivas-Armendáriz, Martínez-Pérez CA, Hernández T, Acosta-Gómez EI, Chacón-Nava JG, Jiménez-Vega F, García-Casillas PE. J Mater Sci : Mater Med. 2012; 23:2893. [PubMed: 22960878]

323. Li M, Liu W, Sun J, Xianyu Y, Wang J, Zhang W, Zheng W, Huang D, Di S, Long Y-Z, Jiang X. ACS Appl Mater Interfaces. 2013; 5:5921. [PubMed: 23790233]

324. Foroughi MR, Karbasi S, Ebrahimi-Kahrizsangi R. J Nanosci Nanotechnol. 2013; 13:1555. [PubMed: 23646681]

325. Kushwaha M, Pan X, Holloway JA, Denry IL. Dent Mater. 2012; 28:252. [PubMed: 22078764]

326. Mayingi, J.; Hélary, G.; Noirclere, F.; Bacroix, B.; Migonney, V. Proceedings of the 29th Annual International. Conference of the IEEE EMBS; Lyon, France. August 23–26; 2007.

327. Oughlis S, Lessim S, Changotade S, Poirier F, Bollotte F, Peltzer J, Felgueiras H, Migonney V, Lataillade JJ, Lutomski D. J Biomed Mater Res Part A. 2013; 101A:582.

Biographies

Liliana Polo-Corrales is a Postdoctoral Scholar in the Engineering Science and Materials Department at the University of Puerto Rico—Mayaguez (UPRM). She has undergraduate graduate and degrees in Chemical Engineering from Universidad del Atlántico—Barranquilla, Colombia and UPRM, respectively. During her graduate studies she worked with magnetic nanoparticles for biomedical applications. Her research interests include nanomedicine in the development of multifunctional nanoparticles for cancer detection and

treatment, and regenerative medicine of the bone in the development of biomimetic 3D scaffolds with electromagnetic stimulation.
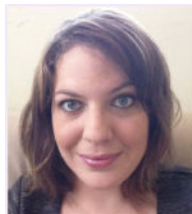
Magda Latorre-Esteves is an Assistant Researcher in the Chemical Engineering Department of the UPRM. She has an Undergraduate Degree in Biology from UPRM and a Graduate Degree in Microbiology and Molecular Genetics from Harvard Medical School. Her postdoctoral training was in nanoparticle/cell interactions at the Chemical Engineering Department in UPRM. Her research interests include nanomedicine for the treatment of genetic diseases, regenerative medicine, and molecular mechanisms of disease.


Jaime E. Ramirez-Vick is Professor and Director of the Engineering Science and Materials Department at UPRM. He has graduate and undergraduate degrees in Chemical Engineering from UPRM and Arizona State University, with postdoctoral training at the Lawrence Berkeley National Lab and the Cancer Center of the University of California—San Francisco. He is co-founder of two microarray-based diagnostic companies in northern California. His research interests include nanomedicine for cancer detection and treatment, regenerative medicine of the bone, and biosensors based on nanostructures.
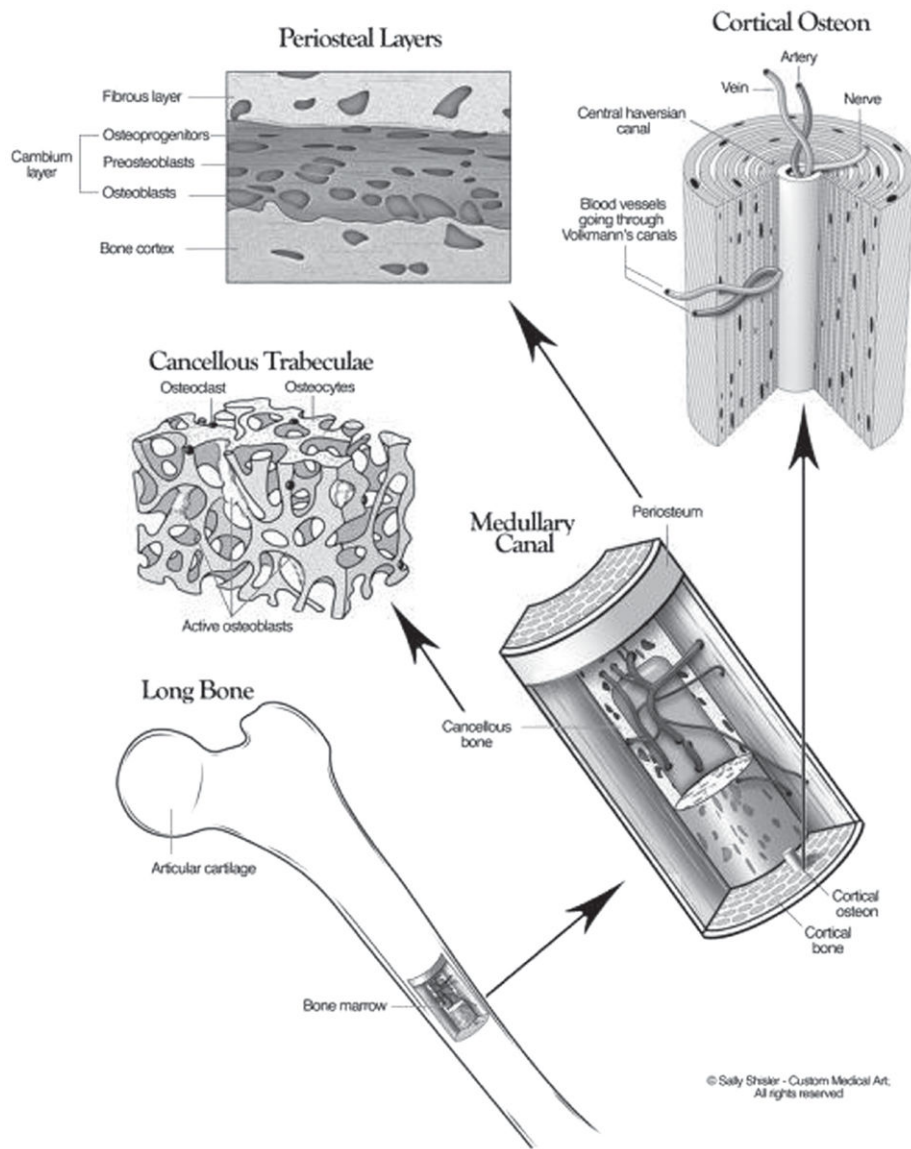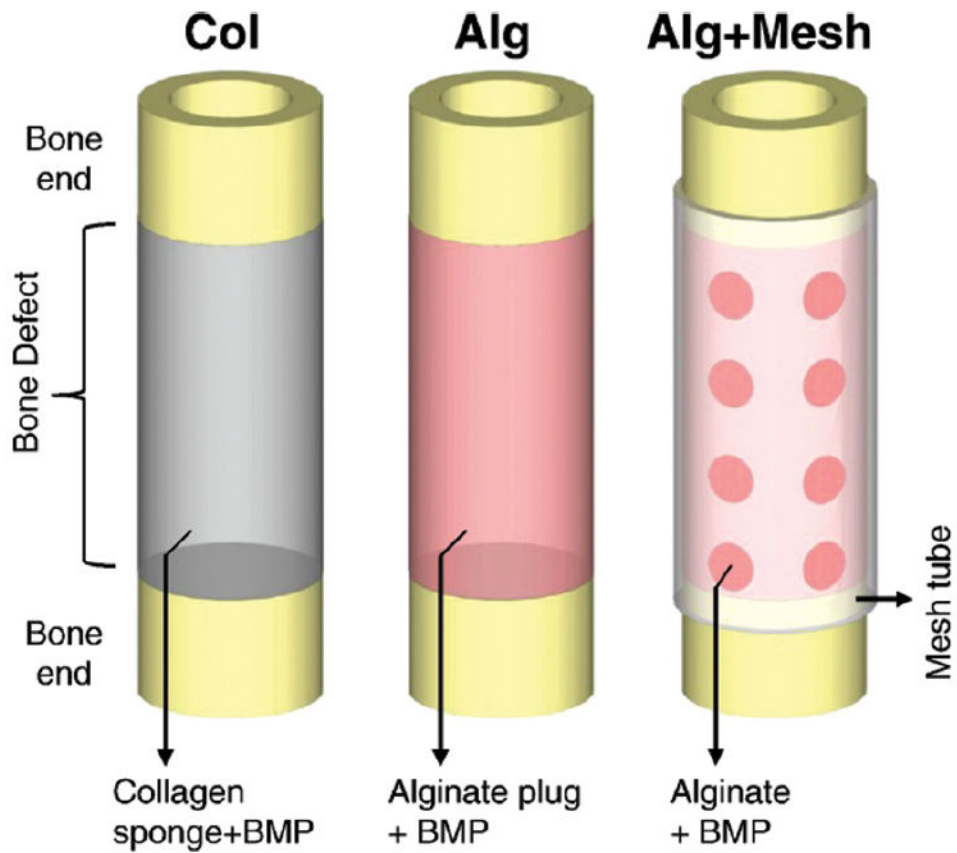
Figure 1.
The three-dimensional structure of bone, which includes the cortical and a cancellous/trabecular component. Reprinted with permission from [12], D. Buck II and G. Dumanian, *Plast Reconstr Surg*. 129, 1314 (**2012**). © 2012, American Society of Plastic Surgeon.
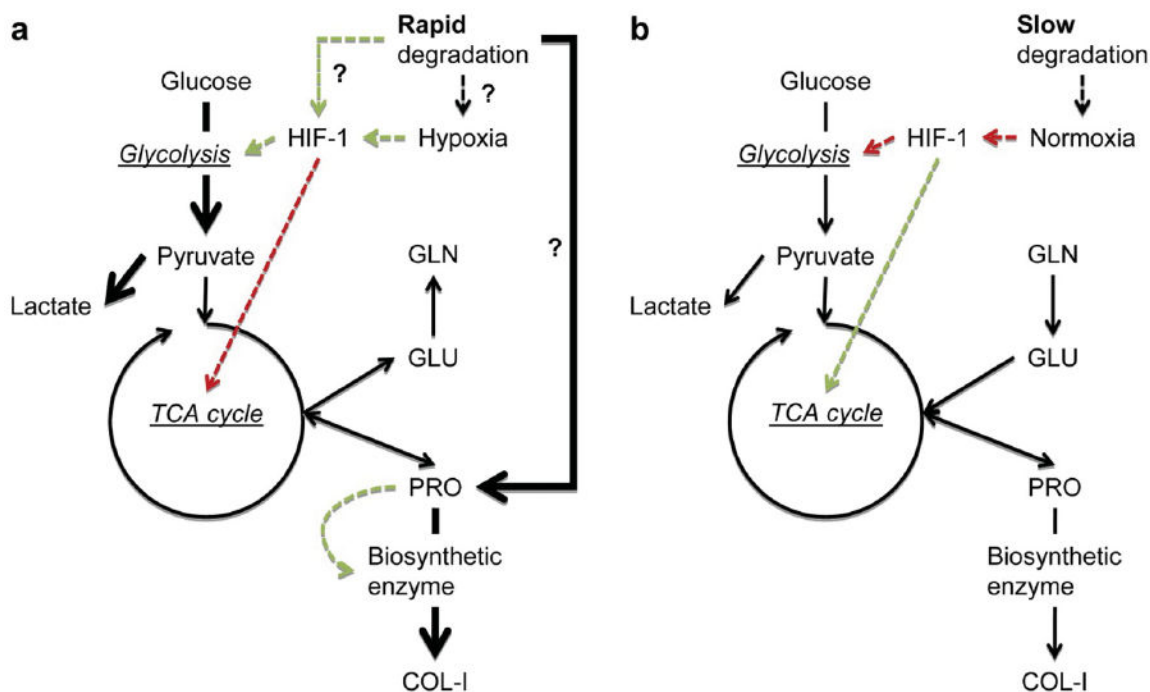
Figure 2.
Illustration of cellular metabolism-scaffold degradation model describing bone remodeling with fluxes representing expected pathways leading to the formation of new bone. (a) Model for rapidly degrading scaffold, and (b) model for slow degrading scaffolds. Solid arrows: metabolic flux. Dashed arrows: signal transduction. Colors: red a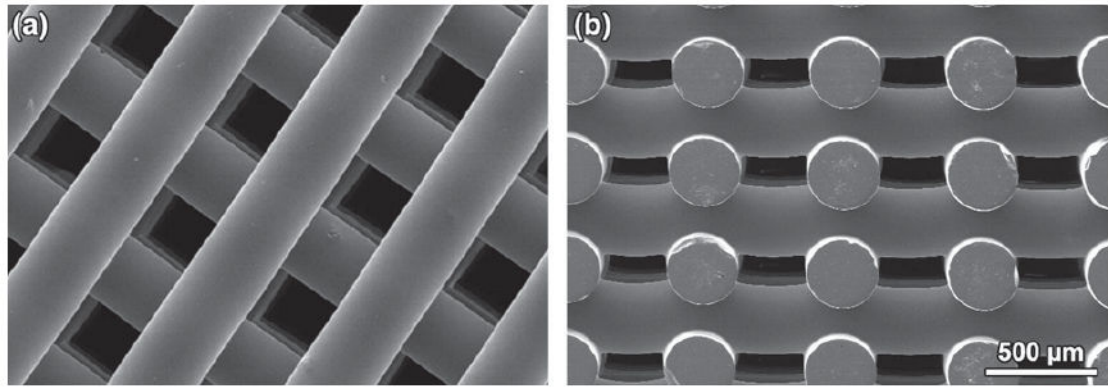nd inhibition; green and activation. Reprinted with permission from [77], S.-H. Park, et al., *Biomaterials* 31, 6162 (**2010**). © 2010, Elsevier.
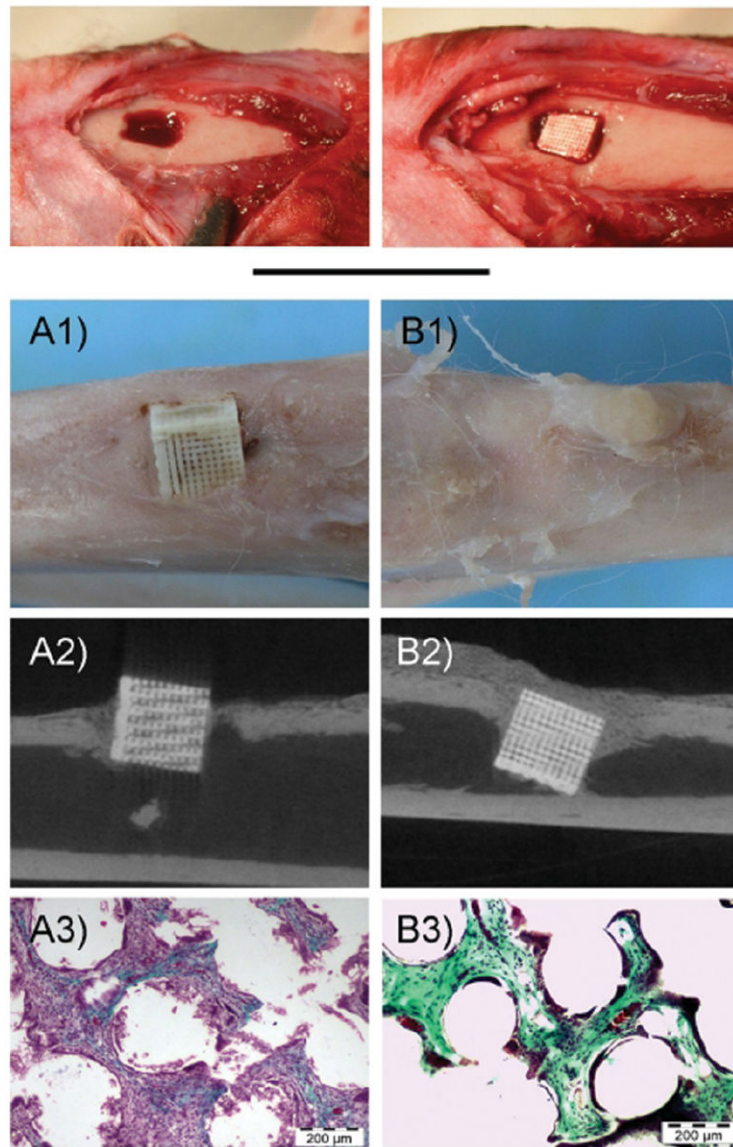
Figure 3.
Schematic representations of the three protein delivery strategies: Collagen sponge-rhMBP-2, Alginate-BMP-2 and Alginate-rhBMP-2. Reprinted with permission from [86], Y. M. Kolambkar, et al., *Bone* 49, 485 (**2011**). © 2011, Elsevier.

Figure 4.
SEM images of silicate 13–93 bioactive glass scaffolds which were prepared by robo-casting: (a) plane of deposition (xy plane); (b) perpendicular to the deposition plane (*z* direction). Reprinted with permission from [144], X. Liu, et al., *Acta Biomaterialia* 9, 7025 (**2013**). © 2013, Elsevier.
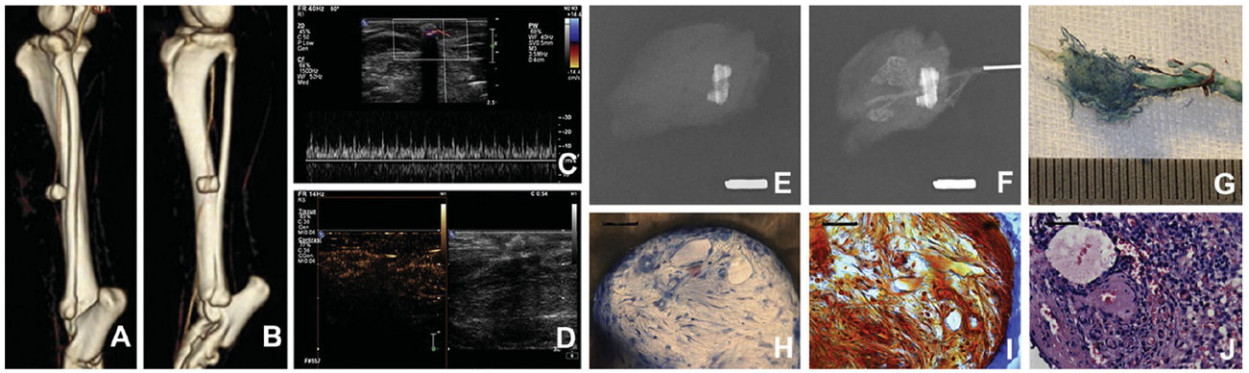
Figure 5.
Photograph showing the Implantation of Ceramic Scaffolds with BMP-2 in rabbit bone. Top, images of the surgical procedure. (A) control scaffolds, (B) BMP-2 adsorbed scaffolds. (1) Gross appearance of harvested samples, (2) Representative mCT slides, (3) Representative histological images (Massons tricrome stainings). Reprinted with permission from [155], A. Abarrategi, et al., *PLoS ONE* 7, 34117 (**2012**). © 2012, PloS ONE.

Figure 6.
Images demonstrating the vascularization of cell-CHA constructs at 4 weeks post-implantation using MSC-coral hydroxyapatite scaffold. CT angiography (A), (B) and ultrasonic inspection (C), (D). X-ray before and after vascular corrosion cast (E), (F) and vascular corrosion cast (G). HE and Masson's trichrome staining of cell-CHA constructs in undecalcification sections (H), (I); and HE staining in decalcification sections (J). Scale bars: 10 mm (F), (G), 50 mm (H)–(J). Reprinted with permission from [177], L. Cai, et al., *Biomaterials* 32, 8497 (**2011**). © 2011, Elsevier.
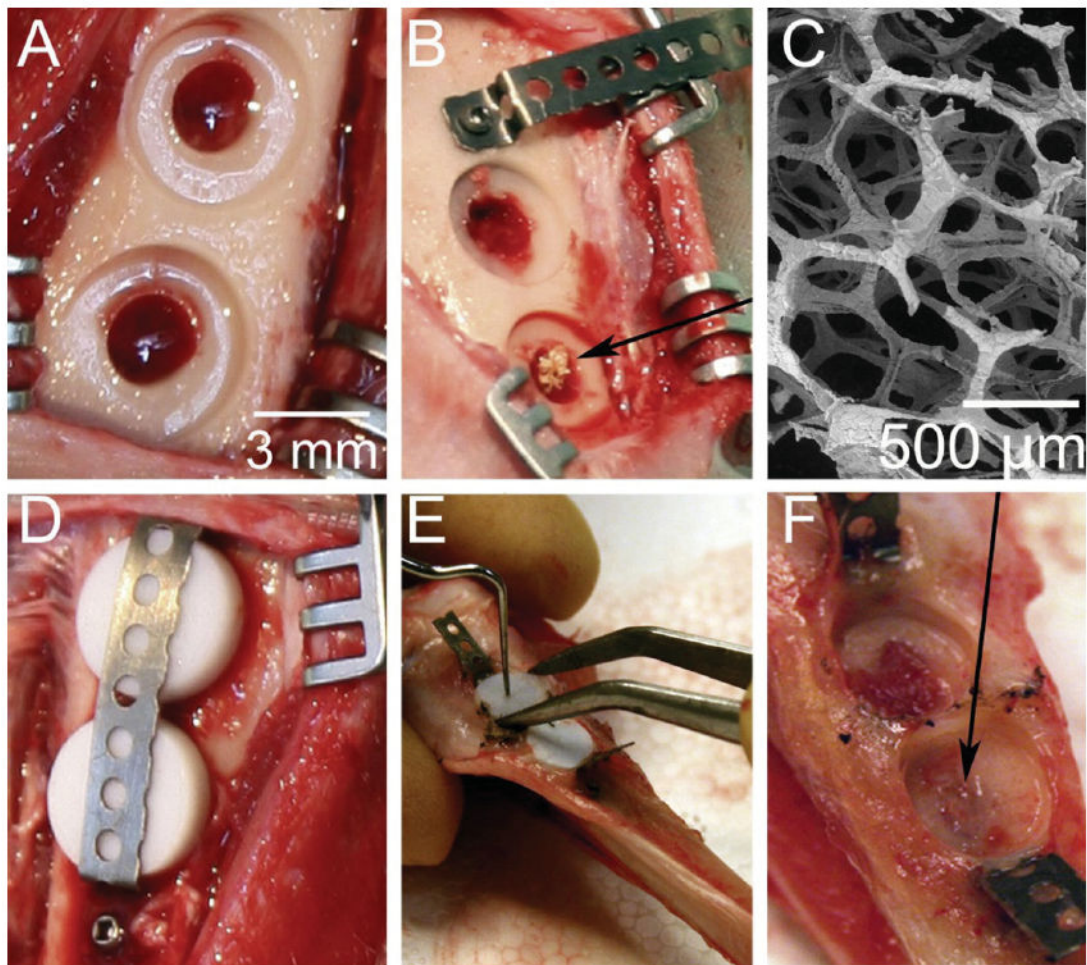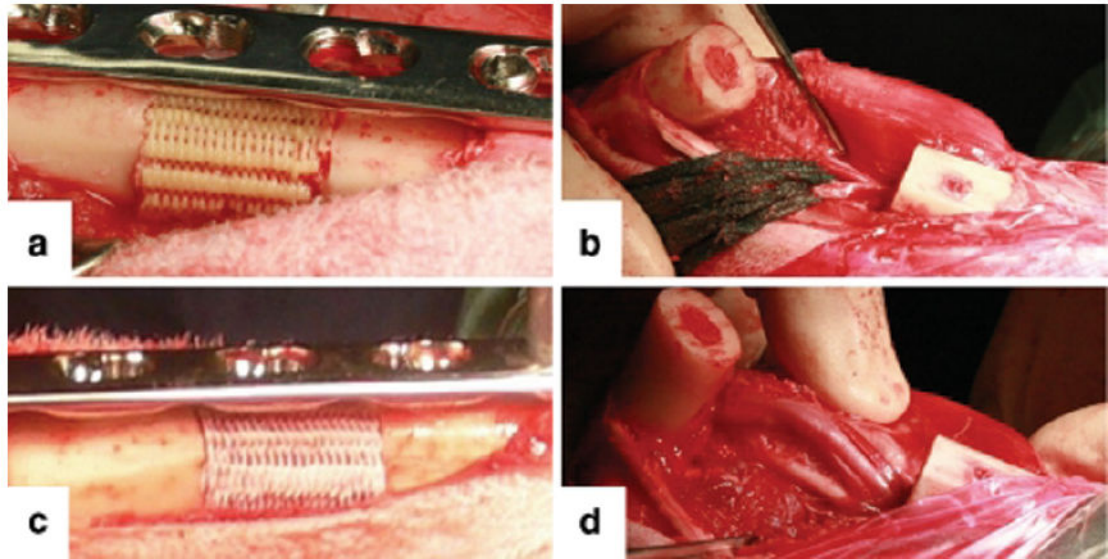
Figure 7.

Illustration showing the Wound chamber model in the tibia of New Zealand White rabbits using Ti and TiO$_2$ scaffolds. Two defects of diameter 3 mm were made in the rabbit tibia (A) and the TiO$_2$ scaffold (black arrow) was placed through the cortical defect and into the bone marrow and the sham defect left empty (B). SEM images of the TiO$_2$ scaffold prior to implantation (C). Titanium coins which were placed on top of the defect to simulate a peri-implant situation. Teflon caps were placed on top of the coins to prevent bone growth on the side and a titanium band was placed to prevent the discs falling out (D). After healing, the band was carefully cut, and the Teflon caps were removed (E). The peri-implant bone attached to the extracted titanium discs was analyzed with real-time RT-PCR. The wound fluid was collected from the wound site with filter papers to test for cytotoxicity (F). The bone tissue was further analyzed with micro-CT and histology. The black arrow shows that the TiO$_2$ scaffold promoted a complete healing of the cortical defect. Reprinted with permission from [191], H. J. Haugen, et al., *Acta Biomaterialia* 9, 5390 (**2013**). © 2013, Elsevier.

Figure 8.
Photograph showing the tibial segmental bone defect of 2 cm length stabilized with a limited contact locking compression plate (LCLCP, Synthes) and filled with a PDLLA-TCP-PCL (a) and mPCL-TCP scaffold (c). Prior to scaffold insertion, the periosteum (b), which is in close proximity to the neurovascular bundle, was entirely removed within the defect area (d). Reprinted with permission from [211], J. C. Reichert, et al., *Int Orthop (SICOT)* 35, 1229 (**2011**). © 2013, Springer.
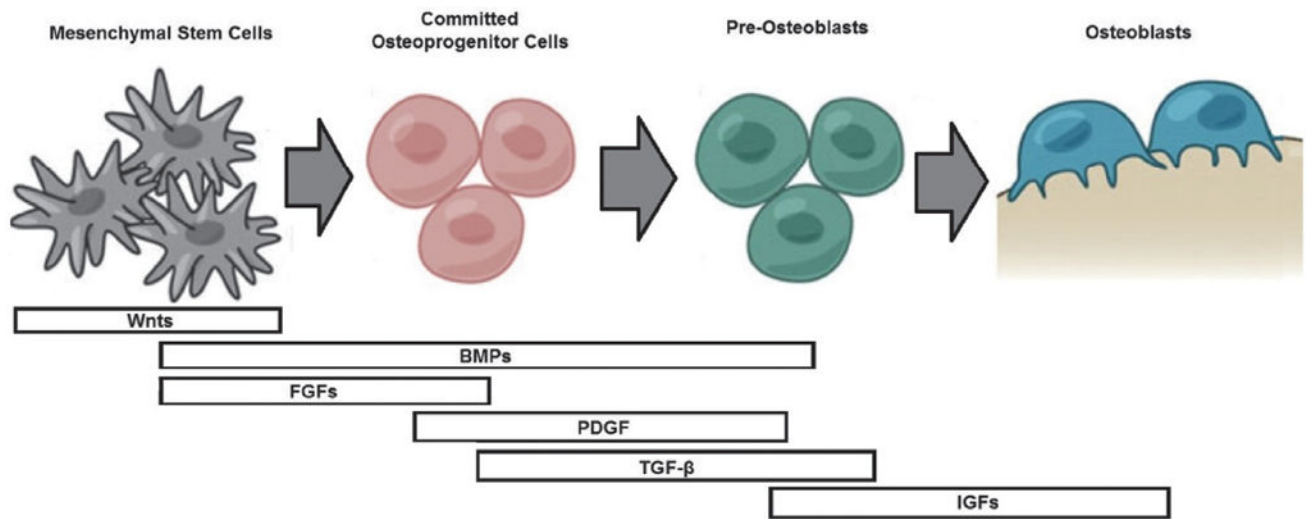
Figure 9.
Differentiation of the osteoprogenitor cells and the role of growth factors during the temporal progression. Adapted from [33], F. Hughes, et al., *Periodontol 2000* 41, 48 (**2006**). © 2006, Blackwell Munksgaard; From [279], Y. Luu, et al., *Bonekey Osteovision* 6, 132 (**2009**). © 2009, Nature Publishing Group.

Table I

Structural and mechanical properties of cortical and trabecular bone.

Bone type—Loading	Porosity[*] (%)	Density (g/cm³)	Volume fraction[∥] (mm³/mm³)	Surface/bone volume[¶] (mm²/mm³)	Young's modulus[¥] (GPa)	Tensile strength[¥] (MPa)	Compressive strength[¥] (MPa)
Cortical—Longitudinal	5–10	1.99[†]	0.85–0.95	2.5	17–20[¥]	79–151[¥]	131–224[¥]
Cortical—Transverse					6–13[¥]	51–56[¥]	106–133[¥]
Cancellous—Longitudinal	75–90	0.05–1.0[‡]	0.05–0.60	20	20[§]		2–5
Cancellous—Transverse					14.7[§]		

Notes: Reference

[*]19-21,

[†]296,

[‡]21,

[∥]297,

[¥]298,

[§]299.

Table II

Natural polymer used for scaffold fabrication and their properties.

Natural polymer	Study	Porosity (%)	Pore size (µm)	Compressive stress (MPa) (CS), Work-of-fracture (J/m²) (WOF), Flexural strength (MPa) (FS), Matrix stiffness (Pa) (MS)	Tangent modulus (kPa) (TM), Elastic modulus (Pa) (EM), Compressive modulus (kPa) (CM), Linear modulus (kPa) (LM), Modulus of resilience (kPa) (MR), Shear modulus (Pa) (SM)	Ref.
Gelatin/chitooligosaccharide	*In vitro/in vivo*		70–105			[300]
Collagen	*In vitro/in vivo*				296.5 ± 107.5 to (0 to 5)% strain-TM 74.5 ± 18.4-MR	[254]
Chitosan	*In vivo*	85 ± 2	70–900			[301]
Chitosan/collagen/beta-glycerophosphate (β-GP)	*In vitro*		3–4		3 times more stiffer than pure chitosan to (0–8)% strain-LM	[302]
Silk fibroin	*In vitro*		(lamellar) 250–500 (spherical) 500–1000			[303]
Silk fibroin	*In vitro/in vivo*	85 ± 5	10–250		25.69 ± 1.61-CM	[304]
Alginate/CPC/hUCMSC	*In vitro*			4-FS > 400-WOF	0.7 GPa-EM	[305]
Alginate	*In vitro*		~200			[306]
Hyaluronic acid	*In vitro*				21-CM	[307]
Hyaluronic acid	*In vitro/in vivo*				2520 ± 30–2600 ± 30-EM	[308]
RAD16-I BD™ (PuraMatrix)	*In vitro*			100-MS	9500-SM	[309]
Chitosan/RGD peptides	*In vitro*		110–149	9.81 ± 0.738-CS		[310]

Table III

Synthetic polymer used for scaffold fabrication and their properties.

Synthetic polymer	Study	Porosity (%)	Pore size (μm)	Compressive stress (MPa) (CS), Tensile strength (MPa) (TS), Tensile stress (MPa) (TSS), Elongation-at-break (%) (EAB), Breaking-elongation-rate (%) (BER)	Elastic modulus (EM), Compressive modulus (CM) (MPa)	Ref.
PLAGA	In vitro		500–710	(14.6 ± 2.9)-CS	402.6 ± 61-CM	[311]
PCL or pHMGCL	In vitro	69.7-PCL 72.8-pHMGCL	900		10-CM	[312]
PLGA-PEO	In vitro	64	8.8			[313]
poly(LLA-co-CL)/poly(LLA-co-DXO)	In vitro	~90				[314]
PPHOS/PLAGA	In vitro	87.2		1.5 ± 0.4-TS	151 ± 14-EM	[257]
PCL/PDIPF	In vitro			7.5 ± 0.7-TSS 60 ± 12-EAB	143 ± 12-EM	[315]
PEA-g-TA	In vitro			105 ± 10-BER		[122]
PLGA-(PEG-ASP)	In vitro/in vivo	> 80				[316]
PEOT/PBT	In vitro					[317]

Table IV

Bioactive glass used for scaffold fabrication and their properties.

Bioactive glass	Study	Porosity (%)	Pore size (µm)	Compressive strength (MPa)	Elastic modulus (GPa) (EM), Compressive modulus (MPa) (CM), Weibull modulus (MPa) (WM)	Ref.
45S5 Bioglass®	In vitro		Macropores: 420 Mesopores: 25–80	5.4–7.2		[318]
CaMgSi$_2$O$_6$	In vitro		300	1.36–0.2	68 ± 20–10 ± 3.3 -CM	[135]
45S5 bioactive glass®	In vitro				0.037–0.482-CM	[140]
45S Bioactive glass®			10–100			[138]
Bioactive glass (BG20)	In vitro	40%PEG 58–52 (T = 800–950 °C) approx. 70%PEG 75–70 (T = 800–950 °C) approx.	400–450	40%PEG 5–7.2 (T = 800–950 °C) approx. 70%PEG 2–3 (T = 800–950 °C) approx.		[141]
Bioglass® and CEL2-derived scaffolds	In vitro		100–600	2.5–4.5		[143]
Bioactive glass® (13–93)	In vitro and in vivo	47	300	86 ± 9	13 ± 2-EM 12-WM	[144]

Table V

Calcium phosphates used for scaffold fabrication and their properties.

Calcium phosphate	Study	Porosity (%)	Pore size (μm)	Flexural strength (FS), Compressive strength (CST), Fracture toughness (FT) (MPa)	Ref.
Calcium Phosphate Cement CPC	*In vitro*			4-FS	[154]
Hydroxyapatite/*β*-TCP/rhBMPP-2	*In vitro/in vivo*	34			[155]
Hydroxyapatite HA	*In vitro/in vivo*		300–800		[156]
Calcium Aluminate/melatonin	*In vivo/in vivo*		100		[164]
Hydroxyapatite HA	*In vitro/in vivo*	50	0.1–500		[157]
		70	50–300		
β-Tricalcium phosphate *β*-TCP	*In vitro*		6	1.10 ± 0.13 -FT	[319]
HA/*β*-TCP	*In vitro*	25–80 vol		3–50-CST	[161]
HA/b-TCP	*In vitro/in vivo*	7.48 ± 0.45 and 9.10 ± 0.57			[162]
CPC/Bioglass®	*In vitro/in vivo*	Microporosity		26–40-CST	[151]

Table VI

Coral used for scaffold fabrication and their properties.

Natural coral	Study	Porosity (%)	Pore size (μm)	Ref.
Natural corals (Hainan, China)	*In vitro/in vivo*	57 ± 6.5 vol	140–260	[172]
			mean pore diameter: 195 ± 75	
Porites sp.	*In vitro*		60–800	[173]
			pore mean size: 280	
Goniopora coral	*In vivo*		600	[174]
Natural coral (Regemed Inc., batch number BS05312)	*In vitro/in vivo*			[176]
Coral hydroxyapatite (CHA, Beijing Yi-Hua-Jian Technology & Trade Co., Ltd., China	*In vitro/in vivo*	30–70	Average pore diameter: 100–600	[177]
Condyle-shaped coralline	*In vitro/in vivo*		100–300	[178]
Porites lutea	*In vitro*			[179]
Acropora sp. (Biocoral_; Inoteb)	*In vitro/in vivo*	4–12	200 to 800	[320]
			Mean pore diameter: 500	
Natural coral scaffolds (Hainan island, China)	*In vitro/in vivo*		100 to 300	[181]

Table VII

Metals used for scaffold fabrication and their properties.

Metal	Study	Porosity (%)	Pore size (µm)	Tensile strength (MPa) (TS), Compressive strength (MPa) (CST)	Young's modulus (GPa) (YM)	Ref.
NiTi/Ti	*In vitro*	3D microporous				[190]
Titanium fiber-mesh sheets	*In vitro*	40 ± 3				[194]
Ti wires	*In vitro*	40				[195]
Ti and TiO$_2$	*In vivo*		500–1000			[192]
TiO$_2$		80–90	400	2.5-CST		[196]
Ti$_6$Ta$_4$Sn alloy	*In vitro*	25–75	75–900			[198]
Magnesium alloy W$_4$(MgY$_4$)	*In vitro/in vivo*		10–250	15–22-CST	0.8–2.9	[199]
TiO$_2$	*In vivo*	91	1 and 500	1.2-CST		[191]
Iron-manganese alloy		36.3		106.07 ± 8.13-TS	32.47 ± 5.0	[200]

Table VIII

Polymer/ceramic composites used for scaffold fabrication and their properties.

Polymer/ceramic	Study	Porosity (%)	Pore size (μm)	Flexural strength (MPa) (FS), Normal stress (Pa) (NS), Strain (MPa) (S), Toughness (J/m^2) (T), compressive stiffness (N/mm) (CSS), Deformation at break (%) (DAB), Strain break (%) (SB)	Elastic modulus (MPa) (EM), Compressive modulus (MPa) (CM), Young's modulus (MPa) (YM), Tensile modulus (MPa) (TSM)	Ref.
Nano-apatite/PCL	In vitro			121 ± 13–161 ± 15-SB	6.77 ± 0.31–13.46 ± 1.29-TSM	[210]
PLGA-PCL-Calcium phosphate	In vitro			0.3–2.2-S	40–120-YM	[207]
PEOT/PBT-CP	In vitro/in vivo	68.5 ± 2.2				[208]
Collagen-CPC	In vitro			0% collagen: (2.0–0.4)-FS		[216]
				8% collagen :(3.4–1.0-FS		
				0% collagen:(368–80)-T		
				8% collagen: (840–173)-T		
PCL-TCP	In vivo		350–500	446–418-CSS	22.17–24.70-EM	[211]
Chitosan-CPC	In vivo			1766 ± 221 N-CST		[321]
Magnesium phosphate-PCL					3.62 ± 1.15, 2.37 ± 1.15 and 4.32 ± 0.13-CM	[228]
PLGA-βTCP	In vitro	Ratio: 88.1 ± 1.2 and 86.7 ± 3.6		0.68 ± 0.04 and 0.70 ± 0.07 MPa-CST	17.91 ± 2.12 and 18.16 ± 3.21-YM	[214]
PCLF-PVA-HA	In vitro/in vivo	80			0.193–0.502-CM	[222]
Chitosan/poly(DL, lactide-co-glycolide)	In vitro			0.589–0.733 MPa–CST	3.79–11.4-EM	[322]
				10.25–22.98-DAB		
				1.77×10^5–7.33×10^5-NS		
PLGA-nHA	In vitro		5.8 ± 3.3–10.9 ± 6.9			[323]
P3HB-HA		86	100–400	1.51 MPa-CST	22.73-CM	[324]
			Average pores size 250			

Table IX

Metal/ceramic composites used for scaffold fabrication and their properties.

Metal/ceramic	Study	Porosity (%)	Pore size (μm)	Compressive strength (CST), Yield stress (YS) (MPa)	Compressive modulus (CM), Young's modulus (YM) (GPa)	Ref.
SiO$_2$/CaO/Na$_2$O/MgO/B$_2$O$_3$			110–550	(0.6–1)-CST		[202]
Niobium/fluorapatite	In vitro	Macroporous structure	Average pore size 325			[325]
Ti-HA	In vitro					[244]
TiO$_2$	In vitro/in vivo	91		> 1.2-CST		[191]
ZrO$_2$–CP/PCL	In vitro	78 vol		12.7-CST		[237]
K/Sr–CPP(calcium polyphosphate)	In vitro	40		1.51 ± 0.47–2.40 ± 0.27-CST		[241]
ZrO2/HAp	In vitro/in vivo	72–91		2.5 to 13.8-CST		[225]
Porous cobalt-containing mesopore-Bioglass (Co-MBG)	In vitro		Macroporous 300–500 mesoporous 0.0045–0.005			[234]
Copper (Cu)-containing mesoporous bioactive glass (Cu-MBG)			Macroporous 300–500 mesopores 0.0038–0.0052			[243]
β-TCP/Mg	In vitro	42 y 50	500	8–12-CST	0.3–0.6-CM	[230]
Sr/calcium polyphosphate (CPP)	In vitro	Irregular porosity		90.72-YS	15.41-YM	[239]

Table X

Metal/ceramic composites used for scaffold fabrication and their properties.

Metal/ceramic	Study	Pore size (μm)	Elasticity (E) (MPa)	Ref.
polyNaSS/Ti	*In vitro*			[326]
PLLA/PLGA/Ti		10	Maximum elasticity: 500 MPa (approx.) at 43 °C	[246]
polyNaSS/Ti	*In vitro*			[247]
NaSS/methacrylic acid, MA/Ti6Al4V alloy	*In vitro/in vivo*			[248]
polyNaSS/Ti	*In vitro*			[327]

Table XI

Co-Culture studies.

Author	Culture system	Cells	Outcome
Buschmann et al. 2011	DegraPol®	Human osteoblasts/Human endothelial cells	Increased cell proliferation, increased growth into scaffold, higher perfusion
Aguirre et al. 2012	Matrigel™	Endothelial progenitor cells/ Mesenchymal stem cells	Increased cellular migration and organization, increased tubulogenic activity, gene expression consistent with an angiogenic phenotype
Unger et al. 2010	Silk fibroin	Human microcapillary endothelial cells/Primary human osteoblast cells	Increased microcapillary formation around and within scaffold
Xing et al. 2013	Poly(L-lactide)-co-(1,5-dioxepan-2-one)	Human umbilical vein endothelial cells/Human osteoblast-like cells	Ability to form microcapillary-like structures in scaffold, increased expression of osteogenesis-related genes
Tortelli et al. 2009	Resorbable porous ceramic scaffold	Murine primary osteoblasts/ Murine osteoclast precursors	Enhancement of osteoblast and osteoclast differentiation.
Ruggiu et al. 2012	Resorbable porous ceramic scaffold	Murine primary osteoblasts/ Murine osteoclast precursors	Superior organization of bone tissue, higher amounts of fibrous osteoid tissue, increased scaffold degradation
Schloßmacher et al. 2013	Alginate, Alginate/Silica Hydrogels	SaOs-2 cells/RAW 264.7 cells	Osteoblast activation, osteoclast inhibition
Pirraco et al. 2013	Porous trans-wells	Monocytes + macrophages/ Human bone marrow stromal cells	Increased hBMSC proliferation, enhanced ALP activity, increased osteocalcin and osteopontin expression, all effects abrogated with the addition of BMP-2 antibody into system